Pathogenesis and treatment of Rift Valley fever virus

by

Haley Nicole Cartwright

BA, Kalamazoo College, 2015

Submitted to the Graduate Faculty of the

Dietrich School of Arts and Sciences in partial fulfillment

of the requirements for the degree of

Doctor of Philosophy

University of Pittsburgh

2022

UNIVERSITY OF PITTSBURGH

DIETRICH SCHOOL OF ARTS AND SCIENCES

This dissertation was presented

by

Haley Nicole Cartwright

It was defended on

April 4, 2022

and approved by

Amy Hartman, PhD, Associate Professor, Department of Infectious Disease and Microbiology

John Williams, MD, Professor, Department of Pediatrics

John Alcorn, PhD, Professor, Department of Pediatrics

Laurie Silva, PhD, Assistant Professor, Department of Pediatrics

Dissertation Director: Anita McElroy, MD, PhD, Assistant Professor, Department of Pediatrics

Pathogenesis and treatment of Rift Valley fever virus

Haley Nicole Cartwright, PhD

University of Pittsburgh, 2022

Rift Valley fever virus (RVFV) is a mosquito-transmitted bunyavirus causing periodic outbreaks of severe disease in humans and livestock. Currently endemic to most of Africa and the Arabian Peninsula, RVFV threatens to spread into new regions of the world due to its many competent mosquito vectors and the effects of climate change. Rift Valley fever (RVF) in humans generally causes a self-limiting febrile illness; however, it can progress to severe forms of disease including hepatitis, hemorrhagic fever, or encephalitis. Unhindered spread of RVFV would cause major human health and agricultural economic consequences. Therefore, RVFV is classified as a NIAID category A priority pathogen and a WHO priority disease for research and development. Despite this, the field lacks tractable high-throughput animal models of the various forms of RVFV disease and there are no licensed human therapeutics. Here I address these gaps in the RVFV field by developing and characterizing both novel mouse models and therapeutically relevant antibodies. First, I evaluate RVFV susceptibility and pathogenesis across five commonly used inbred laboratory mouse strains to determine phenotypic baselines, identify potential sex differences, and determine challenge dose. Second, I screen 20 recombinant inbred Collaborative Cross mouse strains to identify and characterize novel murine models of RVFV disease. Third, I develop RVFV monoclonal antibodies, establish therapeutic efficacy, and show that Fc-mediated functions are a critical component of humoral protection from RVFV. Together this work answers critical questions about RVFV pathogenesis and treatment. Importantly, this work yielded both a novel model of RVF encephalitis and multiple monoclonal antibody therapeutic candidates.

Table of Contents

List of Tables

List of Figures

Preface

The completion of this dissertation would not have been possible without financial support from multiple funding sources. I am extremely grateful to the RK Mellon Institute for Pediatric Research for awarding me a trainee award, which supported all monoclonal antibody work in this dissertation. Work involving the Collaborative Cross resource was performed thanks to the support of an NIH R21 from the National Institute of Allergy and Infectious Diseases (AI145352 to AKM). Additionally, I am thankful for funding provided by the Pediatric Infectious Disease Society Stanley and Susan Plotkin and Sanofi Pasteur Fellowship Award (trainee award to JDD), the Children's Hospital of Pittsburgh of the UPMC Health System (Startup Award to AKM) and the Burroughs Wellcome (CAMS 1013362.01 to AKM) that have all helped to support my research.

I would also like to thank the University of Pittsburgh Clinical and Translational Science Institute (CTSI) Biostatistics, Epidemiology, and Research Design (BERD) Core for providing statistical consultation (supported by NIH grant UL1 TR001857) as well as the Division of Laboratory Animal Resources of University of Pittsburgh staff for their assistance throughout the project. This work used the UPMC Hillman Cancer Center and Tissue and Research Pathology/Pitt Biospecimen Core shared resource which is supported in part by award P30CA047904.

I am an extremely lucky student to have done my graduate studies in Dr. Anita McElroy's lab. I am eternally grateful to my PhD mentor Anita McElroy for being so supportive, encouraging, and motivational throughout my dissertation research. She is the hardest working person I know and her dedication to science, human health, and her team are awe-inspiring. Despite being one of the busiest people I know, Anita has dedicated significant time to teaching me how be an excellent

scientist, how to think critically, communicate effectively, and lead by example. She truly set me up for success and never complained once about my frequent trips to her office for advice.

What is a PhD without the people that make up your lab? I am forever grateful to the members of the McElroy lab that have made my PhD years not only bearable but also fun. Thank you, Dominique Barbeau, for being the most incredible lab manager to ever exist. I am sure I would have hit many more bumps in the road without your help. Also thank you to Josh Doyle and Ling Xu for their support and willingness to listen to me complain. I would also like to offer a sincere thanks to the incredible scientists that surrounded the McElroy lab during my dissertation including Natasha Tilston-Lunel, Lola Alcorn, and Madeline Schwarz who did the most amazing job at supporting both my scientific endeavors and my emotional wellbeing.

Members of my thesis committee have also been an essential part of my dissertation journey. They have provided so much encouragement, structure, and advice along the way, which both sped along and improved the quality of my thesis research. Thank you, Amy Hartman, John Williams, John Alcorn, and Laurie Silva.

I could not have gotten through all the ups and downs of a PhD without the support of my friends. I would like to sincerely thank Rhodes Ford and Ben Murter, my fellow PMI buds, for being with me from day 1 and for supporting me through rotations, classes, comprehensive exams, failed experiments, manuscript submissions, and now dissertation writing. I would also like to thank Sarah Baehr for being my best friend and the most amazing support system through everything.

Finally, I must extend the greatest thanks to my family. To my mom, Marjorie Boulden you are the kindest and most compassionate person I know. The sacrifices you have made in your life for me have allowed me to get where I am today. You have taught me to follow my dreams,

to never give up even when things get hard, and to never stop asking questions. To my dad, Jim Cartwright, you are truly the smartest person I know. You have been there for me through every milestone of my life, and I cannot express adequately how lucky I am to be your daughter. I look up to your drive, your huge heart, and of course your incredible sense of humor. The best compliments of my life have been when people compare me to you.

Thank you to my stepmom and biggest cheerleader Benilde Rocha-Cartwright. To my little brother, Nate Cartwright, I am so lucky to be your big sister and to have grown up alongside you. I wouldn't be the person I am today without you. Finally, to my life partner, Andrew Frisch, you have been my rock through everything and have always believed in me even when I didn't believe in myself. Your determination, compassion, and love inspire me every day. I couldn't imagine being on this crazy ride through life with anyone else.

1.0 Introduction

Rift Valley fever virus (RVFV) is an arbovirus, first discovered in 1931, that causes periodic bouts of endemic disease in Africa and the Arabian Peninsula in both humans and ruminants (1). Due to the many RVFV transmission-competent mosquito vectors and the effects of climate change on mosquito habitats, RVFV has the potential to spread into new geographic regions (2, 3). Rift Valley fever (RVF) in humans is generally self-limiting with recovery occurring after a febrile illness. However, in a subset of individuals RVF can manifest as severe hepatitis, hemorrhagic fever, or encephalitis (4-6). The threat RVF poses to human health illustrates an urgent need to understand how RVFV causes disease as well as the need for RVF-directed therapeutics. Despite being studied for over 90 years, many aspects of RVFV pathogenesis remain unanswered and there are no licensed therapeutics for human use. The study of RVFV pathogenesis and the development of effective therapeutics have been impeded, in part, by the lack of animal models that recapitulate the breadth of RVF disease manifestations.

In chapter 1, I review RVFV epidemiology, replication cycle, human disease, current animal models, and the current state of vaccines and therapeutic development. In chapter 2, I describe RVFV pathogenesis in five commonly used inbred laboratory mouse strains to determine phenotypic baselines, identify potential sex differences, and determine challenge dose for subsequent experiments. In chapter 3, I detail the screening of 20 recombinant Collaborative Cross mouse strains and identify and characterize a novel mouse model of RVF encephalitis. In chapter 4, I develop and characterize anti-RVFV monoclonal antibodies, establish their in vivo efficacy, and show that Fc-mediated functions are a critical component of humoral protection from RVFV. Chapter 5 entails a detailed description of all methods and materials used for my dissertation

research. Finally, in Chapter 6 I summarize my thesis studies and discuss directions this research could take in the future. Altogether, the research described in this dissertation answers critical questions about RVFV pathogenesis and provides novel insight into mechanisms of antibody-mediated protection. Notably, this work has resulted in the detailed characterization of a novel mouse model of RVF encephalitis and the development of multiple monoclonal antibody therapeutic candidates.

1.1 Bunyavirales

In 1975, the International Committee on Taxonomy of Viruses (ICTV) created the *Bunyaviridae* family (7). This family originally comprised a group of serologically related, negative-sense RNA viruses that contain three linear genomic segments. The term 'Bunyavirus' is derived from the Bunyamwera village in Uganda where the Bunyamwera virus was first isolated from *Aedes* mosquitoes during a yellow fever surveillance program (8). The ICTV elevated the *Bunyaviridae* family to an order in 2016 to include the increasing number of closely related viruses. With the most recent update occurring in 2019, the current *Bunyavirales* order comprises of 13 families of viruses: *Mypoviridae, Wupedeviridae, Nairoviridae, Tospoviridae, Peribunyaviridae, Arenaviridae, Hantaviridae, Leishbuviridae, Phenuiviridae, Cruliviridae, Fimoviridae, Phasmaviridae,* and an "unassigned" family (**Figure 1**).

Viruses within the order *Bunyavirales* infect a large variety of life including plants, insects, and animals. Five families within the order contain viruses that are serious human pathogens (*Nairoviridae, Peribunyaviridae, Arenaviridae, Hantaviridae*, and *Phenuiviridae*). These families contain viruses that cause illness in humans spanning from mild self-limiting illness to severe

diseases including hemorrhagic disease, respiratory disease, and encephalitic disease (9). Bunyaviruses are primarily transmitted by arthropods (arboviruses) including mosquitos, ticks, and sandflies. However, some viruses can also be spread through aerosols or through direct contact from the infected animal to humans. Viruses within the order *Bunyavirales* pose a major threat to public health due to the severity of disease they cause in humans, their potential for spread into new regions of the world, and the damage they inflict on agricultural and livestock systems.

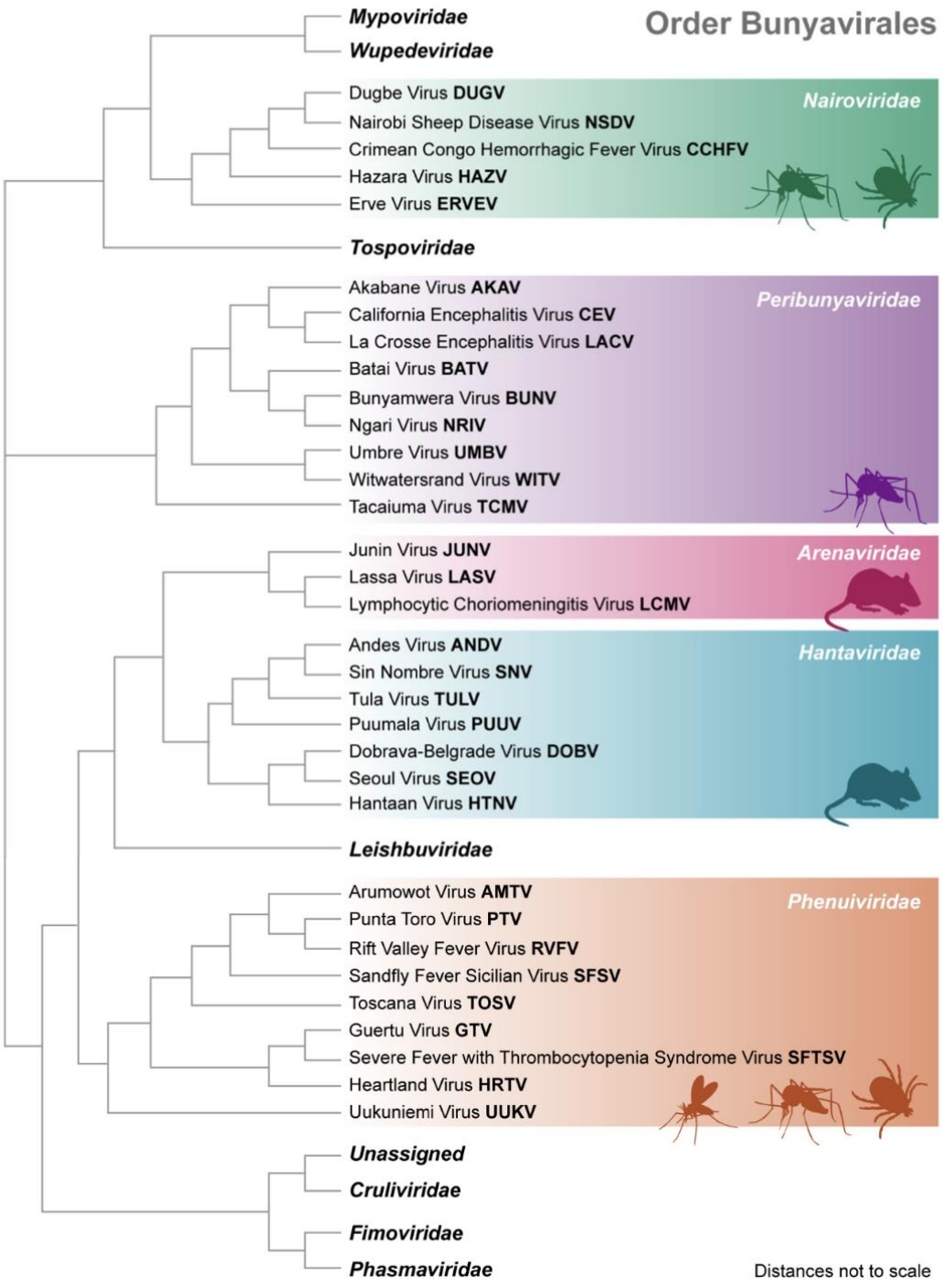

Figure 1 Phylogenetic tree of the order Bunyavirales

Arrangement of the 13 families within the order Bunyavirales are based on the amino acid sequences of the nucleoprotein. Species capable of serving as vectors to any virus within each family are depicted by illustrations. Figure reproduced from Leventhal et al. (2021) (10). Creative Commons license

https://creativecommons.org/licenses/by/4.0/legalcode.Arrangement of the 13 families within the order *Bunyavirales* are based on the amino acid sequences of the nucleoprotein. Species capable of serving as vectors to any virus within each family are depicted by illustrations. Figure reproduced from Leventhal et al. (2021) (10). Creative Commons license .

1.2 Rift Valley Fever Virus

RVFV belongs to the *Phenuiviridae* family and is a member of the phlebovirus genus. RVFV, named after the Rift Valley in Kenya where it was first isolated in 1931, is a zoonotic pathogen that causes disease in both humans and livestock (1). For most of the 20th century RVFV was contained to the continent of Africa, where it continues to this day either to be either endemic or to cause sporadic outbreaks (11) (**Figure 2**). However, in the 1990s, RVFV showed the potential to breach geographical boundaries by spreading off the coast of Africa to the island of Madagascar (12, 13). This was followed by RVFV emergence in Saudi Arabia and Yemen in the early 2000s (14). RVF outbreak data (**Figure 2)** greatly underestimates the true burden of disease, however, as up to 60% of adults are seropositive in countries of endemicity (15-20). The ability of the virus to spread to new regions is due to 1) the many mosquito species capable of transmitting RVFV; 2) the effects of climate change on geographical ranges of mosquitos; and 3) global livestock trade. The potential for emergence of RVFV into new areas of the world as well as its ability to impact human health has led to its classification as a NIAID category A priority pathogen and a WHO priority disease for research and development. The true burden of RVFV in endemic regions is not fully defined due to factors including misdiagnosis due to non-specific disease manifestations, inaccurate or unavailable testing, and subsequent underreporting. Hallmarks of RVFV outbreaks

are clear, however, and include sudden illness, death, and abortion storms in domesticated herds with ensuant illness in humans that live or work near livestock.

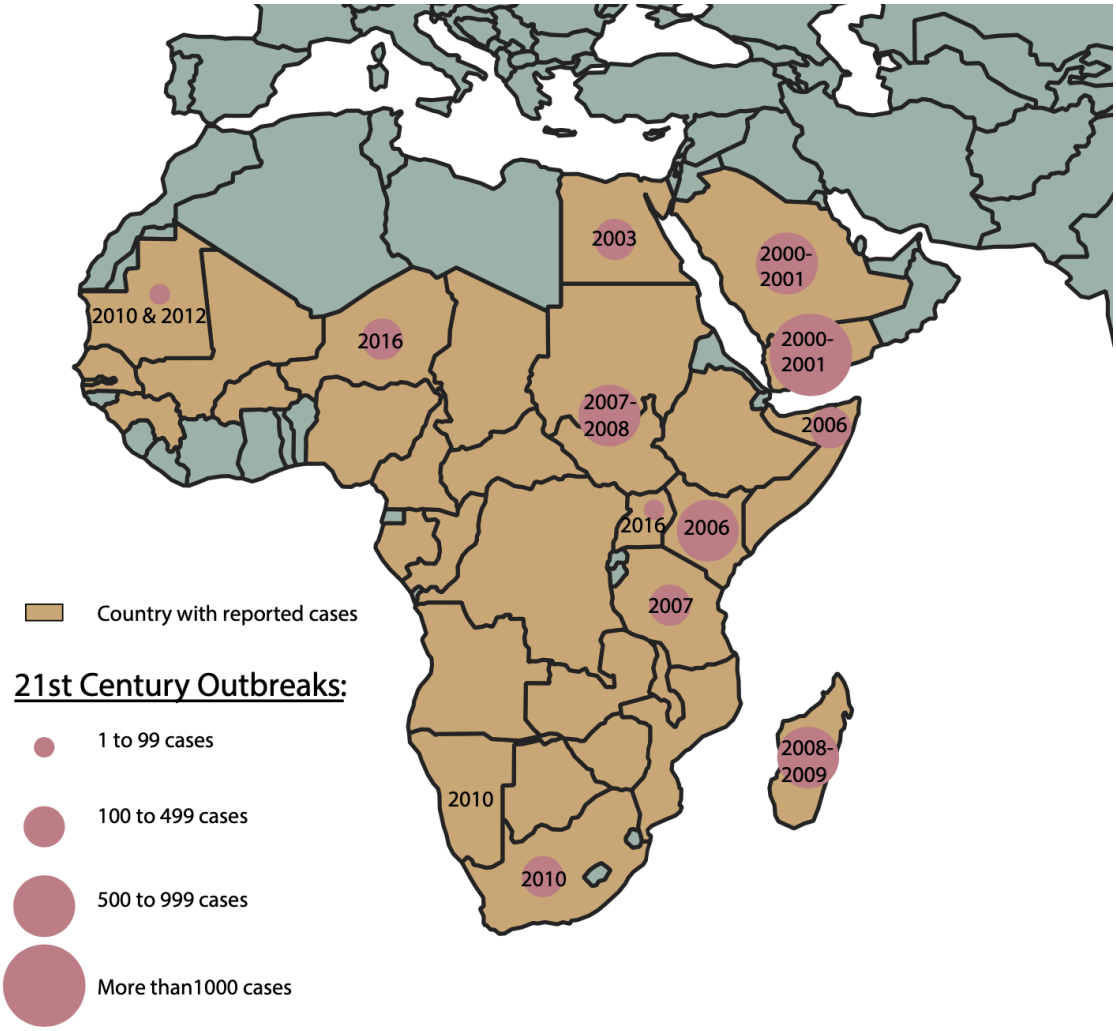

Figure 2 Endemic regions of Rift Valley fever virus and outbreaks since 2000

Countries where RVFV is endemic are colored in gold. Red circles represent human outbreaks of various sizes dating from the beginning of the 21st century. Figure reproduced from Javelle et al. (2020) (21). Creative Commons license https://creativecommons.org/licenses/by/4.0/legalcode.

Countries where RVFV is endemic are colored in gold. Red circles represent human outbreaks of various sizes dating from the beginning of the 21st century. Figure reproduced from Javelle et al. (2020) (21). Creative Commons license

.

RVFV is typical of the genus *Phlebovirus* with a spherical virion measuring 80 to 120 nm in diameter and a negative-sense tri-segmented RNA genome that is encased in a lipid bilayer (envelope). The lipid envelope of RVFV is obtained from the Golgi complex during assembly (22). The tri-segmented genome of RVFV is made up of small (S), medium (M) and large (L) segments **(Figure 3)**. The S segment encodes in an ambisense fashion the nucleoprotein (N) and non-structural protein (NSs) while the L segment encodes the RNA-dependent RNA polymerase (23). The M segment encodes both the envelope glycoproteins Gn and Gc as well as the non-structural proteins Nsm and the 78kDa Gn/Nsm fusion protein (23-25).

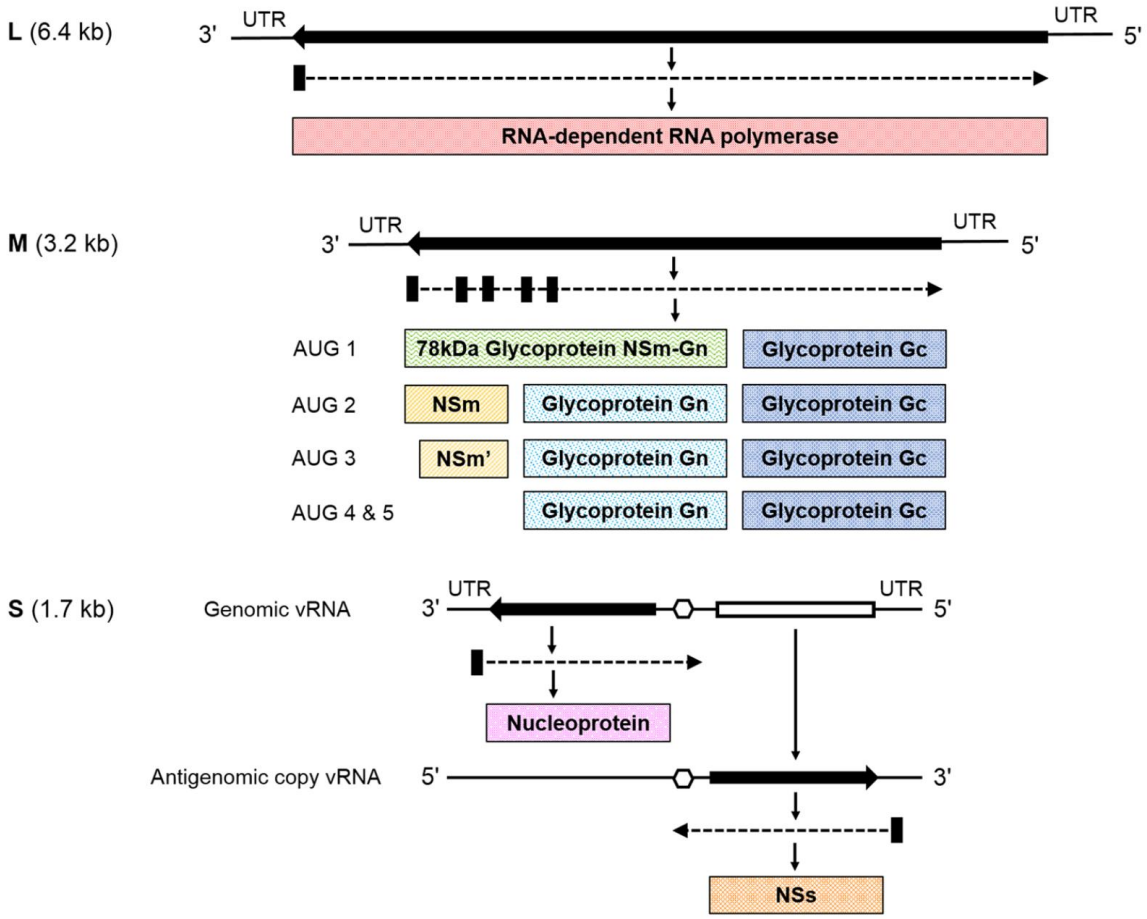

Figure 3 Genome organization of Rift Valley fever virus

The three segments of the RVFV genome are presented here as large (L), medium (M), and small (S). Open reading frames for each genome segment are shown by the black arrows while the respective protein products appear in boxes. Figure reproduced with permission from Gaudreault et al. (2019), copyright 2018, Springer Nature (24).The three segements of the RVFV genome are presented here as large (L), medium (M), and small (S). Open reading frames for each genome segment are shown by the black arrows while the respective protein products appear in boxes. Figure reproduced with permission from Gaudreault et al. (2019), copyright 2018, Springer Nature (24).

1.3 Rift Valley Fever Virus Replication Cycle

Replication of RVFV, like other Bunyaviruses, occurs in the cytoplasm (**Figure 4**). Following Gn-mediated cellular attachment via LRP-1 on a permissive cell, fusion between the plasma and RVFV membranes occurs (26). The RVFV receptor LRP-1 is highly conserved across species and is widely distributed throughout tissue types making the cellular tropism of RVFV very broad (26). Some of the many cell types able to be infected by RVFV include macrophages, dendritic cells, epithelial cells, neuronal cells, adrenal cells, and placental cells (26-30). After receptor binding on these cells and upon endosomal fusion under low pH conditions, the viral RNA-dependent RNA polymerase (RdRp) and viral ribonucleoproteins (RNPs), viral genomic RNAs (vRNAs) complexed with N, are released into the cytosol. Immediately upon entry, transcription of RNPs occurs to produce mRNAs followed closely by translation of viral proteins (31, 32). RVFV transcription and translation are coupled, with protein translation occurring before the completion of viral mRNA transcription (31, 32). Genome replication also takes place in the cytoplasm where complementary full-length template RNA (cRNA) is used to produce vRNAs. These vRNAs are used by the virus both as templates for additional mRNA synthesis and as the genomic segments of progeny virions (33-35). The viral glycoproteins Gn and Gc are translated as a precursor protein in the endoplasmic reticulum (ER) (36). The Gn/Gc precursor is then cleaved by signal peptidases in the ER to produce the functional Gn and Gc glycoproteins (37). After Gn/Gc dimerization occurs, the heterodimer travels from the ER to the Golgi. Genome segments, RNPs, and the RdRp are recruited to the Golgi likely by interacting with the Gn cytoplasmic tail (38). Once localized to the Golgi, progeny virions assemble then RVFV buds from the Golgi (34, 35). Finally, RVFV progeny are transported to the cell surface via secretory vesicles where they are released after fusion with the cellular plasma membrane.

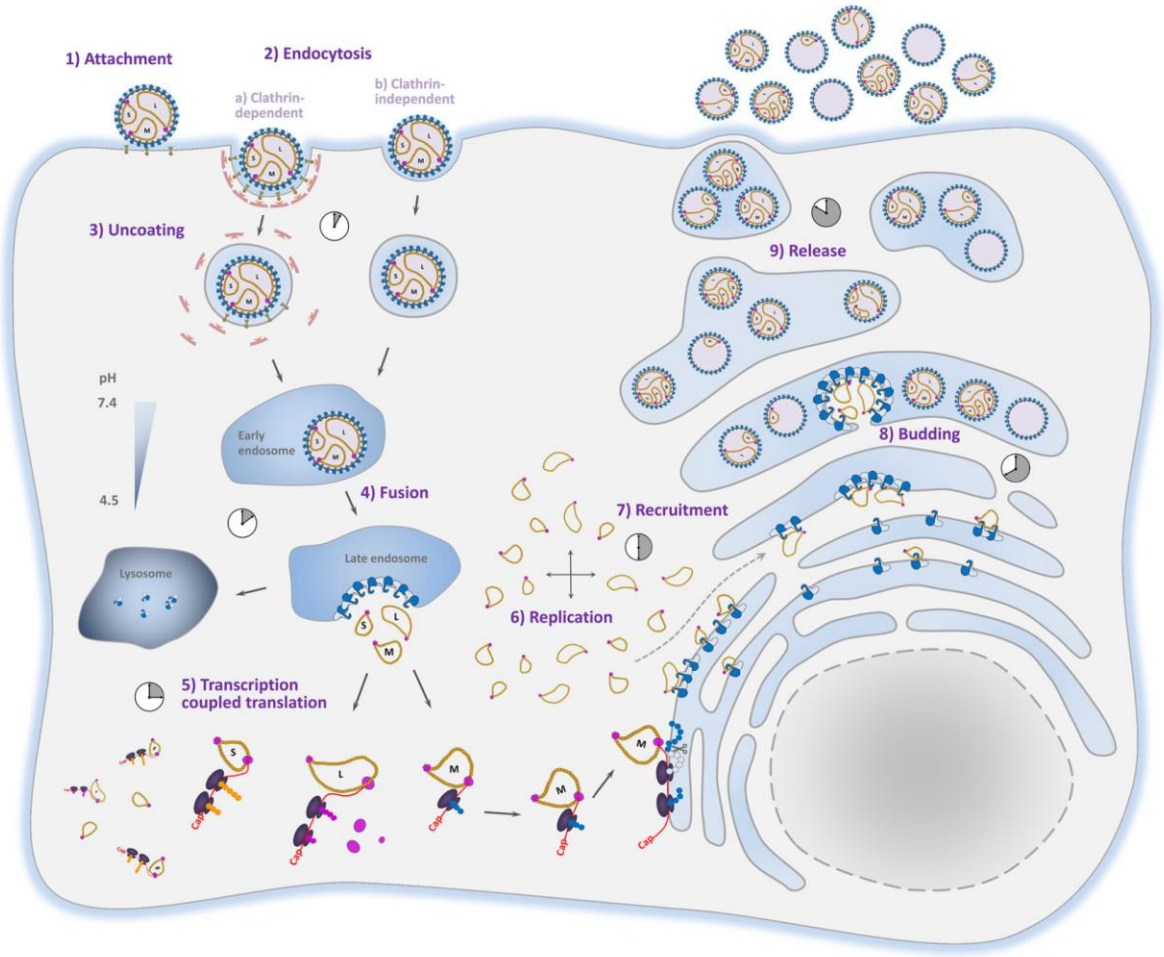

Figure 4 Rift Valley fever virus replication cycle

1) Viral attachment occurs by Gn binding to LRP-1 on a permissive cell. 2) Endocytosis occurs either by a) clathrin-dependent or b) independent mechanisms. 3) Uncoating occurs due to endosomal acidification followed by 4) fusion of the viral and endosomal membranes and subsequent release of RNPs into the cytosol. 5) RNPs are used as templates for transcription of mRNAs and translation of viral proteins. 6) vRNAs are produced via cRNAs. 7) Glycoprotein Gn-mediated recruitment to the Golgi occurs for genome segments, RNPs, and the RdRp. 8) Once accumulated, virions are packaged at the Golgi then budding occurs into the Golgi lumen. 9) Mature viral particles are released from the cell via exocytosis. Figure reproduced from Wichgers et al. (2016) (39). Creative Commons license https://creativecommons.org/licenses/by/4.0/legalcode.1) Viral attachment occurs by Gn binding to LRP-1 on a permissive cell. 2) Endocytosis occurs either by a) clathrin-dependent or b) independent mechanusms. 3) Uncoating occurs due to endosomal acidification followed by 4) fusion of the viral and endosomal membranes and subsequent release of RNPs into the cytosol. 5) RNPs are used as templates for transcription of mRNAs and translation of viral

proteins. 6) vRNAs are produced via cRNAs. 7) Glycoprotein Gn-mediated recruitment to the Golgi occurs for genome segments, RNPs, and the RdRp. 8) Once accumulated, virions are packaged at the Golgi then budding occurs into the Golgi lumen. 9) Mature viral particles are released from the cell via exocytosis. Figure reproduced from Wichgers et al. (2016) (39). Creative Commons license .

1.4 Rift Valley Fever Virus Ecological Replication cycle

The RVFV lifecycle is inextricably linked to the conditions and interactions of humans, livestock, and the environment. This intersection of human and animal health makes RVFV exemplary of the One Health concept (acknowledgment that optimal health outcomes will only be achieved by recognizing the interconnection of animals, people, and the earth) and adds a layer of complexity to control efforts. Among the animals able to be infected by RVFV, those most severely affected are ruminants including goats, sheep, and cattle. Transmission of RVFV among livestock occurs primarily via mosquito vectors. RVFV-transmitting mosquitos consist primarily of *Culex* spp. and *Aedes* spp, which breed in floodwaters (40-43). Outbreaks of RVFV in livestock are therefore highly driven by the abundance of mosquitos in surrounding areas. Mosquito population levels fluctuate considerably based on local rainfall. This is due to the breeding behavior of these species of mosquito, which lay their eggs (infected with RVFV due to transovarial transmission) after a period of flooding in water-filled depressions in the earth (dambos) (44). Subsequently, drought cycles cause these dambos to dry out, however, the desiccated mosquito eggs remain viable for long periods of time. When heavy rainfall occurs next, often in 10-year cycles, the mosquito eggs hatch. This translates to an abundance of RVFV-infected mosquitos, which then feed on livestock herds thereby infecting them with RVFV. These mosquito amplification events, driven by flooding, result in large-scale outbreaks of RVFV in

animal herds as well as in humans. This inter-epizootic versus epizootic-epidemic cycle is further detailed in **Figure 5**.

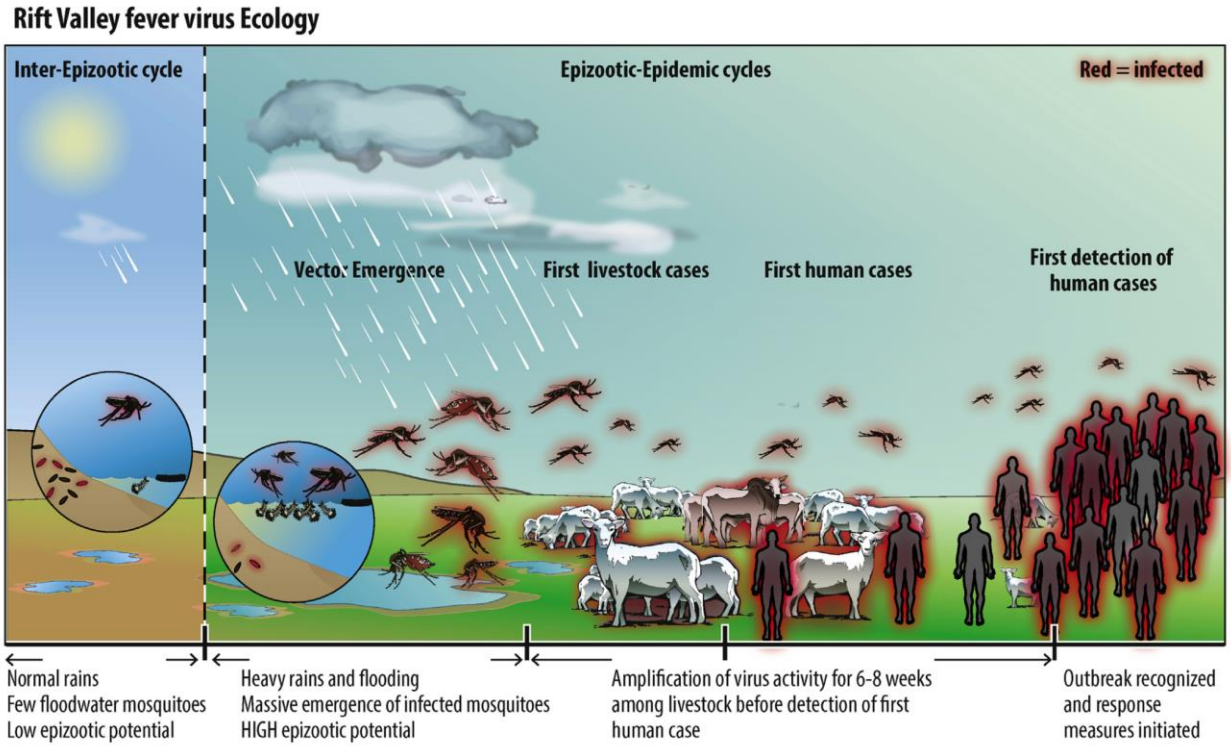

Figure 5 Rift Valley fever virus ecological lifecycle

Inter-Epizootic and Epizootic-Epidemic cycles of Rift Valley fever virus shown. RVFV emerges with mosquitos after heavy rainfalls, is transmitted to livestock where it is amplified, then is passed to nearby humans via mosquito bite or mucus membrane exposure. Figure reproduced with permission from Bird et al. (2016), copyright 2016, Elsevier (45).

Although transovarial transmission of RVFV within mosquitos has been suggested to be an important mechanism of viral persistence in areas where RVFV is endemic, it is likely not the only factor (46). Long-term maintenance of RVFV in an area could be aided by smaller scale vector-host interactions in which small local mammals keep RVFV circulating at low levels between the epidemic periods (47, 48). Although the role of wild animals as amplifying hosts remains unclear, infected livestock herds clearly serve as amplifying hosts for RVFV (49). When

infected mosquitos feed off domesticated livestock, animals display signs of illness including listlessness, diarrhea, and vomiting. Infected pregnant animals suffer frequent abortion of fetuses while younger animals often die. Mosquitos that take blood meals from these sick animals subsequently serve as vectors by spreading RVFV on to other animal herds or nearby humans.

An added complexity to RVFV human outbreaks is the sheer number of exposure methods. People can become exposed to RVFV by an infected mosquito bite, mucous membrane exposure to infected blood or tissues such as those from aborted fetuses, or contact with contaminated animal products such as meat or milk (50). The frequency of human exposure to RVFV via mosquito bite is debated. However, RVFV cases where infected individuals reported no known contact with infected livestock demonstrate that mosquitos are an important human transmission mechanism (51). In many human cases, the infection route is unclear due a history of exposure to both infected livestock and mosquitoes. RVFV human exposures are often driven by occupational, geographic, and lifestyle factors. Occupations such as herdsmen, farmers, abattoir workers, and veterinarians are high risk for RVFV exposure in endemic regions (52-56). Handling animal organs, aborted fetuses, or blood are all known risk factors associated with a higher likelihood of RVFV infection (56-58). These methods of mucous membrane exposure via handling carcasses or aborted fetuses are also known to be associated with more severe disease manifestations (56). The higher proportion of severe disease development from this exposure type is likely due to the extremely high viral titers present in aborted fetuses as well as the exposure being via mucous membrane contact. Regardless of how humans acquire RVFV, they serve as dead-end hosts, for RVFV is not transmitted from person to person (57, 59, 60).

1.5 Rift Valley Fever in Humans

RVFV is the causative agent of RVF. After viral exposure, via either the bite of a mosquito or mucous membrane exposure through high-risk activities involving livestock, humans develop RVF. The first descriptions of human disease appeared shortly after discovery of the veterinary illness in 1931 (1). Most human RVF cases described around this time were of scientists and veterinarians involved in the study. The disease was described as "dengue-like" with symptoms being similar to that of influenza including fever, headache, emesis, sweating, arthralgia and myalgia, retro-orbital pain, hepatic symptoms, hemorrhage, and abdominal pains (1, 61). From these observed disease manifestations in humans, the previously named "enzootic hepatitis" was changed to "Rift Valley fever".

Although the first human cases were described in the 1930s, the first major human outbreak of RVF did not occur until the 1970s. Beginning in 1974, the South African outbreak comprised 110 laboratory-confirmed human cases of RVF with 7 fatalities due to liver damage and hemorrhage, 15 encephalitic cases, and 10 retinitis cases (58). A second large outbreak occurred in Egypt at the end of the decade where detailed descriptions of human RVF illness were reported. Human manifestations were described as being disparate illnesses including self-limiting febrile illness, hemorrhagic disease, encephalitis, and ocular disease (4). Following the Egyptian outbreak, RVF outbreaks were reported in West Africa, Madagascar, Saudi Arabia, Yemen, as well as other places (12, 62-65) (**Figure 2**). The Saudi Arabian outbreak was particularly significant for it represented the first time that RVFV had impacted human health outside of the African continent.

Although RVF is often described as an acute viral hemorrhagic fever, the most common manifestation in humans is a self-limiting febrile illness. The incubation period is typically 3-6

days post-infection (dpi), after which humans develop headache, myalgia, and fever (4). In the majority of cases, this febrile illness lasts 3-5 days at which time the fever recedes and a full recovery is made. In the minority of cases, estimated at 1-2%, people proceed to more severe forms of disease after the initial febrile illness (66). RVF severe manifestations include retinitis, encephalitis, hepatitis and hemorrhagic fever. More severe RVF cases such as neurologic dysfunction and hemorrhagic manifestations have a mortality rate of up to 50% (67).

In cases of hepatitis, patients progress after the initial febrile illness and symptoms can include jaundice and sometimes hemorrhagic manifestations (4). Acute hepatitis can occur at the same time or before hemorrhaging and can also precede encephalitis. Hepatic disease in humans presents commonly with elevated levels of alanine transaminase (ALT) and aspartate transaminase (AST) as well as prolonged blood coagulation time, anemia, and thrombocytopenia (51, 62, 68, 69). Anemia is often due to microangiopathic destruction but in some cases hemolysis was found to be immune-mediated RBC destruction (62). Renal failure has also been found to be a common complication of severe RVF often accompanying hepatitis, and in certain cohorts affected one quarter of patients (62). At autopsy, patients' livers display evidence of severe necrosis (58, 70). RVF hepatitis and hemorrhagic fever are severe forms of disease, which, when lethal, can result in death within 1 week of onset of symptoms (71).

Cases of delayed-onset encephalitis typically appear in humans 14-28 days post-symptom onset; however, CNS symptoms have also appeared past 60 days (66, 72). Patients with neurological RVF disease have symptoms including headaches, delirium, hallucination, vertigo, and paralysis (58, 62). Case reports of human encephalitis are rare and few encephalitic autopsy samples have been studied. However, human autopsy specimens showed focal necrosis in the brain accompanied by the presence of macrophages and lymphocytes (58). Meningeal involvement has

also been noted in human cases due to the presence of lymphocytic CSF pleocytosis and nuchal rigidity (58, 72). Blood creatine kinase level increases have also been noted in a quarter of RVF patients manifesting with CNS symptoms (62). RVF encephalitis is highly lethal with 53% of encephalitic patients in the 2000 Saudi Arabian outbreak succumbing to disease (62). Even when non-lethal, RVF encephalitis can leave lasting impacts including brain damage and paralysis (4). Finally, one of the most common complications of RVF in humans is the development of ocular symptoms and vision problems (73, 74). Visual disturbances generally present 1-3 weeks post-initial symptom onset and include reduced vision, blind spots, and photophobia that can be permanent (74).

An important part of the study of RVF in humans has been determining the underlying host factors that are responsible for progression to severe disease. It has been suggested by multiple studies that route of exposure to RVFV has a minimal impact on disease severity; however, exposure to infected livestock does increase the risk for severe disease implicating route and dose of infection as playing some role (56, 57). However, humans have been seen to develop a wide spectrum of disease manifestations after presumed infection via mosquito bite, due to a lack of reported exposure to infected livestock. This indicates that gene polymorphisms or co-morbidities within the host could be the factors responsible for the development of severe RVF manifestations. Early activation of innate immune signaling has been suggested to provide the greatest protection from severe or lethal RVF. Therefore it is unsurprising that cross sectional studies performed in Kenya described innate immune response gene polymorphisms that were associated with severe disease progression (56, 75). Mutations were found in TLR3, TLR7, TLR8, MyD88, TRIF, MAVS, and RIG-I that were repeatedly associated with severe RVF manifestations (75). It has also been noted during multiple outbreaks that HIV positive patients have a higher rate of RVF

encephalitis than the general population and are at greater risk of death (76, 77). This as well as numerous studies in animal models demonstrates that later-onset disease manifestations like encephalitis can be modulated by host adaptive immunity (78).

Two pro-inflammatory cytokines (sCD40L and GRO) were elevated in non-fatal human cases from the 2000 Saudi Arabia outbreak (68). Additionally, the immunosuppressive receptor antagonist IL-1RA and IL-10 were elevated in fatal cases of RVF (68). This suggests an association between a pro-inflammatory cytokine response and increased RVF survival. Contrastingly, human cases from the South African 2010 outbreak revealed that fatal RVF cases corresponded with increases in pro-inflammatory cytokines IL-8, IP-10, CXCL9, and MCP-1(77). These fatal cases did show elevation in the anti-inflammatory cytokine IL-10 as the previous study. Evidence of endothelial activation and dysfunction was found in RVFV disease patients with elevation in ICAM, L-selectin, and E-selectin (69). Thrombomodulin, E-selectin, and ICAM were also associated with fatal disease (69). In human hemorrhagic cases, viral load has also been shown to be positively associated with markers of inflammation (IP-10, CRP, eotaxin, MCP-2, granzyme B), markers of endothelial function (ICAM-1), and markers of fibrinolysis (tPA and D-dimer) (52). Together, these studies demonstrate that an inflammatory response is initiated following infection; however, upregulation of certain inflammatory signals may be harbingers of immunologic dysfunction and associated with fatal RVFV infections.

1.6 Rift Valley Fever Animal Models

Immediately after its discovery in 1931 as a novel disease-causing agent, infectious blood samples containing RVFV were sent to London for experimental inoculation of a variety of animal

species by G.M. Findlay (61). There was a broad range in susceptibility among the animals tested. Mice, rats, and hamsters were found to be extremely susceptible similar to young livestock. On the other hand, RVFV was found to be much less severe and deadly in various non-human primate (NHP) species, cats, and rabbits (61). Since these initial animal experiments in the 1930s, many additional models of RVF have been developed and more fully characterized. Established models today serve distinct uses to aid in the study of RVFV pathogenesis and therapeutic development.

RVF manifestations vary widely in NHP models depending on the species and the exposure (61). Findlay et al. in the 1930s first showed that rhesus macaques developed non-fatal disease when infected with RVFV (61). Initial clinical readouts of disease included fever and leukopenia in the animals. Later studies using RVFV ZH501 strain resulted in a broader model for human infections when rhesus monkeys were infected (79-81). Challenge with ZH501 intravenously (IV) resulted in 18% of monkeys developing severe hemorrhagic fever. These NHPs developed weakness and fever starting at 2-4 dpi and developed facial and abdominal petechial hemorrhaging and lesions. Illness in these animals was accompanied by liver necrosis, disseminated intravascular coagulation and anemia. This model is very useful for clinical studies that require a spectrum of disease that mirrors human disease manifestations. However, only 18% lethality does not lend this model to vaccine or therapeutic assessment studies and NHP studies are resource intensive. Finally, the infection route (IV) is not a clinically relevant exposure route of RVFV.

Additional NHP models of RVF have been developed in the last few decades including the African Green monkey and the common marmoset models. When given via aerosol exposure, RVFV causes viral meningoencephalitis in African green monkeys (82). Hematological analysis indicated decreases in platelet counts as well as leukocytosis. African green monkeys therefore serve as a useful large animal model for late-onset encephalitis as well as a model of human aerosol

exposure. Marmosets were found to be more susceptible to RVFV than other NHPs. Marmosets were also found to develop encephalitis when challenged via aerosol, but had a lower LD_{50} for challenge dose (82). When challenged via subcutaneous (SC) injection, marmosets experience high rates of mortality succumbing primarily to acute hepatic disease (83). Marmosets experienced changes in their hematological and chemistry values and displayed signs both of hemorrhage and neurological disease. Marmosets therefore provide an excellent NHP model for the evaluation of vaccines and therapeutics due to the severity of RVF manifestations they exhibit.

Ferrets were both among the first and the most recently developed non-rodent models of RVFV. In the 1930s, ferrets were infected via pharyngeal washes and were interestingly found to develop disease with pulmonary involvement (84). More recently, a ferret model of RVF has been developed in which ferrets develop encephalitis after intranasal (IN) exposure (85). This model offers an alternative to NHP models for the study of RVF CNS disease and its prevention.

Rats offer an interesting and useful alternative to NHPs for modeling diverse manifestations of RVFV and uncovering the contribution of host genetics on RVFV susceptibility. Susceptibility between rat strains varies widely from 100 percent lethality to subclinical disease (86). Wistar-Furth (WF) and Brown Norway (BN) rats are highly susceptible to RVFV SC infection even at very low doses (87, 88). Both WF and BN rat strains die within 3-5 days of classical acute hepatitis. In contrast to these highly susceptible strains, ACI and MAXX rat strains experience only 50% mortality after either IP or SC challenge (88, 89). These rats succumb later in infection, 7-14 dpi, compared to WF and BN rats, and develop a late-onset CNS disease instead of hepatitis. At necropsy, ACI and MAXX rats were found to be completely devoid of hepatic lesions and only had detectible virus in the brain (88, 89). In contrast to all previously developed

models, the Lewis rat strain was found to be completely resistant to clinical RVF disease when challenged via SC exposure (86, 88, 90).

Recently, WF, ACI, and Lewis rat strains were challenged with RVFV by aerosol exposure and developed wildly different disease manifestations. While WF and ACI rats developed the same disease manifestations as when challenged previously by SC, hepatitis and encephalitis respectively, the Lewis rat RVF phenotype changed drastically (91, 92). Instead of showing complete resistance to clinical disease, as upon SC challenge, aerosol-challenged Lewis rats developed severe late-onset RVF encephalitis. This discovery added an aerosol infection model to the already diverse array of rat models of RVFV. These rat models enable study of various forms of RVF disease in a small animal model as well as offering the potential to correlate host genetics to disease manifestation. Despite the diversity of RVF models available, some rat strains are outbred and therefore cannot offer the consistency and genetic tractability of inbred mouse models. Additionally, rats pose challenges as animal models due to the lack of available knockout models and immunologic resources.

Historically, mice have displayed the most consistent manifestations of RVF. Infection of immunocompetent inbred mouse strains with wild-type (WT) RVFV via peripheral exposure almost universally results in an acute lethal hepatitis within 3-5 dpi (93). Mouse models of hepatitis that have been tested and developed over the years include murine strains C57BL/6J, 129/SV/Pas, and MBT (94-97). From this dissertation work, NOD/ShiLtJ, A/J, NZO/HILtJAs mice were added to this list as novel RVF hepatitis models [Chapter 2 and (94)]. These mice, upon challenge with WT RVFV via either a SC or IP route, succumb universally to acute hepatitis displaying liver necroses, elevated ALT levels, leukopenia, lymphopenia, and anemia. These clinical readouts

mirror human hepatic manifestations of RVF closely therefore serve as appropriate models for the study of RVF pathogenesis in the context of the liver.

The only immunocompetent mouse strain to display a divergent manifestation to hepatitis is the BALB/c mouse model. Upon challenge with WT RVFV, BALB/c mice display a split phenotype with some mice succumbing early of hepatic disease while others progress quickly on to CNS disease (96-98). Until the completion of my dissertation, the BALB/c model was the only murine model that developed encephalitis following RVFV infection via a clinically relevant peripheral exposure route. This murine model of encephalitis has aided in the study of RVF pathogenesis, however, working in a split phenotype model has challenges. Due to its inconsistent phenotype and early progression to encephalitis, the BALB/c model has limitations for the study of RVF encephalitic disease or for the assessment of therapeutics to treat RVF CNS disease.

An alternative for the study of encephalitis in murine models has been to administer virus directly into the nose or via aerosol (78, 91, 99, 100). Recent studies in BALB/c mice have found that the development of RVF neurological disease is faster and more severe upon aerosol challenge (78, 99). Although these models offer increased resources for the study of RVF encephalitis, they do not model the natural route of infection. Thus, a murine model of consistent encephalitis following peripheral RVFV exposure would be valuable to the field.

RVFV encephalitis has been observed in immunodeficient mice following peripheral challenge with attenuated virus (delNSs – RVFV lacking the NSs protein). μMT mice lacking B-cells were shown to only develop lethal encephalitis $1/10^{th}$ of the time using an attenuated RVFV strain (delNSs) inoculated SC (101). Additionally, mice with various defects in cellular immunity developed late-onset encephalitis following delNSs infection of different frequencies, but in no case was the phenotype 100% penetrant (101-103). Immunodeficient mice have also been useful

models for studying viral dissemination using a tagged attenuated RVFV. Non-pathogenic in immunocompetent mice, attenuated and tagged versions of RVFV can be used in immunodeficient IFNAR KO mice to investigate tissue and cell tropism as well as to track virus over time through the course of hepatic infection. Although these models provide a clinically relevant exposure route and insights into the requirements of innate and adaptive immunity, they have drawbacks for the study of pathogenesis as they are lacking an intact immune system.

In conclusion, mice are excellent models to study pathogenesis of RVF as they mimic multiple forms of human RVF disease, most importantly hepatitis. They are also the most convenient rodent to use for the assessment of therapeutics and vaccines due to their price, ease of handling, and reagents available. Murine models are extremely useful for the study of host genetics and immunity as well as high-throughput pre-clinical evaluation of vaccines and therapeutics. The main drawbacks to using murine models are the lack of consistent models of encephalitis, retinitis, and hemorrhagic fever outcomes. Additionally, all murine models are overwhelmingly lethal unlike human RVFV disease.

1.7 Rift Valley Fever Virus Vaccines

Although the history of RVF vaccine research is almost as old as the discovery of RVFV, there are currently no licensed commercial vaccines available for use in humans. All vaccines currently in use today in both humans and animals are made using virus isolated from early outbreaks ranging from 1948 to 1977 (104). Fortunately, RVFV does not contain significant heterogeneity among circulating strains (105). The lack of viral serotypes greatly increases the

chance of developing a vaccine that could both protect from any RVFV strain infection and could offer lasting protection over a human lifetime.

The first developed RVFV vaccine was the formalin inactivated NDBR103. This vaccine was developed from the Entebbe strain of RVFV through hundreds of passages in mice then subsequently in green monkey kidney cells (106) This vaccine strain was used for human vaccination in 1997 of volunteers and UN soldiers (107). Although this vaccine was found to elicit neutralizing antibodies, it took a course of three vaccinations followed by a booster dose (107). This resulted in a vaccine that was both expensive and required repeated immunizations. These represent major obstacles to use in resource-limited settings.

One of the oldest RVF vaccines is the Smithburn live-attenuated vaccine. This vaccine has been the most widely used vaccine throughout Africa. Isolated from a mosquito in Uganda in 1944, the vaccine strain was developed in South Africa through serial passage in various animals then, since 1971, propagation in BHK-21 cells. This vaccine has been given to livestock in multiple African countries including South Africa, Kenya, and Egypt, as well as in Saudi Arabia. The popularity of this vaccine for the protection of livestock has been due to its low cost and extreme potency. However, the Smithburn vaccine does have disadvantages which include residual pathogenicity, fetal deformities, sudden-onset abortions, and reversion to virulence (107, 108). Due to these risks, the vaccine has been relegated to use in only non-pregnant animals in RVF-endemic countries, excluding Egypt (109, 110)

MP-12 is another live-attenuated RVFV strain which was produced by the U.S. Army Medical Research Institute of Infectious Diseases (USAMRIID) from the repeated passage of the WT RVFV ZH548 strain (111-113). This passaging was done in the presence of the mutagen 5-fluorouracil, making it both temperature sensitive and carrying redundant mutations in all three

gene segments (111-113). When MP-12 was initially assessed in livestock few side effects were noted (109). However, farmers have reported low levels of MP-12 vaccination-induced spontaneous abortion in pregnant animals, specifically when the vaccine was administered early in pregnancy (109, 114). Despite this, MP-12 has been shown to be effective at preventing RVF disease and was shown to be safe in humans when it was given to more than 100 healthy volunteers (115, 116). The longevity of the protection (i.e., neutralizing antibody levels) has not yet been established.

As opposed to live-attenuation, the Clone 13 vaccine is a naturally attenuated RVFV strain. Clone 13 contains a natural deletion of 549 nucleotides in the NSs gene (the main virulence factor of RVFV). This vaccine strain was plaque-isolated from an immunocompetent patient in the Central African Republic (116, 117). Similar in potency to the Smithburn vaccine, Clone 13 is also highly safe for it has not been shown to cause abortions or teratogenicity in pregnant animals (118). However, if given in too high of a dose in the first trimester of pregnancy, Clone 13 can lead to fetal defects and even stillbirth due to its ability to cross the placenta (119). A primary disadvantage of this vaccine is also its inability to produce a long-term immune response in animals, however, it has been licensed in some countries in Africa (107).

In 2019, the Coalition for Epidemic Preparedness Innovations (CEPI) released a call for development of a RVFV vaccine for use in humans. CEPI has chosen to prioritize soliciting a RVFV vaccine due to RVFV's inclusion on the World Health Organization's list of priority pathogens. CEPI has stated that they chose to invest in RVFV vaccine development due to its feasibility and the potential for it to greatly impact human health. The many decades of vaccine development, animal model testing, reverse genetics platform development, and licensure for animal use have all laid the groundwork for the successful development of a safe and effective

human RVF vaccine. Currently, two RVF vaccines are in clinical trials for human use while many others are working their way through the phases of preclinical development (120).

1.8 Rift Valley Fever Virus Therapeutics

Most human cases of RVF do not require active treatment. However, for patients that develop severe RVF manifestations there are no specific treatments available other than general supportive care. Several drugs have been tested for their efficacy in treating RVF, with ribavirin and favipiravir having accumulated the most data to date. Developed in the 1980s, the nucleoside analog ribavirin was one of the first drugs tested for efficacy against RVFV. In initial screens it showed promise for it had high efficacy in vitro (121). However, in an aerosol challenge study by Reed et al., ribavirin failed to protect mice (99, 122). Enhanced efficacy was achieved by combination treatment of ribavirin plus immunostimulant poly(ICLC) (99, 122). Intravenous ribavirin treatment was used in the 2000 Saudi Arabia outbreak, however, was reported in a WHO report in 2016 to be ineffective in treating or lessening severity of RVFV (unpublished data). This ribavirin trial in Saudi Arabia was halted due to the apparent increase in neurological manifestations of disease in patients treated with the drug (123).

Favipiravir is a nonnucleoside inhibitor of the influenza A virus (IAV) polymerase that has also been assessed for its effectiveness at inhibiting RVFV. Favipiravir has been shown to effectively work as an antiviral against a wide range of RNA viruses including bunyaviruses. This drug was shown to be more effective than ribavirin at protecting hamsters from lethal RVFV challenge as well as preventing progression to late-onset encephalitis (124, 125). Favipiravir treatment post-RVFV infection was effective at significantly decreasing death even when

administered up to 48 hours post-infection (125). Despite decreasing death, some animals did go on to develop neurological disease when treated with favipiravir. Study of various molecules targeting viral components, host cellular pathways, and autophagy systems have demonstrated some in vitro efficacy against RVFV (126). However, surprisingly few antiviral candidate drugs have been tested in vivo for their effectiveness in treating RVF (127-131).

1.9 Monoclonal Antibodies and Fc effector functions

The lack of effective or even adequate therapeutics for severe RVF disease underscores the importance of efforts to develop novel therapies. Although monoclonal antibodies (mAbs) currently make up the main class of biotherapeutics, their application for treating viral infections has, until recently, received limited attention. It is now clear that therapeutic mAbs have viable potential for targeting pathogens with advantages including rapid development, high specificity, and low toxicity (132). MAbs have already shown efficacy in the treatment of multiple infectious diseases, with many in clinical development (133). MAb therapies have been successfully developed for post-exposure treatments to Ebola virus (EBOV), human immunodeficiency virus (HIV), and Hepatitis C virus (HCV) (134-136).

MAb therapy is a form of passive immunotherapy that intends to blunt viral infections via direct interaction with the virus or a virally infected cell. MAbs can decrease viral dissemination through mechanisms involving their Fab and Fc fragments. Neutralization is mediated by the Fab region, which directly contacts a viral surface glycoprotein, blocking entry into host cells via either blocking attachment to the host cell, preventing penetration into the host cell membrane, or interfering with viral uncoating within the cell. In addition to neutralization, mAbs provide

protection through a variety of mechanisms via their ability to interact with Fc gamma receptors (FcγRs) on innate immune cells. MAbs bind FcγRs through their Fc domain to mediate functions, including antibody-dependent cellular cytotoxicity (ADCC), antibody-dependent cellular phagocytosis (ADCP), and complement-dependent cytotoxicity (CDC) (137, 138). Multiple innate immune cells can perform ADCC including monocytes, macrophages, neutrophils, and NK cells. ADCC involves the release of cytotoxic granules, which results in the direct killing of infected cells. ADCP, otherwise called opsonophagocytosis, is the uptake by phagocytic cells of virally infected cells coated by antibody or antibody-virus complexes. Cells capable of performing ADCP include monocytes, macrophages, neutrophils, DCs, and eosinophils. After phagocytic uptake, immune complexes and infected cells are cleared by trafficking these complexes to lysosomes for degradation. This process also results in the increase in antigen processing and presentation on Major Histocompatibility Complex (MHC) molecules on the innate immune cell's surface. In addition to ADCC and ADCP, antibodies can induce complement activation. The complement cascade contributes to viral elimination via both direct (complement-dependent cytotoxicity) and indirect (phagocytic clearance of complement-coated targets) means.

The essential role of Fc-mediated immune effector functions in providing protection from viral disease has been reported for Ebola virus (EBOV), human immunodeficiency virus (HIV), IAV, chikungunya virus (CHIKV) and others (139-144). The induction of ADCC has been shown to be a critical component of immunity to both HIV and influenza virus (145-147). ADCP has been shown to be of major importance in the protection against many viruses including influenza, WNV, and HIV (148-150). Finally, complement has been shown to have a protective role during viral infections including WNV, CMV, and HIV (149, 151, 152).

1.10 Monoclonal Antibodies as a potential Rift Valley Fever Virus Therapeutic

RVFV displays two surface glycoproteins, Gn and Gc, as highly ordered heterodimers and has icosahedral symmetry with a T12 triangulation number (153, 154). The icosahedral lattice is made up of 110 hexameric and 12 pentameric capsomers – in total 720 Gn/Gc heterodimers. Gn comprises the spike of the capsomers with Gc laying underneath partially occluded. This Gn/Gc complex mediates viral entry and fusion in permissive cells. Recently, Gn has been shown to directly bind the newly identified RVFV receptor LRP-1 (26). Inhibition of the Gn/LRP-1 interaction resulted in blocked RVFV entry into target cells (26). This confirms that Gn plays a key role in the infection process by physically binding the RVFV receptor and initiating cellular entry. To date, a crystal structure of Gn/LRP-1 has not been achieved therefore the exact Gn epitope(s) required for LRP-1 binding have not been determined. Gc on the other hand plays a key role in the fusion process displaying typical structural characteristics of a class II fusion protein (155). With Gn and Gc making up the two major antigenic components on the viral surface and playing such key roles in RVFV infection it is not surprising that they are the targets of neutralizing antibodies (156).

Natural infection with RVFV results in the production of antibodies against Gn, Gc, and N RVFV proteins. Recent RVF vaccine studies demonstrated that antibodies play a major role in mediating protection from RVFV infection (107). Vaccines targeting one or both major antigenic RVFV components, the Gn and Gc glycoproteins, have been shown to induce strong humoral responses in animals (157). Mice treated with attenuated RVFV showed strong neutralizing antibody responses which correlate with increased survival after WT RVFV challenge (101, 120, 158-160). Humoral immunity alone has been shown to be protective in historical passive antibody administration studies (161). Protection against RVFV infection has long been associated with the

induction of neutralizing mAbs, directed against Gn and/or Gc (101, 162, 163). However, protection can be elicited through other mechanisms. Mice vaccinated with the immunodominant N protein, for example, demonstrated partial protection from RVFV challenge despite the absence of neutralizing mAbs (164, 165). Non-neutralizing mAbs have also been shown to improve protection through cooperative effects (166). Taken together, vaccine studies echo the results of previous passive transfer experiments demonstrating that RVFV protection can be conferred by antibodies alone (162, 167). Together, these data suggest the potential use of mAbs as an RVF biotherapeutic or prophylaxis.

Select studies have investigated the use of anti-RVFV mAbs as a potential therapeutic. To date, RVFV mAb research has focused on the development and evaluation of neutralizing mAbs. This is likely due to their ease of identification (by classical in vitro neutralization assays) and the long-held belief that the hallmark of an antibody's protective potential is its ability to directly neutralize virus. Rabbit, human, monkey, and mouse mAbs directed against the two RVFV glycoproteins—Gn and Gc—have been recently developed and demonstrated protective efficacy in mice (166, 168-171). Gn- and Gc-neutralizing mAbs have demonstrated protection in vivo by blocking attachment, entry, or fusion of RVFV (168-171). The RVFV Gn protein is made up of A, B, and beta domains. Domain B, which is the most outward facing, has been suggested as an immunodominant region of Gn. To date, studies on neutralizing anti-RVFV mAbs have mapped protective mAbs to the most membrane distal apex region of domain B (168). Additional work has identified domain A as a hot spot for highly neutralizing mAb binding (169, 171). Protective epitopes being present in both domains A and B, both outward face and farthest from the viral envelope, imply that the entire outward facing surface of Gn can be targeted by mAbs to elicit in vivo protection. Recent increased understanding of the importance of Fc-mediated functions in the

protection against viruses such as EBOV, IAV, and CHIKV implies the potential for Fc effector functions to be an essential component of mAb-mediated protection from RVFV, a role that has yet to be investigated. Understanding the contribution of antibody effector functions is essential to optimizing the development of an effective antibody therapeutic.

2.0 Rift Valley Fever Virus Is Lethal in Different Inbred Mouse Strains Independent of Sex

Rift Valley fever virus (RVFV) is a zoonotic arbovirus affecting humans and livestock in Africa and the Arabian Peninsula. The majority of human cases are mild and self-limiting; however, severe cases can result in hepatitis, encephalitis, or hemorrhagic fever. There is a lack of immunocompetent mouse models that faithfully recapitulate the varied clinical outcomes of RVF in humans. However, there are easily accessible and commonly used inbred mouse strains that have never been challenged with wild-type RVFV. Here, RVFV susceptibility and pathogenesis were evaluated across five commonly used inbred laboratory mouse strains: C57BL/6J, 129S1/SvlmJ, NOD/ShiLtJ, A/J, and NZO/HILtJ. Comparisons between different mouse strains, challenge doses, and sexes revealed exquisite susceptibility to wild-type RVFV in an almost uniform manner. Never before challenged NOD/ShiLtJ, A/J, and NZO/HILtJ mice showed similar phenotypes of Rift Valley fever disease as previously tested inbred mouse strains. The majority of infected mice died or were euthanized by day 5 post-infection due to overwhelming hepatic disease as evidenced by gross liver pathology and high viral RNA loads in the liver. Mice surviving past day 6 across all strains succumbed to late-onset encephalitis. Remarkably, sex was not found to impact survival or viral load and showed only modest effect on time to death and weight loss for any of the challenged mouse strains following RVFV infection. Regardless of sex, these inbred mouse strains displayed extreme susceptibility to wild-type RVFV down to one virus particle. Data presented in this chapter have been previously published in Frontiers in Microbiology. Manuscript information: Cartwright HN, Barbeau DJ, McElroy AK. Rift Valley Fever Virus Is Lethal in Different Inbred Mouse Strains Independent of Sex. Frontiers in Microbiology 2020; 11 (94).

2.1 Introduction

Rift Valley fever (RVF) is a disease of humans and livestock causing severe economic and human health impacts (123). Outbreaks of veterinary and human RVF occur throughout the Middle East and Africa with serosurveys indicating widespread human infection (15, 172, 173). In people, RVF spans a variety of clinical manifestations, ranging from an acute flu-like illness to a more severe and sometimes lethal form of disease (4). The vast majority of human RVF virus (RVFV) infections result in self-limited febrile illnesses, but 10–20% of identified human cases progress to severe hepatitis, hemorrhagic fever, or encephalitis (5, 6, 174). These large variations in human RVF disease progression and outcome are inadequately represented in the current small animal models. This lack of accurate recapitulation of human disease continues to limit our understanding of RVFV pathogenesis.

Currently, the most faithful recapitulation of human disease is displayed in various non-human primate models (79, 93, 175). However, the use of non-human primate models is not feasible for large-scale or high-throughput studies. To date, all tested inbred mouse models are highly susceptible to wild-type RVFV and nearly all die of severe and early-onset hepatic disease. A major exception to this are BALB/c mice that live longer following infection and are more prone to develop neurological disease (96-99). On the other side of the spectrum exist the highly susceptible MBT and C57BL/6J mice that exhibit 100% mortality in 3–4 days (95-97). Although these models demonstrate the existence of some variation in RVFV disease outcome in inbred mice, they are still overwhelmingly lethal unlike human RVFV disease. Additionally, they only recapitulate severe hepatitis and inconsistently display late- onset encephalitis. However, the notable differences in survival times and disease skewing between these strains do point to the possibility of identifying mice with additional RVFV phenotypes.

Inbred rats have shown impressive differences in disease susceptibility to RVFV between strains. RVFV infection in rats ranges from extreme lethality in the highly susceptible Wistar-Furth (WF) rat to a complete absence of symptoms or death in subcutaneously infected Lewis rats (86, 88, 90). Distinct clinical outcomes of RVFV infection also exist between inbred rat models, with WF rats dying of acute hepatitis while August-Copenhagen-Irish (ACI) rats die of a late-onset encephalitic disease (86, 88-90). Interestingly, upon aerosol challenge, Lewis rats display a distinct phenotype, succumbing almost uniformly to encephalitis (91).

Due to these divergent clinical outcomes from RVFV infection in both mice and rats, we deemed it useful to investigate other classically used inbred mouse strains for their susceptibility to and disease manifestations of RVFV. Three out of five of the chosen strains for this study had never been investigated in the context of wild-type RVFV infection and the 129S1/SvlmJ strain had only briefly been studied(96). Using the C57BL/6J mouse genome as a reference, the other four selected inbred mouse strains (129S1/SvlmJ, NOD/ShiLtJ, A/J, and NZO/ HILtJ) vary at 4 million single nucleotide polymorphisms (SNPs) (176). Due to this existing genetic variability between strains, these inbred mouse strains have been able to capture a range of human disease manifestations for other viral infections. Leist et al. discovered highly variable disease phenotypes, including survival, body weight, and viral load, across investigated mouse strains with even inbred strains showing clear divergence in their susceptibility to H3N2 infection (177). Significant differences in SARS-CoV pathogenesis and disease severity were also found by Gralinski et al. upon challenge of various inbred and outbred mice (178). While this paper found fascinating differences in the outbred mouse resource, they were even able to identify an expansion of SARS-CoV phenotypes within common inbred mouse strains.

The study described here was undertaken to assess the susceptibility of five commonly used inbred laboratory mouse strains to wild-type RVFV. We investigated mouse strain, viral dose, sex, weight loss, and viral load following challenge with the wild-type ZH501 strain of RVFV. This report presents evidence for the overwhelming lethality of wild-type RVFV, down to a single virion, across C57BL/6J, 129S1/SvlmJ, NOD/ShiLtJ, A/J, and NZO/HILtJ inbred mouse strains, independent of sex.

2.2 Results

2.2.1 Survival and clinical observations

Female and male mice of five genetically inbred mouse strains (C57BL/6J, 129S1/SvlmJ, NOD/ShiLtJ, A/J, and NZO/HILtJ) were infected by footpad injection with doses ranging from 0.2 to 2,000 $TCID_{50}$ of the wild-type ZH501 strain of RVFV. Weight was recorded daily over the course of 28 days and mice were euthanized upon meeting predefined euthanasia criteria, as outlined in **Table 3**, or at the end of the 28 days. Results from initial survival studies showed that RVFV was highly lethal in the evaluated inbred mouse strains, even down to an infection dose of 2 $TCID_{50}$ (**Figure 6**). Therefore, challenge doses were limited to 0.2 or 2 $TCID_{50}$ for subsequent experiments comparing all strains.

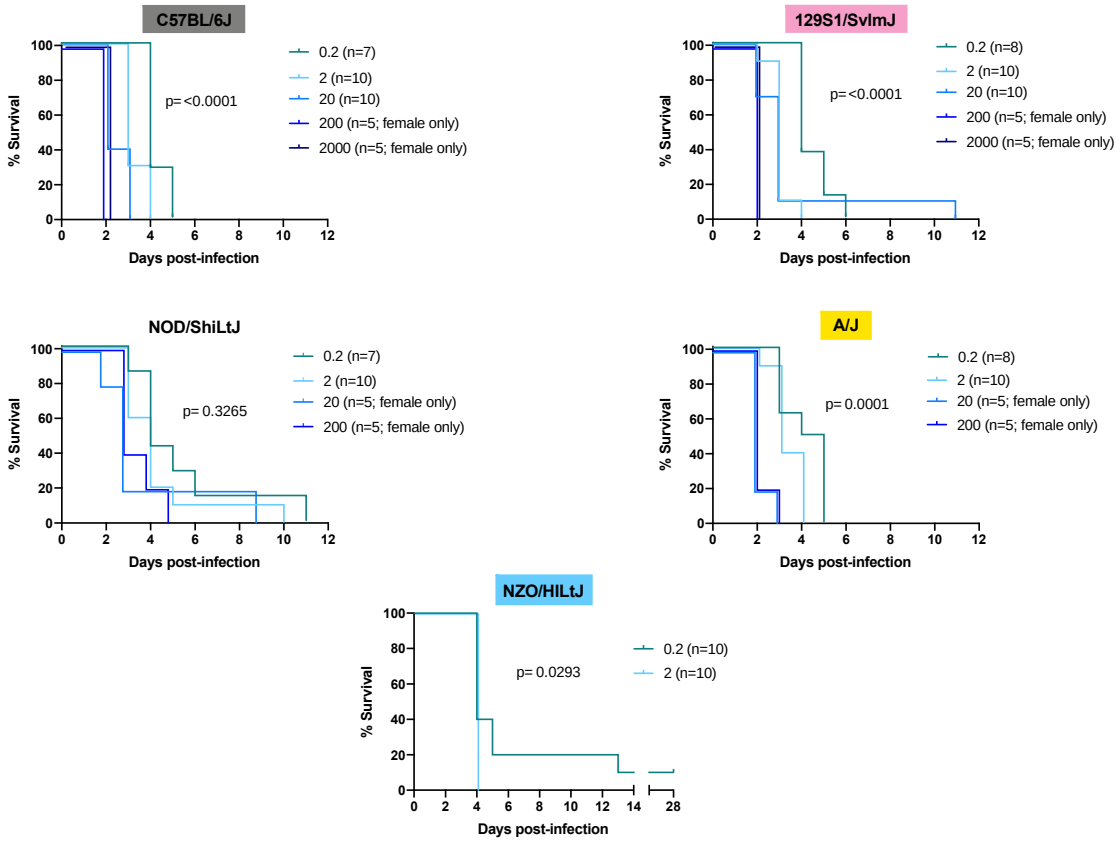

Figure 6 RVFV challenge dose affects time to death in five inbred mouse strains

Survival curves of 5 inbred mouse strains infected via footpad injection with wild-type RVFV at doses of 0.2, 2, 20, 200, 2000 TCID50 show dose-dependent differences in time to death but not survival. Each line represents the percent survival after infection of mice at a given challenge dose. Confirmed uninfected mice from the 0.2 TCID50 dose are excluded from the graphs. Survival statistics were calculated using a log rank (Mantel-Cox) test and P values are marked on all graphs.

At the 0.2 $TCID_{50}$ challenge dose, there were mice that survived to day 28 across all five strains (**Figure 7A**). As would be expected given the probability of delivering a live virus particle to each mouse when administering such a small dose, most of these "survivor" mice at this 0.2 $TCID_{50}$ challenge dose were confirmed to be uninfected by a negative terminal serum ELISA result and negative qRT-PCR of liver, spleen, brain, and testes tissues (**Figure 7B**). These mice were

therefore excluded from subsequent data analysis. The only mouse that lived to the end of the study and was deemed a true survivor was one NZO/HILtJ female mouse. This mouse showed high RVFV-specific terminal serum ELISA titers and detectable tissue viral RNA levels and thus was determined to have been successfully infected at the 0.2 $TCID_{50}$ dose (**Figure 7B**). This mouse was therefore not excluded from subsequent datasets. Apart from this one survivor, all other mice succumbed to RVFV infection from 2,000 $TCID_{50}$ down to the challenge dose of 0.2 $TCID_{50}$ across all five inbred mouse strains (**Figure 6; Figure 8**). These results demonstrate the lethality of RVFV down to a single virion in all five of the tested inbred mouse strains. With an LD_{50} impossible to calculate, to the best we can estimate, the LD_{100} of RVFV for all five of the tested inbred mouse strains is 1 infectious virus particle.

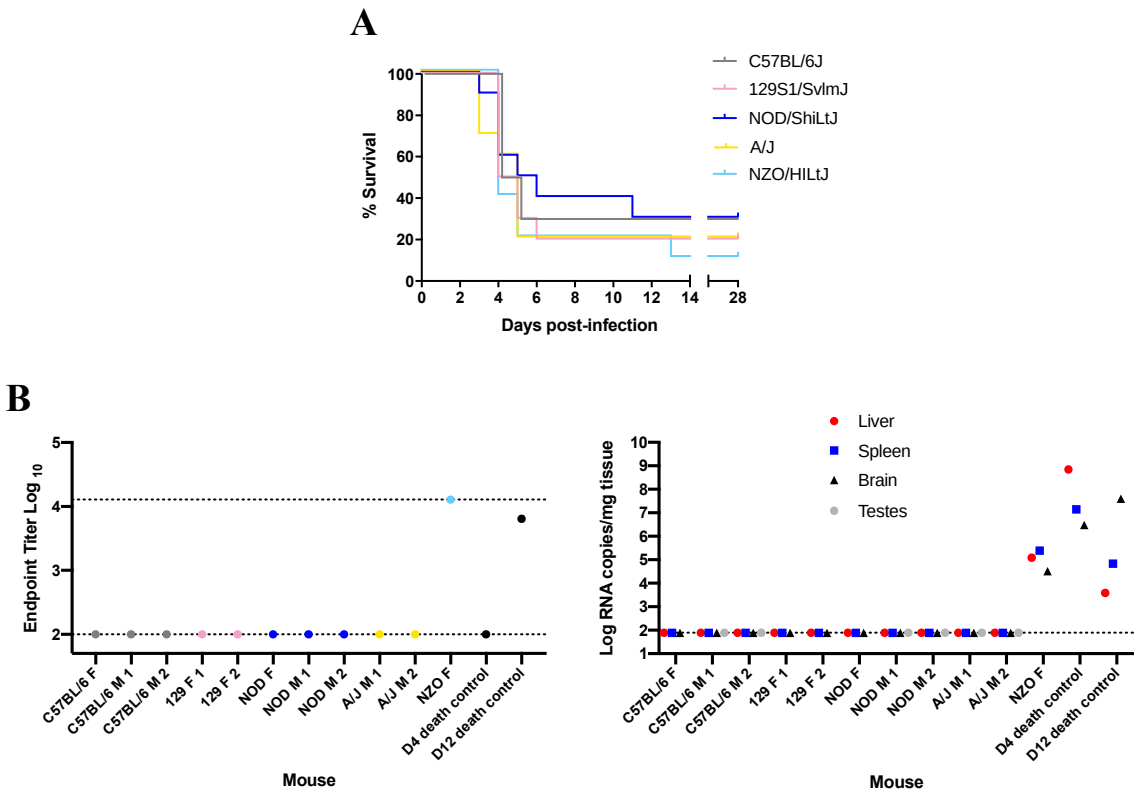

Figure 7 Nearly all "survivor" mice in the 0.2 $TCID_{50}$ challenge group were not infected with RVFV

(A) Survival curve of five inbred mouse strains infected via footpad injection with wild-type RVFV at a dose of 0.2 TCID50 shows "survivor" mice across all five strains. Each line represents the percent survival after infection of five female and five male mice. (B) Enzyme-linked immunosorbent assay (ELISA) and qRT-PCR analysis of "survivor" mice as well as early and late-death 0.2 TCID50-challenged mice as controls. Endpoint RVFV-specific ELISA titer in the serum of mice that survived to day 28 post-infection. Viral load per milligram of tissue in the liver, spleen, brain, and testes of mice that survived to day 28 post-infection was measured by qRT-PCR. The limits of detection for these assays are indicated by dashed lines (ELISA limits of detection due to limited dilutions: lower limit of 100 and upper limit of 12,800; qRT-PCR limit of detection: 77.5 RNA copies/mg).

Log-rank (Mantel-Cox) tests revealed significant differences in the survival curves between challenge dose groups for all strains except for NOD/ShiLtJ mice (**Figure 6; Figure 8A**). All other strains succumbed to RVFV infection in a statistically significant dose-dependent manner

with the 2 $TCID_{50}$ challenge group dying earlier than the 0.2 $TCID_{50}$ challenge group (**Figure 6; Figure 8A**). Across all mouse strains, the median time to death was increased at lower challenge doses. Dose 2 $TCID_{50}$ was the challenge dose that infected 100% of mice while also extending the median time to death by 1 day as compared to higher challenge doses (for example, C57BL/6J mice had a median time to death of 3 days at dose 2 $TCID_{50}$ instead of 2 days at doses 20, 200, and 2,000 $TCID_{50}$). Log-rank (Mantel-Cox) tests resulted in significance between strain survival curves ($p = 0.0022$) at dose 2 $TCID_{50}$ (**Figure 8B**). However, the difference in time to death between strains is minimal as all inbred mouse strains succumb within 5 days of infection (apart from the one NOD/ShiLtJ female who died at day 10; **Figure 8B**). Minimal but statistically significant differences in weight loss were observed between strains (**Figure 8C**). The greatest difference in weight trajectories was the NOD/ShiLt mouse that died of late-onset encephalitis. This mouse lost weight consistently for 4 days, and then exhibited an abrupt increase in weight on the day leading up to its death (**Figure 8C**).

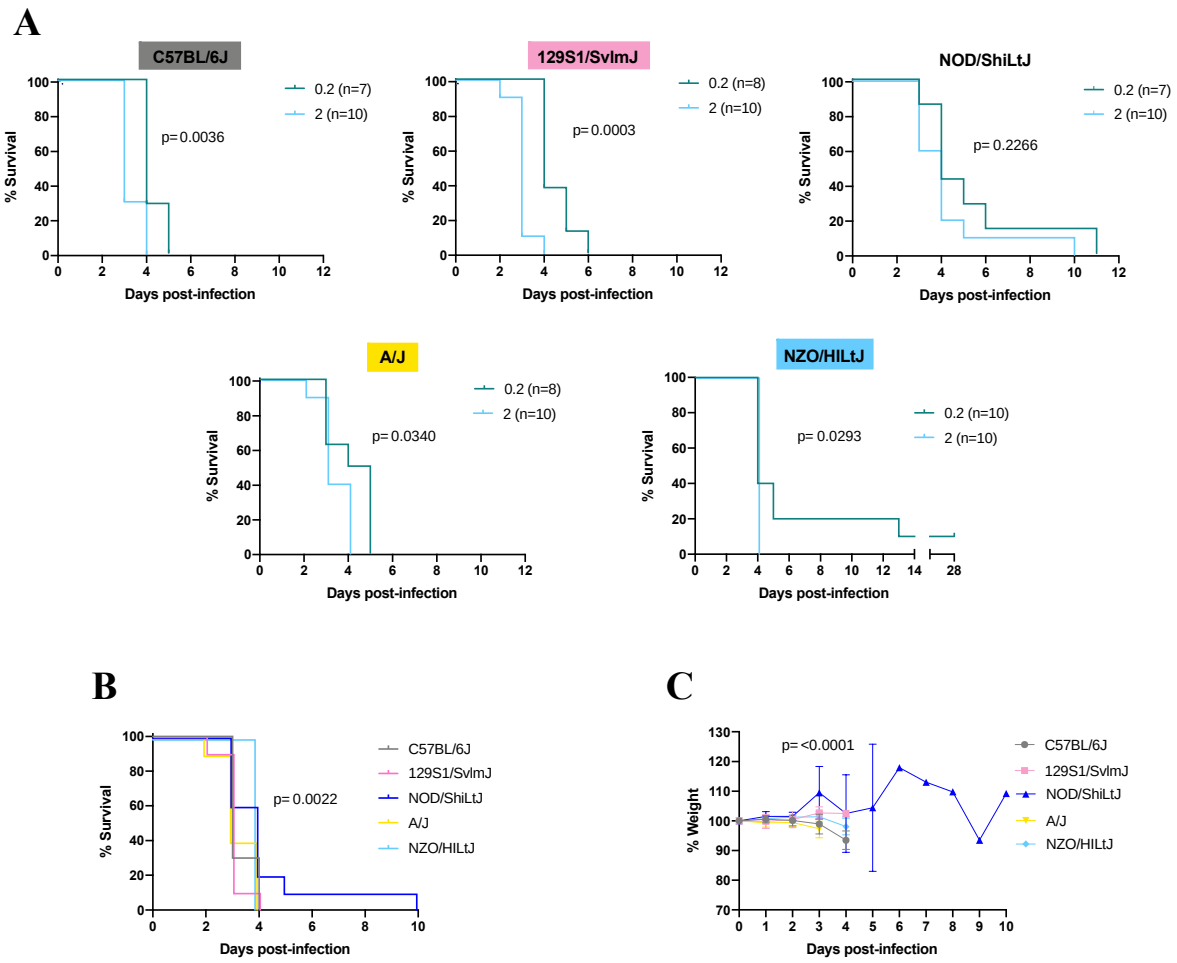

Figure 8 Lethality in five inbred mouse strains following RVFV infection

(A) Survival curves of five inbred mouse strains infected via footpad injection with wild-type RVFV at doses of 0.2 or 2 TCID50 show dose-dependent differences in time to death but not survival. Each line represents the percent survival after infection of female and male mice at a given challenge dose. Confirmed uninfected mice from the 0.2 TCID50 dose are excluded from the graphs. (B) Percent survival of all five inbred mouse strains when infected with 2 TCID50 RVFV. Each line represents the percent survival after infection of five female and five male mice for a given strain. (C) Percent change in mouse daily weight from baseline in all five inbred strains after infection with 2 TCID50 RVFV. Weight loss curves represent five female and five male mice for a given strain. Survival statistics were calculated using a log rank (Mantel-Cox) test and p are marked on all graphs. The mixed-effects model with the Geisser-Greenhouse correction were used for weight loss comparisons between mouse strains over time.

RVFV-induced death across all five inbred mouse strains tested at a dose of 2 $TCID_{50}$ was consistent with severe hepatic disease. This was evidenced by gross liver pathology including hepatic enlargement and pale foci of necrosis as well as virologic data indicating the liver as the key target of RVFV at the time of death. The only exception to this in the 2 $TCID_{50}$ challenge dose was one late-onset NOD/ShiLtJ death. This mouse cleared most virus from its liver and spleen but died at day 10 of late-onset encephalitis as evidenced by clinical symptoms (tremor) and virologic data. Late-onset encephalitis was also seen in the 0.2 and 20 $TCID_{50}$ dose groups and was the reason for euthanasia for all deaths after day 6. Not all mice showed symptoms of disease before death due to the extremely fast progression of disease. Symptoms, when present before death, were similar among all five inbred mouse strains. Observed symptoms include hunched posture, ruffled fur, piloerection, huddling behavior, eye squinting, and poor response to stimuli. Mice that succumbed or were euthanized past day 6 post-infection displayed symptoms of encephalitis including hind limb paralysis and tremor.

2.2.2 Sex differences

Males and females of all five strains of mice succumbed equally to RVFV infection with 100% lethality at the dose 2 $TCID_{50}$, regardless of sex. Upon comparing female and male mice within each inbred strain using Log-rank (Mantel-Cox) tests, a significant difference in survival curves was only found for A/J mice, with males dying approximately 1 day later than females (**Figure 9A**). For all other strains (C57BL/6J, 129S1/SvlmJ, NOD/ShiLtJ, and NZO/HILtJ) no significant sex-dependent difference was observed between survival curves (**Figure 9A**). Interestingly, only 129S1/SvlmJ and NOD/ShiLtJ mice displayed even a slight sex-specific significant difference in weight loss while showing no sex-specific difference in time to death

(**Figure 9B**). Paradoxically, 129S1/SvlmJ mice and female NOD/ShiLtJ mice actually gained weight leading up to death (**Figure 9B**). All NOD/ShiLtJ female mice gained weight before death; however, the one mouse that succumbed to late-onset encephalitis in this group gained weight suddenly at day 3 post-infection, and then slowly dropped weight until finally gaining weight on the day leading up to euthanasia at day 10.

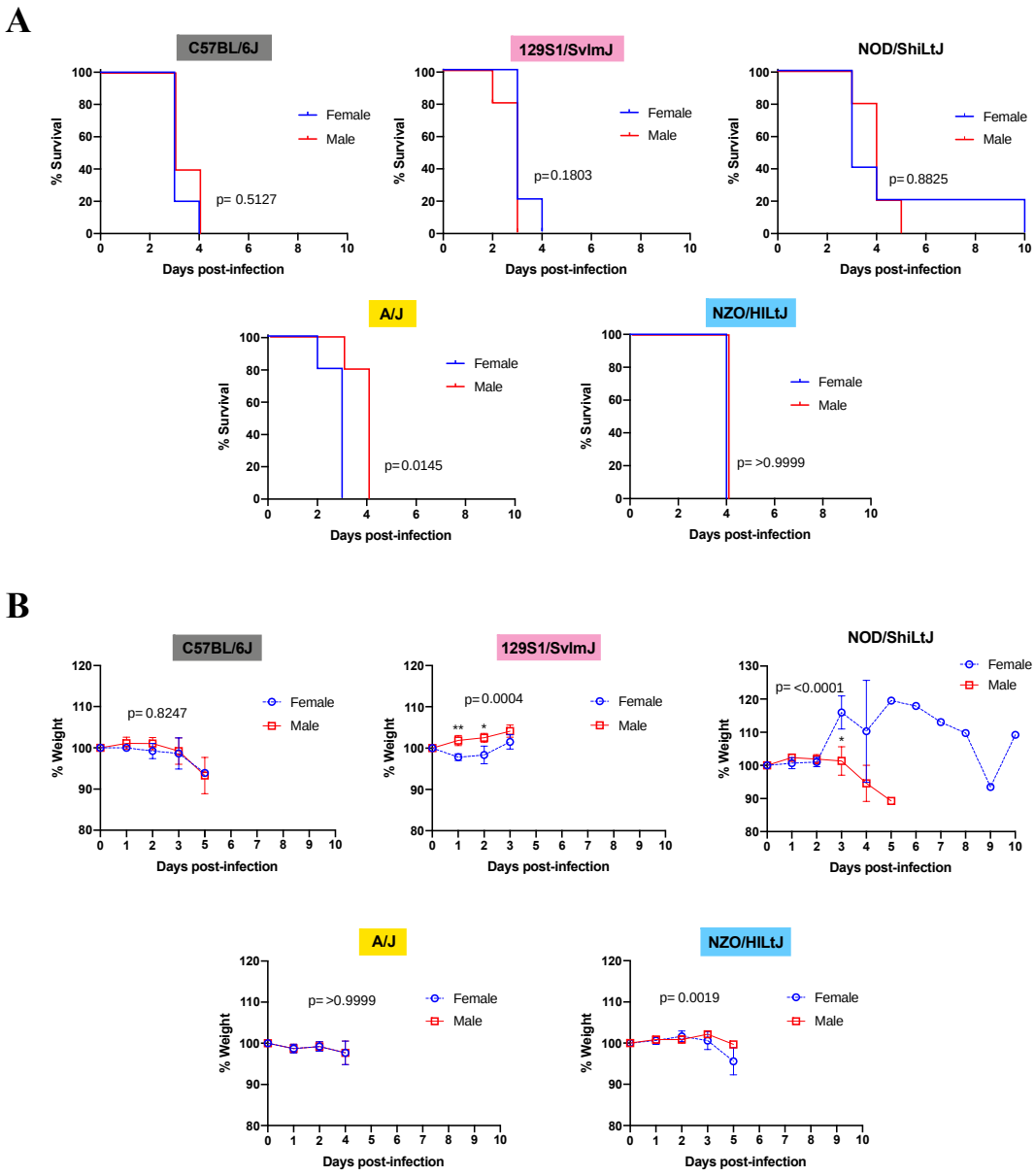

Figure 9 Sex does not impact survival and has only a modest effect on time to death and weight loss in five inbred mouse strains following RVFV infection

(A) Survival curves of five inbred mouse strains infected via footpad injection with 2 TCID50 RVFV show no difference between female and male mice. Each line represents the percent survival after infection of five mice of each sex. (B) Percent change in mouse daily weight from baseline after infection with 2 TCID50 RVFV. Each weight loss line represents five mice. Survival statistics were calculated using a log rank (Mantel-Cox) test and p are marked on all graphs. The mixed-effects model with the Geisser-Greenhouse correction and Bonferroni's multiple comparisons

test were used for weight loss comparisons between sexes and over time for each mouse strain. An asterisk at a particular time point indicates significance ($p \leq 0.05$) in post hoc analysis.

2.2.3 Viral titers

Liver, spleen, and brain tissue samples were harvested from all mice for viral RNA level analysis by qRT-PCR. RVFV challenge dose did not significantly affect the viral RNA levels in the liver, spleen, or brain of mice at the time of death/euthanasia (**Figure 10A**). An assessment of viral load in different tissues as a function of sex or strain was performed using the 2 $TCID_{50}$ dose. This dose was chosen since it uniformly resulted in 100% of the mice being infected. qRT-PCR data are presented as the viral RNA levels in tissues at the time of death for both female and male mice of all five inbred strains (**Figure 10B**). For male mice, testes were collected to investigate any differences in viral RNA load between strains. There were no significant differences in RNA levels in the liver, spleen, or brain when comparing between the five inbred mouse strains either with sexes combined or separate (**Figure 10B**). Although there appeared to be sex-specific trends in liver viral load for C57BL/6J, 129S1/SvlmJ, and A/J mouse strains, none are statistically significant by two-way ANOVA (**Figure 10B**). No significant difference in viral RNA in testes was found between mouse strains when compared using one-way ANOVA. The two low data points that appear on the graph represent the liver and spleen RNA levels from the late-onset NOD/ShiLtJ encephalitis death. The consistency of these RNA load data across both strain and sex are remarkable but logical due to the similarity of disease manifestations and survival timeframes. All strains consistently carry the highest viral load in the liver and the lowest viral load in the brain with the sole exception being the NOD/ShiLtJ mouse that died of encephalitis.

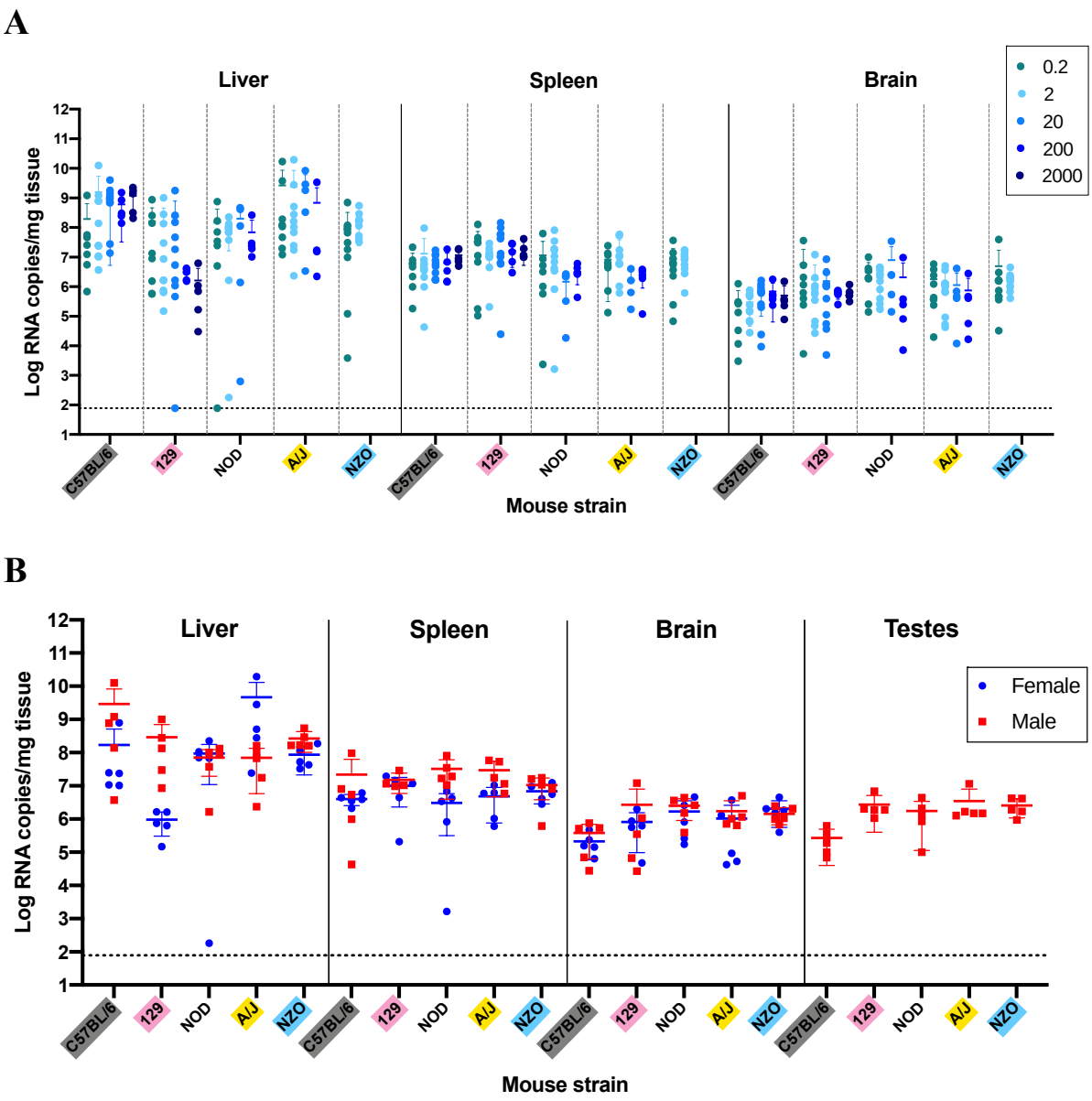

Figure 10 Quantification of viral RNA levels in key tissues of five inbred mouse strains shows no statistically significant dose, sex, or strain differences

(A) Viral load per milligram of tissue in the liver, spleen, and brain of mice at the point of death or euthanasia after RVFV infection at doses of 0.2, 2, 20, 200, and 2,000 TCID50. Confirmed uninfected mice from the 0.2 TCID50 dose are excluded from the graph. (B) Viral load per milligram of tissue in the liver, spleen, brain, and testes of mice that succumbed to infection with 2 TCID50 RVFV was measured by qRT-PCR. A one-way ANOVA was used to compare viral RNA loads within each tissue for each strain across doses. For NZO/HILtJ mice an unpaired t-test was used since

there were only two challenge doses. A two-way ANOVA was used to compare viral RNA loads within each tissue across strains and sex. A one-way ANOVA was used to compare viral RNA loads within the testes across strains. The limit of detection of these assays (77.5 RNA copies/mg) is indicated by a dashed line.

2.3 Discussion

This study evaluated the consequences of RVFV infection in five common inbred laboratory mouse strains: C57BL/6J, 129S1/ SvlmJ, NOD/ShiLtJ, A/J, and NZO/HILtJ. RVFV pathogenicity was studied in these strains with challenge doses ranging from 0.2 to 2,000 $TCID_{50}$. Complete lethality was observed in all five inbred mouse strains down to a dose of 2 $TCID_{50}$. This is consistent with other published studies using different strains of inbred mice (95, 96, 98). It is not possible to infect a mouse with a portion of a virus particle, therefore, mice in the 0.2 $TCID_{50}$ dose group were either infected with 0, 1, or more virus particles depending on the distribution of virions in the 10 $TCID_{50}$/ml dilution stock. Mice in this dose group that "survived" until day 28 and had negative terminal serum ELISA and tissue qRT-PCR were determined to have not been infected. It is interesting to note that these mice were co-housed with sick and dying animals from the same 0.2 $TCID_{50}$ infection group, revealing a lack of RVFV transmission between animals. This is consistent with the reported absence of person-to-person transmission (59). All mice that were successfully infected in the 0.2 $TCID_{50}$ dose group succumbed to disease with the exception of one NZO/HILtJ female mouse that was determined to be a true survivor. From these results, we conclude that one infectious virion is sufficient to cause lethal RVFV disease in C57BL/6J, 129S1/SvlmJ, NOD/ShiLtJ, A/J, and NZO/HILtJ mice.

Throughout the execution of this work consistency in lethality and time to death using a recombinant reverse-genetics generated strain of RVFV was noted. Fully sequence confirmed, early passage recombinant RVFV (rRVFV) strains made through reverse genetics offer far greater reproducibility. This is especially important when evaluating novel mouse strains for their susceptibility to RVFV. Even at a dose of 2 $TCID_{50}$, all mice were successfully infected and time to death was remarkably consistent within each strain. This is likely related to the lack of significant numbers of defective-interfering (DI) particles or viral subpopulations that would accumulate over repeated passaging. In fact, the importance of using recombinant RVFV strains was noted in a recent publication (179). Ikegami et al. found that several genetic lineages of RVFV exhibited differences in virulence in outbred CD1 mice (179). Specific to the ZH501 strain of RVFV, it was found that the ZH501 isolate might contain two distinct viral subpopulations, M847-G and M847-A (160). The two subpopulations were found in a stock of wild-type ZH501 acquired from the CDC, although the authors note that there is no way to determine when the subpopulations arose or if they were present in the infected patient from which the isolate came (160). Infection of mice with the mixture of viral populations was found to be less virulent than the reverse-genetics derived rRVFV M847-A viral variant (160). The increased lethality and reliability obtained by using rRVFV was reflected in our mouse challenge studies.

The inbred mouse strains investigated in this paper were extremely susceptible to RVFV but revealed a significant difference in time to death corresponding to viral dose, with mice challenged at lower doses surviving longer. In this study, the dose of 2 $TCID_{50}$ RVFV was found to be the lowest dose that reliably infects 100% of the tested inbred mice. The 2 $TCID_{50}$ dose was also found to result in the longest median time to death, for C57BL/6J, 129S1/SvlmJ, NOD/ShiLtJ, and A/J mouse strains, as compared to all higher challenge doses. Therefore, this dose allows for

the possibility of dilution errors while still challenging mice with at least one virion of lethal RVFV and extends the survival time by 1 day. Doses higher than 2 $TCID_{50}$ were not used to challenge NZO/HILtJ mice; however, it can be hypothesized that this strain would follow the same trend. The acute hepatic inbred mouse challenge models described in this paper, therefore, permit the reliable administration of a low dose of virus, while also consistently extending the intervention window for post-exposure studies or serial euthanasia. These models could be used alongside the highly established BALB/c mouse model, which is undoubtably a useful model for post-exposure studies due to its longer time to death and greater resiliency to RVFV infection. However, time to death in BALB/c mice is varied as well as their course of disease. Therefore, for the study of RVFV hepatic disease, the presented five inbred mouse models represent a consistent model for pathogenesis and intervention studies.

Interestingly, RVFV challenge dose did not affect viral RNA load in mouse tissues at the time of death or euthanasia. This result is comparable to work performed in rats showing no correlation between the dose of administered virus and the amount of infectious virus (PFU) at the time of death (91). A lower challenge dose of virus could be slower at establishing infection; however, a maximal viral set point is reached by the time of death/euthanasia regardless of challenge dose. Serial sacrifice studies at early time points post-infection would likely reveal initial differences in viral establishment between infection doses.

Mice from all five strains died of disease consistent with severe acute hepatitis, typically within 5 days of infection at a dose of 2 $TCID_{50}$. Clinical symptoms, gross liver pathology, virologic level trends in key tissues, and time to death were all consistent with the acute RVFV hepatic disease phenotype previously described in BALB/c, C57BL/6J, and MBT mouse models (95-98). The only other disease manifestations observed in the infected mice were hind limb

paralysis and tremor in the three mice that died after day 6 in the 0.2 and 2 $TCID_{50}$ dose groups. These mice displayed clear encephalitic disease with viral titers appearing highest in the brain while viral RNA was nearly cleared from all other organs, mirroring RVFV encephalitic presentation in other mouse models (98, 99).

It is known that genetic variability exists between commonly used laboratory inbred mouse strains and that these genetic differences have substantial influence on mouse phenotypes. These genetic differences are also present between the strains used in this study and influence such things as the skewing of C57BL/6J mice toward a Th1 response, the development of polygenic obesity in NZO/HILtJ mice or the predisposition of NOD/ShiLtJ mice to develop type 1 diabetes. However, it is clear that the five inbred mouse strains used in this study do not contain adequate genetic diversity to elicit increased resistance to RVFV infection or a skewing toward different manifestations of RVF disease. The one exception to the universal death caused by RVFV in this study was a female NZO/HILtJ mouse that survived to the end of the study and was determined to have been successfully infected from a dose of 0.2 $TCID_{50}$. Although this mouse did not show symptoms or die by day 28, it is possible that it would have died of late-onset encephalitis if the study had been prolonged. Although not a direct comparison, encephalitis deaths in CD4-depleted inbred mice have been seen as late as 36 days post-infection with ΔNSs RVFV (101). However, it is also distinctly possible that this mouse did survive productive wild-type RVFV infection. It is interesting to note that NZO/ HILtJ mice are the only strain in this study with a fully functional Mx1 locus (human homologue MxA), which has been shown to have antiviral activity against multiple viruses (177, 180-183). However, as only one out of all challenged NZO/HILtJ mice survived, it is clear that Mx1 is not the main host genetic factor responsible for mouse susceptibility to RVFV.

It is widely accepted that sex significantly influences infectious disease pathogenesis and severity across multiple species (184, 185). Males and females of numerous species differ in disease severity to various viral pathogens due to differences in their hormone environments and immune response potentials (186, 187). These sex influences on viral disease severity are complex and thus must be investigated for each individual pathogen. Although in general males are more susceptible to infection by viral pathogens, there are viruses, such as human Papillomavirus and Influenza A virus, that do not follow this rule and are instead higher risk infections in females (184, 188-190). However, little data exist on the importance of sex in the context of RVFV infection in mice. Historic RVFV studies have used both sexes of mice, but few have directly compared females and males in the same study.

In this study, both females and males of the five inbred mouse strains were challenged with the same doses of RVFV. There was no significant difference in survival curves or time to death between female and male mice except for a 1-day difference in time to death for A/J mice. Although weight loss was found to be statistically different between sexes for 129S1/SvlmJ, A/J, and NZO/HILtJ mice, this is not felt to be of clinical importance given the overall lethality. Additionally, viral RNA load in the liver, spleen, and brain was not found to be significantly different when comparing females and males of any of the five inbred mouse strains. This failure to identify any significant sex difference in percent survival or viral burden and the extremely modest influence of sex on time to death and weight loss is qualified by the relatively low number of animals challenged in these studies. Five mice per group are not of sufficient power to conclude a total absence of sex differences in RVFV infection. However, even with small sample sizes, the almost uniform lethality seen in both sexes suggests that it would be a reasonable approach to use only one sex for initial survival studies in future experiments, saving both time and resources. In

the context of vaccine and therapeutic studies, however, it would still be advisable to evaluate both sexes for potential subtle variation in responses that could be revealed with a more highly powered study.

These data differ from that presented by Tokuda et al. who found that sex influenced susceptibility to RVFV in MBT (n = 90) and BALB/c (n = 96) mice as determined by log-rank tests of survival curves (191). The authors found that males were more susceptible to infection than females, concluding that MBT susceptibility is controlled by multiple genes, of which sex is a contributing factor (191). Generally, differences in the amount of influence attributable to sex between ours and other's research could be caused by a variety of factors. These include the mouse strains used, the age of the mice, the RVFV challenge strain, the power of the study, and whether reverse- genetics derived virus or passaged isolate is used for challenge. Additionally, environmental factors between research facilities could affect such things as the mouse microbiome, which has been shown to influence severity of various infectious diseases (192-194).

In summary, C57BL/6J, 129S1/SvlmJ, NOD/ShiLtJ, A/J, and NZO/HILtJ mice are highly susceptible to lethal RVFV infection. In this study, the dose of 2 $TCID_{50}$ wild-type RVFV was found to be the lowest dose that reliably infected 100% of inbred mice tested. All inbred mice that were tested uniformly died of 2 $TCID_{50}$ RVFV challenge, regardless of sex or inbred strain. No substantial differences in disease phenotype or susceptibility were found between the five chosen inbred mouse strains as most died of acute hepatic disease. Therefore, all of these models could be useful for the study of acute lethal hepatitis caused by RVFV. From these studies, it is clear that the five chosen mouse strains do not contain adequate genetic diversity to identify increased resistance to RVFV in mice. Additional studies aimed at assessing mice for divergent RVFV

phenotypes that better recapitulate human disease could focus on mice with additional genetic diversity.

3.0 Host Genetics Modulate Rift Valley Fever Virus Pathogenesis and Disease Outcome

Rift Valley fever (RVF) is an arboviral disease of humans and livestock responsible for severe economic and human health impacts. In humans, RVF spans a variety of clinical manifestations, ranging from an acute flu-like illness to severe forms of disease, including late-onset encephalitis. The large variations in human RVF disease are inadequately represented in current immunocompetent mouse models, which overwhelmingly die of early-onset hepatitis. Existing mouse models of RVF encephalitis are either immunosuppressed, display an inconsistent phenotype, or develop encephalitis only when challenged via intranasal or aerosol exposure. In this study, the genetically defined recombinant inbred mouse resource known as the Collaborative Cross (CC) was used to identify mice with additional RVF disease phenotypes when challenged via a peripheral foot-pad route to mimic mosquito-bite exposure. Wild-type Rift Valley fever virus (RVFV) challenge of 20 CC strains revealed three distinct disease phenotypes: early-onset hepatitis, intermediate phenotype, and late-onset encephalitis. The strain with the most divergent phenotype, which died of late-onset encephalitis at a median of 11 days post-infection, is the first immunocompetent mouse strain to develop consistent encephalitis following peripheral challenge. The encephalitic strain was directly compared to C57BL/6 mice, which uniformly succumb to hepatitis within 2-4 days of infection. Encephalitic disease was characterized by high viral RNA loads in brain tissue, accompanied by clearance of viral RNA from the periphery, low ALT levels, lymphopenia, and neutrophilia. In contrast, C57BL/6 mice succumbed of hepatitis at 3 days post-infection with high viral RNA loads in the liver, viremia, high ALT levels, lymphopenia, and thrombocytopenia. The identification of an encephalitic strain of CC mice as an RVFV model will allow for future investigation into the pathogenesis of RVF encephalitic disease in an

immunocompetent host and indicates that genetic background is the basis for RVF disease variation. Data presented in this chapter are under revision for publication in *PLOS Pathogens* with authors Cartwright HN, Barbeau DJ, Doyle JD, Klein J, Heise MT, Ferris MT, McElroy AK and under the manuscript title: "Host genetics modulate Rift Valley fever virus pathogenesis and disease outcome".

3.1 Introduction

Rift Valley fever virus (RVFV) is a pathogen of both humans and livestock in endemic regions. In humans, Rift Valley fever (RVF) typically manifests as a self-limiting febrile illness. However, in 10-20% of cases people exhibit severe forms of disease including retinitis, hepatitis, hemorrhagic fever, or delayed-onset encephalitis (4-6). Compared to the breadth of clinical outcomes in humans, inbred immunocompetent mouse strains challenged with wild-type (WT) RVFV are uniformly susceptible to infection and overwhelmingly develop a lethal acute hepatitis with occasional BALB/c mice surviving longer to display encephalitic manifestations (94, 98). There are no murine models that develop either hemorrhagic fever, retinitis, or consistent late-onset encephalitis. Pathogenesis and therapeutic studies for RVFV disease manifestations besides hepatitis have therefore been restricted to larger animal models such as non-human primates (NHP). However, NHP models are expensive and impractical for large throughput studies. An alternative for the study of encephalitis in rodent models has been to administer virus directly into the nose or via aerosol, however, this does not represent the natural route of infection (78, 91, 99, 100). Thus, a murine model of encephalitis following peripheral RVFV exposure is needed.

The divergent RVFV clinical manifestations seen in humans have been associated with polymorphisms in innate immune signaling pathway molecules, suggesting that human clinical outcome is shaped by differences in the quality of the innate immune response (75). Interestingly, unlike inbred mice, rats have shown strain specific differences in disease susceptibility to RVFV. Distinct differences in severity of RVFV infection after peripheral challenge exist between Wistar-Furth (WF) and Lewis rats as well as differences in clinical manifestations between the acute hepatic WF rats and the late-onset encephalitic August-Copenhagen-Irish (ACI) rats (88-90). These divergent clinical outcomes from RVFV infection across different rat strains and among humans suggest a genetic basis for disease variation. In the search for novel murine models of RVFV disease, the genetically outbred Collaborative Cross (CC) resource was investigated in this study.

The CC is a genetically defined recombinant mouse resource derived from the systematic interbreeding of 8 founder strains representing 90% of all genetic variation across Mus musculus: 5 classically used inbred mouse strains (A/J, C57BL/6J, 129S1/SvlmJ, NOD/ShiLtJ, NZO/HILtJ) and 3 wild-derived strains (CAST/EiJ, PWK/PhJ, WSB/EiJ) (195, 196). These mouse crosses were then inbred for generations so that the resultant CC mouse strains were >90 percent homozygous and genetically defined while also containing a high level of genetic variation distributed randomly across each strain's genome (176, 197). With numerous mouse strains available for purchase, CC strain selection was based on the likelihood of each strain to exhibit increased resistance to infection. The interferon-induced GTPase, MxA, has been shown to inhibit RVFV replication in vitro, therefore its mouse homologue Mx1 was used as the selection criteria for this study (181). Twenty CC mouse strains that are known to have a functional wild-derived Mx1 locus were selected for challenge with RVFV (180). These 20 CC strains were evaluated for their

susceptibility to RVFV infection and characterized through clinical, virologic, immunologic, hematologic, and metabolic readouts. A direct comparison of C57BL/6 mice and the CC strain that had the most divergent clinical outcome was used to define differences in disease manifestation and progression over time. This report provides the groundwork for the use of the CC in defining the genetic basis of RVF disease phenotype and details the identification of the CC057 strain as a novel immunocompetent murine model of RVFV encephalitis.

3.2 Results

3.2.1 CC genetic diversity drives divergent RVFV disease manifestations

To evaluate RVF disease phenotypes in genetically diverse mouse strains, 20 CC strains were challenged with 2 $TCID_{50}$ of WT ZH501 RVFV via footpad (FP) injection. All mice universally succumbed to this challenge dose, however, strains varied widely in their time to death (**Figure 11A, B**). Three categories of RVF disease outcome were identified based on gross pathology, clinical symptoms, and median time to death: hepatitis, intermediate phenotype, and encephalitis (**Figure 11**). Strains classified as hepatic died early in infection; median of 3-4 days post-infection (dpi), within the timeframe of known inbred mouse models of RVFV hepatitis. These mice had grossly enlarged livers and experienced rapid decline in weight immediately before euthanasia criteria was met (**Figure 11C**). In contrast, strains classified as encephalitic died consistently late in infection; median of 9-11 dpi, showing progressive weight loss late in the disease course preceding euthanasia. Clinical symptoms in the encephalitic strains included lateral eye deviation, circling, ataxia, seizure, and hind limb paralysis. These strains lacked gross liver

pathology at time of death. Finally, strains classified as intermediate phenotype, displayed a gradient of hepatic and encephalitic disease symptoms, and met euthanasia criteria between a median of 5-8 dpi.

These three classifications of RVF disease phenotype were supported by distinct viral RNA load patterns within key tissues. Hepatic-classified mice had the highest viral RNA loads in the liver at the time of death while encephalitic mice died with minimal liver viral RNA titers but high brain viral RNA loads (**Figure 11D**). In addition to having high levels of viral RNA in the liver, hepatic mice were viremic with high viral RNA levels also present in the serum and other tissues (**Figure 11D; Figure 12**). In contrast, mice dying of late-onset encephalitis succumbed to disease despite near clearance of viral RNA from peripheral tissues and the blood. Interestingly, serum viral RNA loads taken early in infection (2 dpi) did not correlate with time to death (least squares regression analysis, alpha=0.05, p=0.9452).

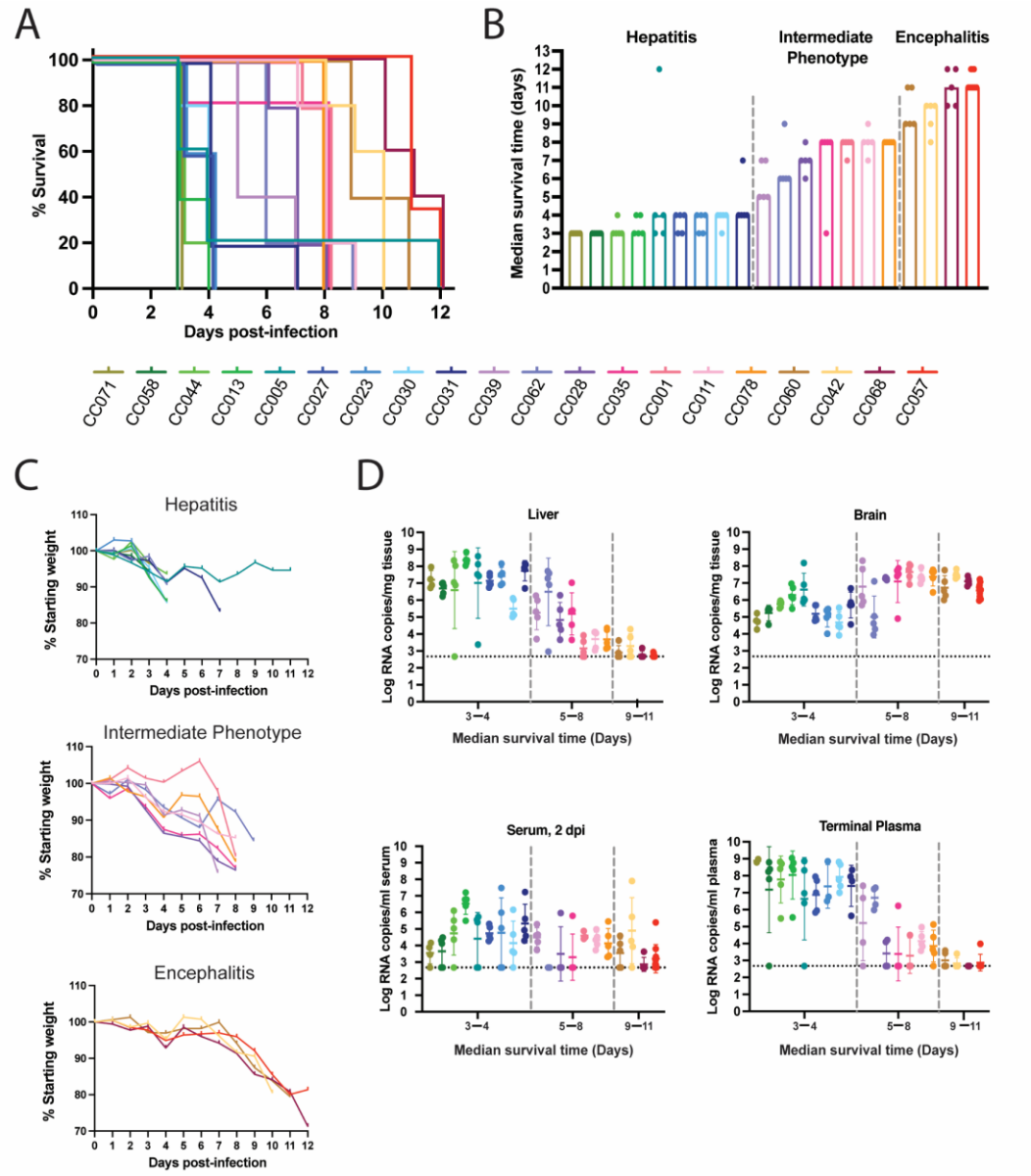

Figure 11 Disease phenotypes identified after RVFV infection in CC strains

(A) Survival curve of CC mouse strains following RVFV challenge. Each line represents 5 female mice apart from CC057 mice (n=9, 5 female and 4 male). (B) Median time to death across CC strains. (C) Mean percent of starting body weight over the course of infection with CC strains split into three categories of disease outcome. (D) qRT-PCR based assessment of viral RNA loads in tissues, serum, and plasma at time of euthanasia. CC strains separated into three categories of disease outcome by two dashed grey lines. Serum and plasma viral loads were assessed if sufficient sample was present (n≤5 per CC strain) with data shown as geometric mean ± geometric SD. LOD of assays noted by dotted horizontal line.

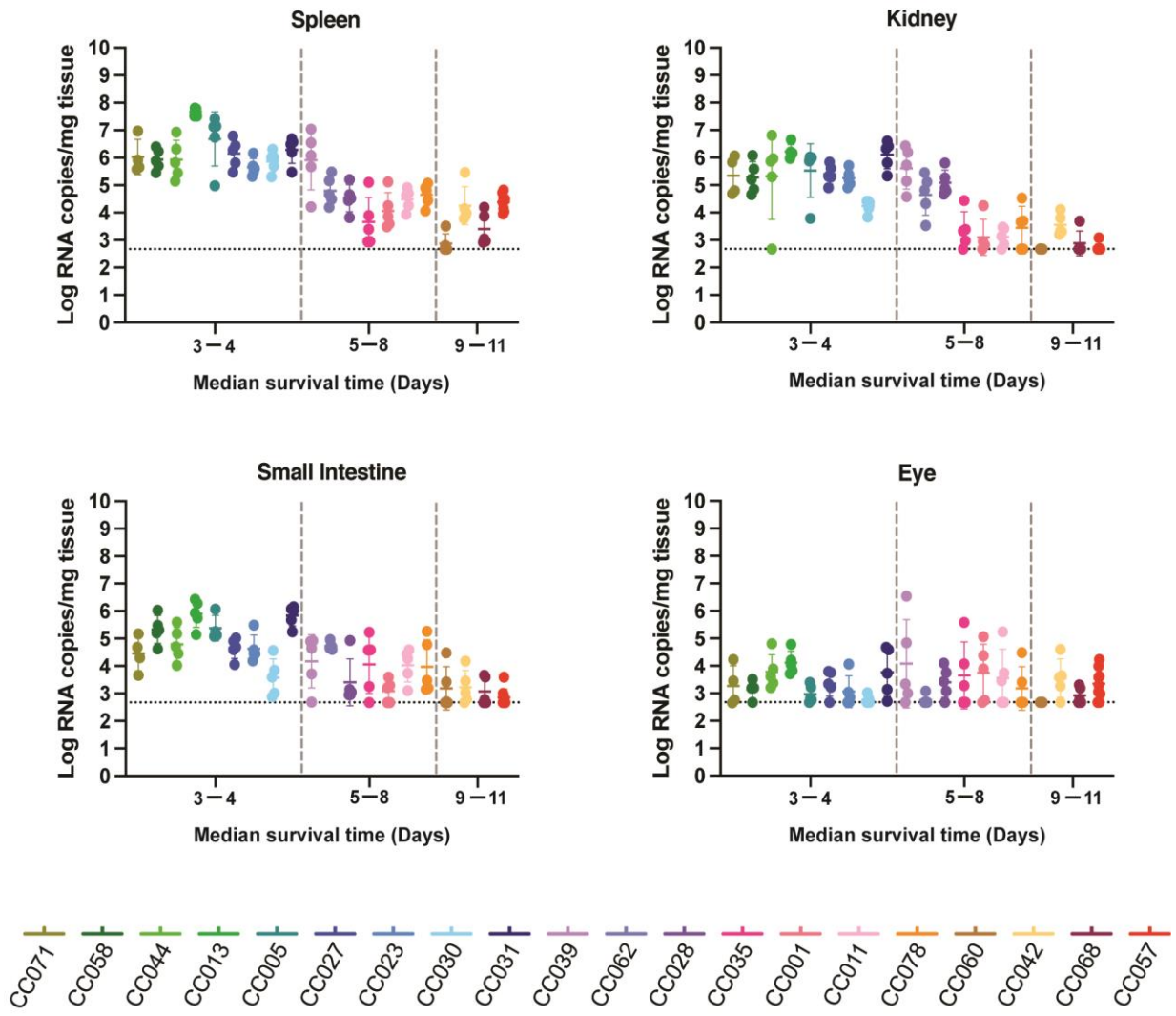

Figure 12 Viral loads across CC strains in other tissues

qRT-PCR based assessment of viral RNA loads in tissues at time of euthanasia. CC strains separated into three categories of disease outcome by two dashed grey lines. Data shown as geometric mean ± geometric SD. LOD of assay noted by dotted horizontal line.

In addition to large differences in viral RNA distribution and load between hepatic and encephalitic mice, these divergent disease phenotypes displayed clinical differences in blood chemistry (CHEM) data at time of death (**Figure 13**). Mice that died early of hepatitis presented with elevated alkaline phosphatase (ALP), alanine aminotransferase (ALT), bile acids, while

encephalitic mice died in the absence of clinical markers of liver involvement. Other serum chemistry markers and complete blood counts (CBC) were not consistently different between the phenotypes (**Figure 13, Figure 14**).

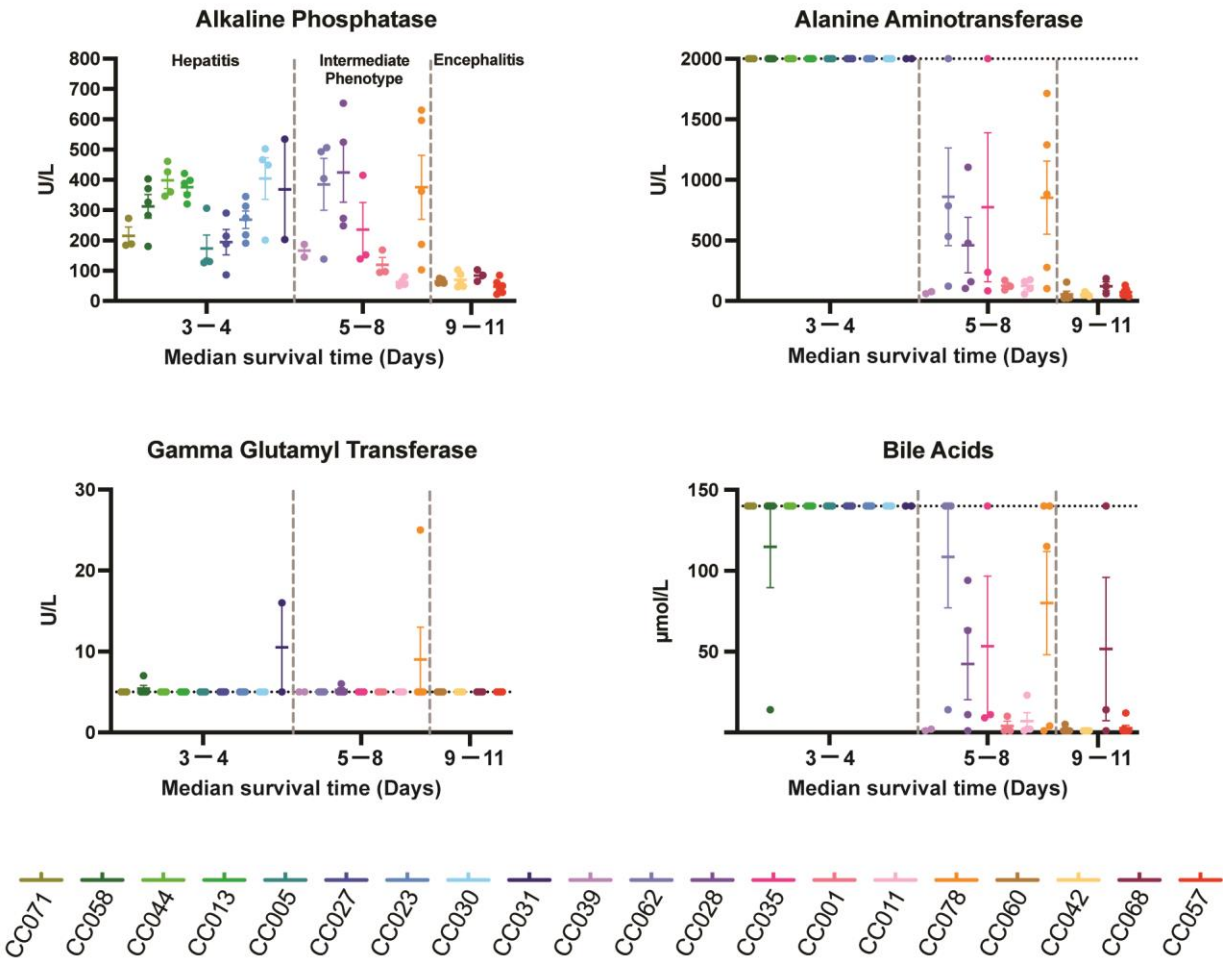

Figure 13 Liver chemistry profiles vary across CC strains according to RVF disease outcome

CC strains separated into three categories of disease outcome by two dashed grey lines. CHEM was run if sufficient sample was present (n≤5 per CC strain). Data shown as mean ± SD. Upper or lower LOD for assays noted by horizontal dotted line. Alanine Aminotransferase upper LOD: 2000 U/L; Gamma Glutamyl Transferase lower LOD: 5 U/L; Bile Acids upper LOD: 140 µmol/L.

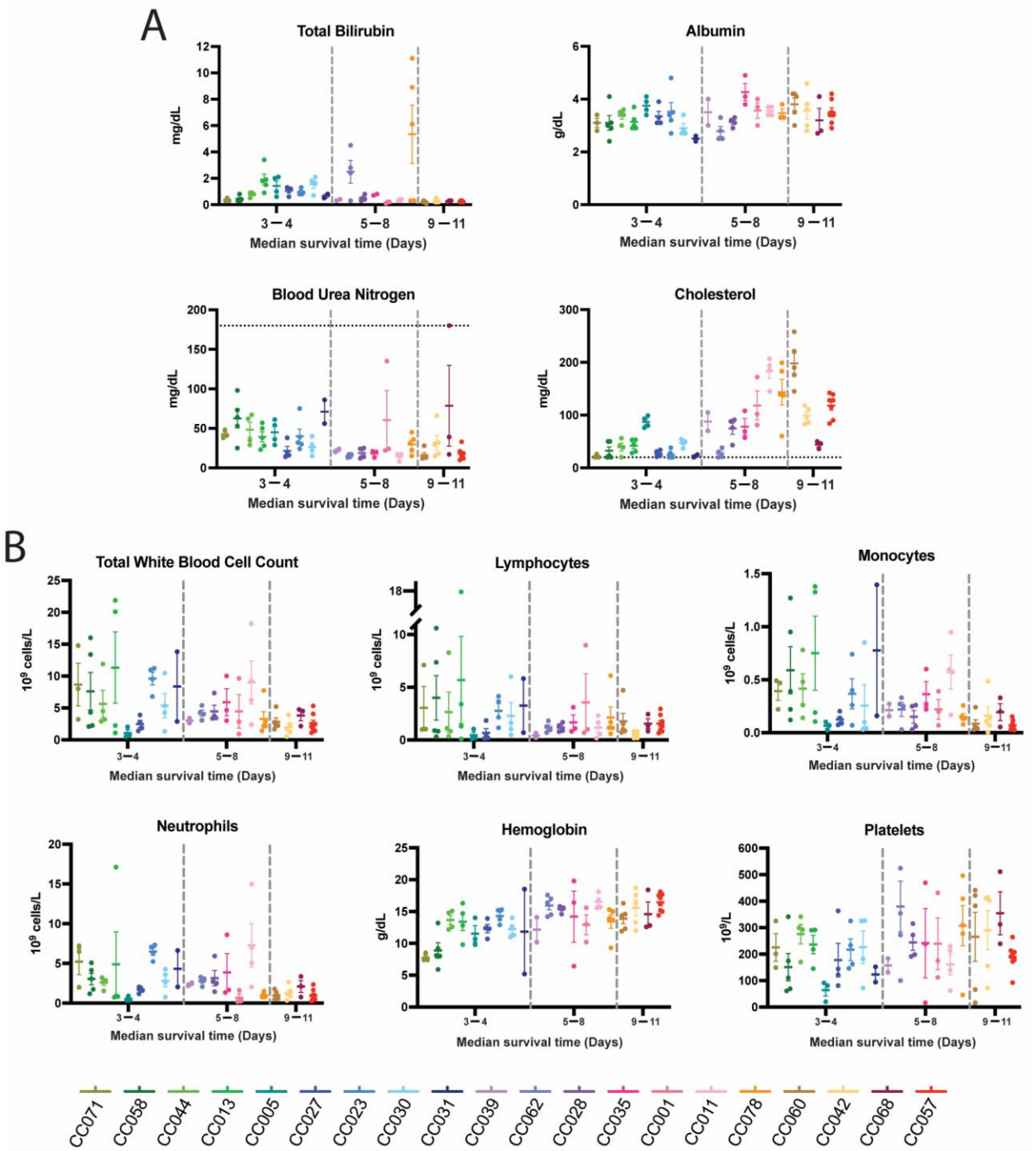

Figure 14 CHEM and CBC profiles vary across CC strains after RVFV infection

CC strains separated into three categories of disease outcome by two dashed grey lines. (A) CHEM and (B) CBC analysis was run if sufficient sample was present (n≤5 per CC strain). Data shown as mean ± SD. Upper or lower LOD for assays noted by horizontal dotted line. Blood Urea Nitrogen upper LOD: 180 mg/dL; Cholesterol lower LOD: 20 mg/dL.

To characterize the humoral response to infection, all mice that succumbed later than 5 dpi were assessed by RVFV-specific enzyme-linked immunosorbent assay (ELISA). Those strains found to be positive for RVFV-specific antibodies were further assessed by focus reduction neutralization test (FRNT). Regardless of CC strain, mice mounted an antibody response starting around 8 dpi (**Figure 15**). Mice that survived longer post-infection had a more robust neutralizing antibody response than those that died earlier. However, even mice with the strongest neutralizing antibody response at their time of death succumbed to RVF encephalitic disease.

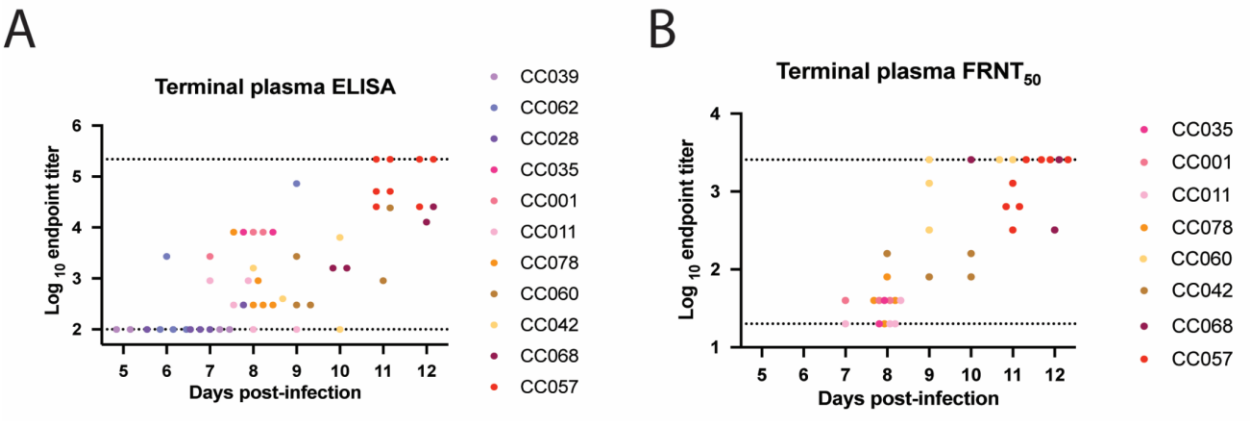

Figure 15 CC strains die of late-onset encephalitis despite the presence of neutralizing antibody levels

(A) ELISA and (B) FRNT of plasma at time of euthanasia after RVFV challenge [n=5/CC strain, except CC057 n=9 (5 female and 4 male)]. Upper and lower LODs for each assay noted by dotted line. ELISA upper LOD: 218,700; ELISA lower LOD: 100; FRNT50 upper LOD: 2,560; FRNT50 lower LOD: 20.

3.2.2 CC057 mice have a unique disease course compared to C57BL/6 mice

From the four CC strains that developed consistent late-onset encephalitic disease, the CC057 strain was selected for additional in-depth studies. The RVFV encephalitic phenotype was found to be sex-independent in the CC057 mouse strain, with both female and male mice displaying nearly identical survival curves and weight loss trends (**Figure 16A, B**). CC057 viral

RNA data revealed uniformity between sexes with viral RNA loads being consistently highest in the brain regardless of sex (**Figure 16C**).

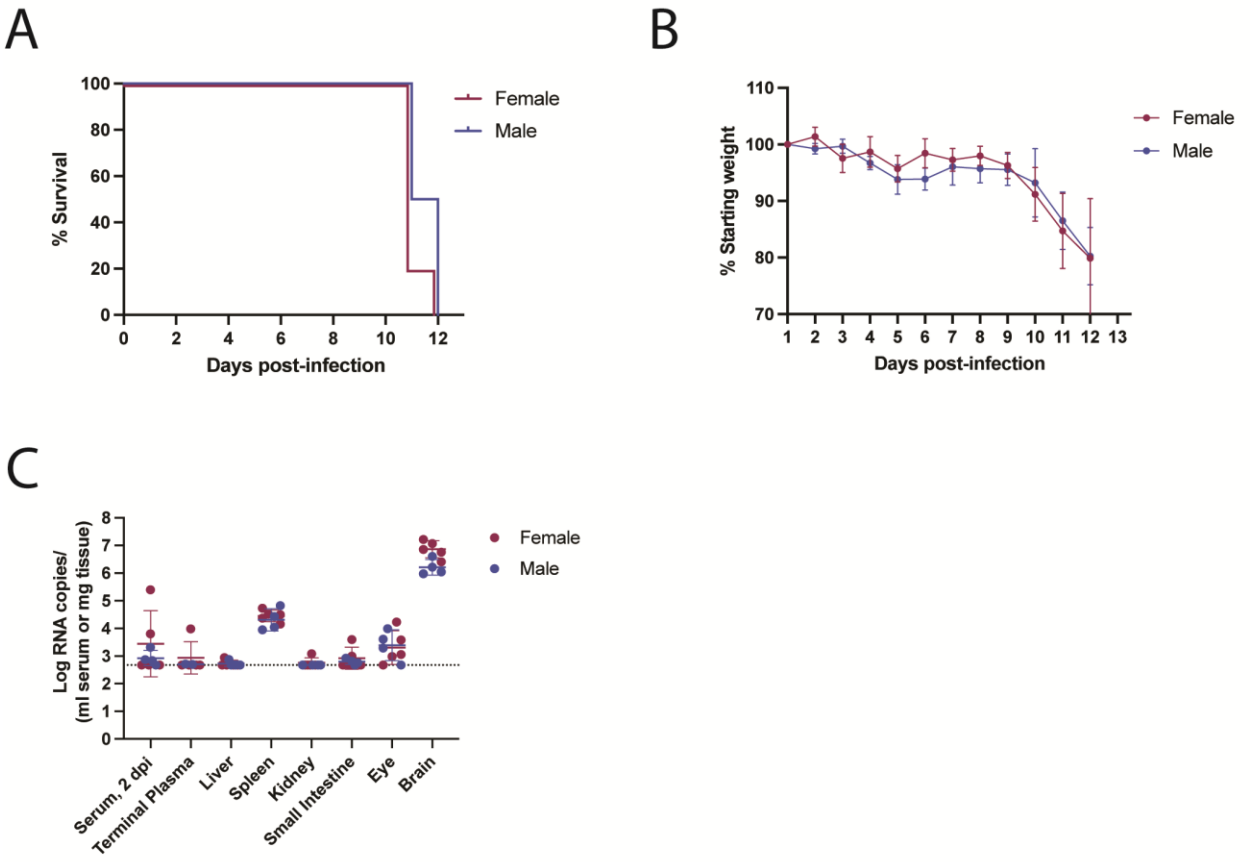

Figure 16 The RVF clinical phenotype in the CC057 mouse strain is not sex-dependent

(A) Survival curve of CC057 mice split by sex (female n=5, male n=4). (B) Percent of starting body weight over the course of infection. Data presented as mean ± SD. (C) qRT-PCR based assessment of viral RNA loads in CC057 mouse tissues, serum, and plasma at time of euthanasia. Data previously presented in Figures 12 and 13, now split by sex. Data shown as geometric mean ± geometric SD. LOD of assay noted by dotted line.

To directly compare hepatic and encephalitic RVF disease progression, the classically used C57BL/6 hepatitis model and the newly identified CC057 encephalitis model were infected with 2 $TCID_{50}$ WT ZH501 RVFV in the left footpad and serially euthanized at various timepoints (**Figure 17A**). At each timepoint, tissue and blood samples were taken to assess virologic,

hematologic, metabolic, histologic, and immunologic readouts. Apart from one viral RNA positive C57BL/6 liver sample at 2 dpi, all other C57BL/6 and CC057 mouse tissues were below the limit of detection (LOD) for viral RNA at 0.5, 1, and 2 dpi (data not shown). In contrast, at 3 dpi, viral RNA titers were present in all sampled tissues in C57BL/6 mice with the highest titers being present in the liver (**Figure 17B**). Viral RNA was also present in various CC057 tissues including the liver, however, C57BL/6 viral RNA titers in the liver, spleen, and brain were significantly higher than those in CC057 mice.

No definitive virus-induced cytopathology was seen in either C57BL/6 or CC057 livers before 3 dpi (data not shown). At 3 dpi, lesions appeared in the livers of all mice; for both C57BL/6 and CC057 mice the most common findings were foci of hepatocellular degeneration and necrosis. These were generally associated with inflammatory, often neutrophilic, infiltrates. Livers varied widely in frequency of necrotic foci, from substantial in C57BL/6 livers to more infrequent focal individual cell degeneration in CC057 livers (**Figure 17C**). Differences in the extent of hepatocellular damage were paralleled by the large difference in viral antigen staining seen by immunohistochemistry (IHC) between the two mouse strains. C57BL/6 mice appropriately had high levels of antigen staining in the liver at 3 dpi (3 of 3 mice) with one mouse staining positive as early as 2 dpi (**Figure 17D**). Contrastingly, at 3 dpi the extent of antigen staining in CC057 livers was considerably lower with only sporadic single hepatocytes staining positive (3 of 3 mice).

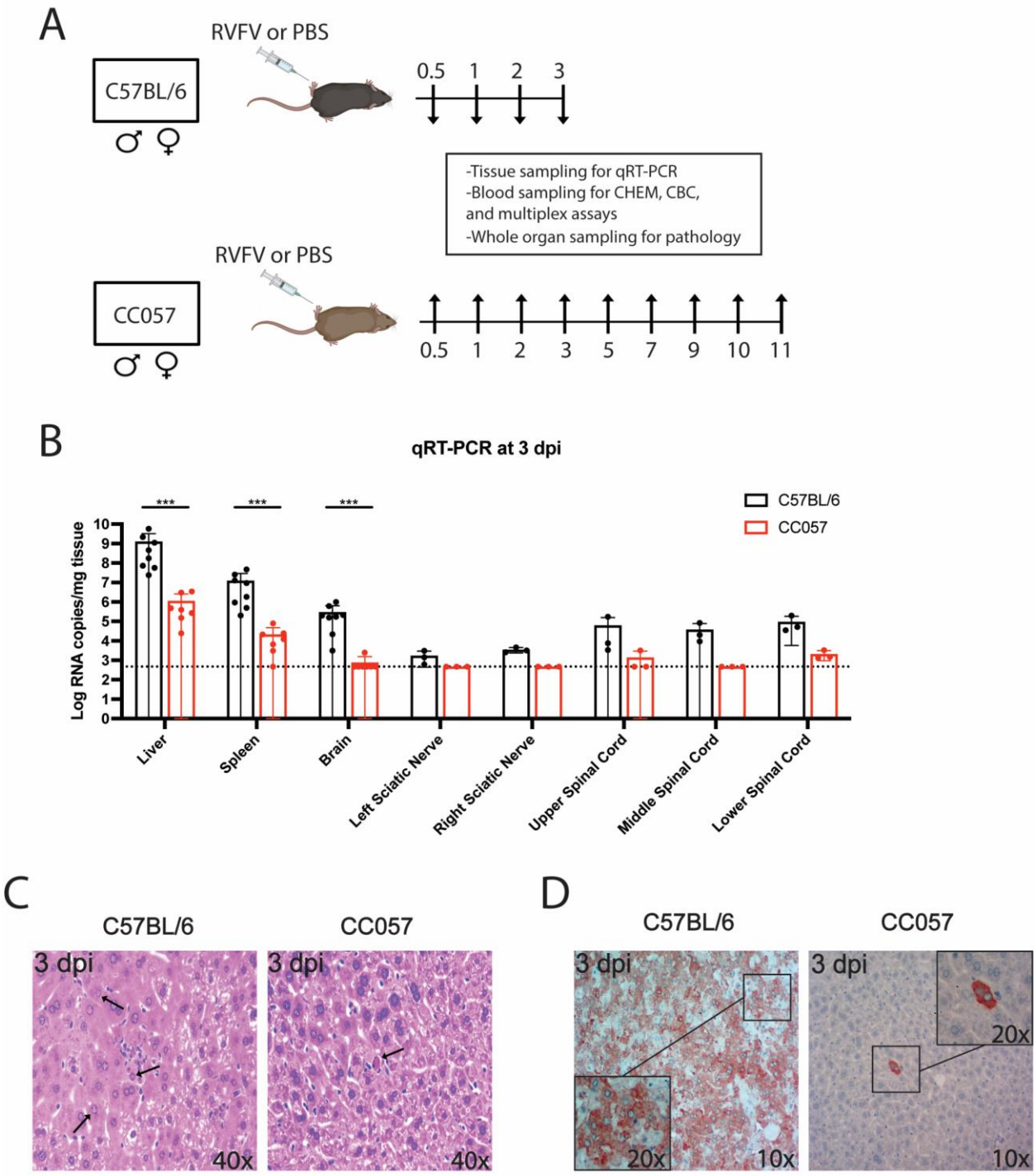

Figure 17 CC057 mice control viral replication and spread in the liver

(A) Experimental design: at each timepoint, tissue and blood samples were taken to assess virologic, immunologic, hematologic, and histologic readouts. (B) qRT-PCR based assessment of viral RNA loads in tissues of C57BL6 and CC057 mice at 3 dpi. Data shown as mean ± SD (n=3-8/tissue type). LOD of assay noted by dotted line. Comparison

of viral RNA load between mouse strains was performed in each tissue by Mann-Whitney (liver p=0.0003; spleen p=0.0003; brain p=0.0003). (C) Representative 3 dpi H&E-stained sections of formalin-fixed paraffin-embedded RVFV-infected livers. Arrows point to intranuclear inclusion bodies (C57BL/6) and focal individual cell degeneration (CC057). (D) IHC of RVFV antigen (brown) in representative 3 dpi sections of formalin-fixed paraffin-embedded livers from RVFV-infected mice.

Serial CBC and CHEM data revealed another critical aspect to the divergence in disease course between hepatic and encephalitic RVF mouse models. Immune cell counts did not vary significantly from baselines in either C57BL/6 or CC057 mice before 3 dpi (**Figure 18A**). At 3 dpi, however, clear differences emerged with C57BL/6 mice alone exhibiting significant leukopenia and lymphopenia. Although some C57BL/6 mice had elevated levels of neutrophils at 3 dpi, CC057 mice displayed significantly higher neutrophilia from baseline at this critical point in infection. Interestingly, only CC057 mice had anemia at 0.5 and 3 dpi while C57BL/6 mice alone exhibited thrombocytopenia. Clinical markers of liver/biliary disfunction, ALT and ALP, were significantly elevated in the hepatic C57BL/6 mouse model at 3 dpi (**Figure 18B**). CHEM data with no physiologically relevant changes from baseline for either C57BL/6 or CC057 mice are included in the supplementary material (**Figure 19**).

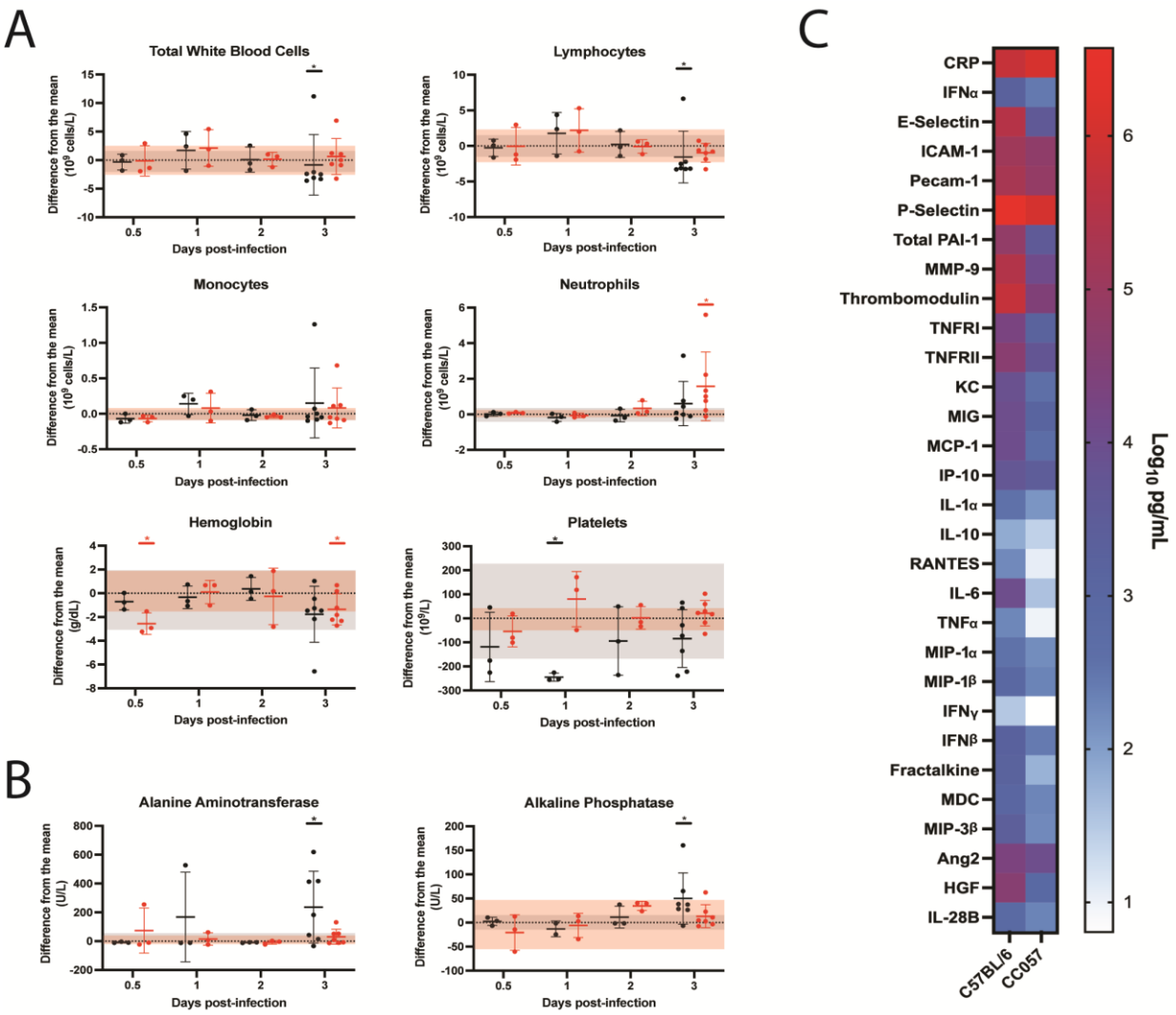

Figure 18 Acute phase blood biomarkers in C57BL/6 versus CC057 mice

(A) CBC and (B) CHEM over time with data presented as a function of difference from the uninfected mean, shown as mean ± SD (n=3-7/time point). Uninfected normal ranges for C57BL/6 and CC057 mice are represented by grey and pink horizontal shading respectively. Comparisons of CBC data were performed at each timepoint by Mann-Whitney to compare RVFV-infected samples to uninfected control samples for each mouse strain separately (Total white blood cells 3 dpi p=0.0164; Lymphocytes 3 dpi p=0.0164; Neutrophils 3 dpi p=0.0098; Hemoglobin 0.5 dpi p=0.0182, 3 dpi p=0.0499; Platelets 1 dpi p=0.0091). Comparisons of CHEM data were performed at each timepoint by Mann-Whitney to compare RVFV-infected samples to uninfected control samples for each mouse strain separately (ALT 3 dpi p=0.0298; ALP 3 dpi p=0.0052). (C) Analyte levels in the plasma at 3dpi. Data shown as the mean (C57BL/6 n=15; CC057 n=3).

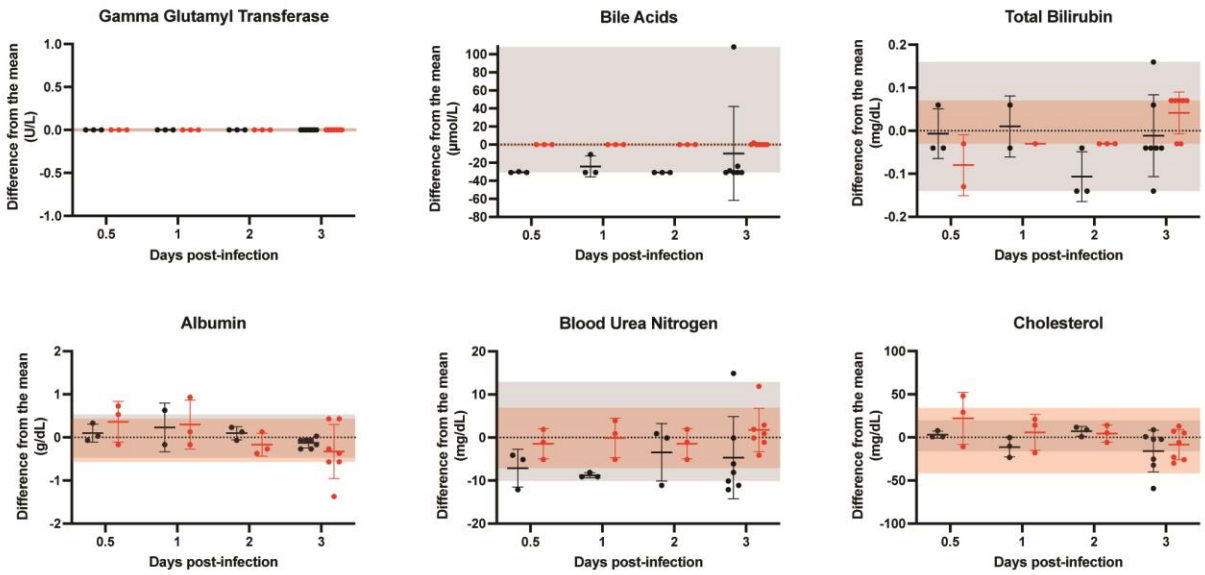

Figure 19 Additional CHEM data presented over the course of disease in C57BL6 and CC057 mice

Data presented as a function of difference from the uninfected mean, shown as mean ± SD (N=3-7/time point). Uninfected normal ranges for C57BL/6 and CC057 mice are represented by grey and pink horizontal bars respectively. Comparisons of CHEM data were performed at each timepoint by Mann-Whitney to compare RVFV-infected samples to uninfected control samples for each mouse strain separately.Data presented as a function of difference from the uninfected mean, shown as mean ± SD (N=3-7/time point). Uninfected normal ranges for C57BL/6 and CC057 mice are represented by grey and pink horizontal bars respectively. Comparisons of CHEM data were performed at each timepoint by Mann-Whitney to compare RVFV-infected samples to uninfected control samples for each mouse strain separately.

To further compare hepatic and encephalitic disease courses, the concentrations of 32 analytes were measured in the plasma of C57BL/6 and CC057 mice over the course of infection using multiplex immune assays. Selected analytes included markers of inflammation and markers of endothelial or barrier function. Baseline levels of 11 analytes were found to be significantly lower in CC057 compared to C57BL/6 mice, suggesting a slightly lower baseline inflammatory environment in the CC057 mouse strain (**Figure 20**). With the goal of identifying early biomarkers

of hepatic versus encephalitic disease outcome, analyte levels at 0.5, 1, and 2 dpi were compared between C57BL/6 and CC057 mice by two-way ANOVA. Unfortunately, of the 32 measured analytes no significant biomarkers of outcome were found at these early timepoints before 3 dpi with 3 mice per strain analyzed per timepoint (data not shown). However, at the critical 3 dpi timepoint when most C57BL/6 mice succumbed to hepatitis, nearly all measured C57BL/6 analyte levels were highly elevated including IL-6 and HGF (**Figure 18C**). To compare analyte levels between C57BL/6 and CC057 mice, data were normalized to their respective uninfected mean (**Table I**). By Mann-Whitney, 21 of 32 analyte levels were significantly higher in C57BL/6 mice as compared to CC057 mice (**Table I**). Multiplex data are not shown for CD40L and IL-9 at 3 dpi due to a lack of data points above the limit of detection for either C57BL/6 or CC057 mice.

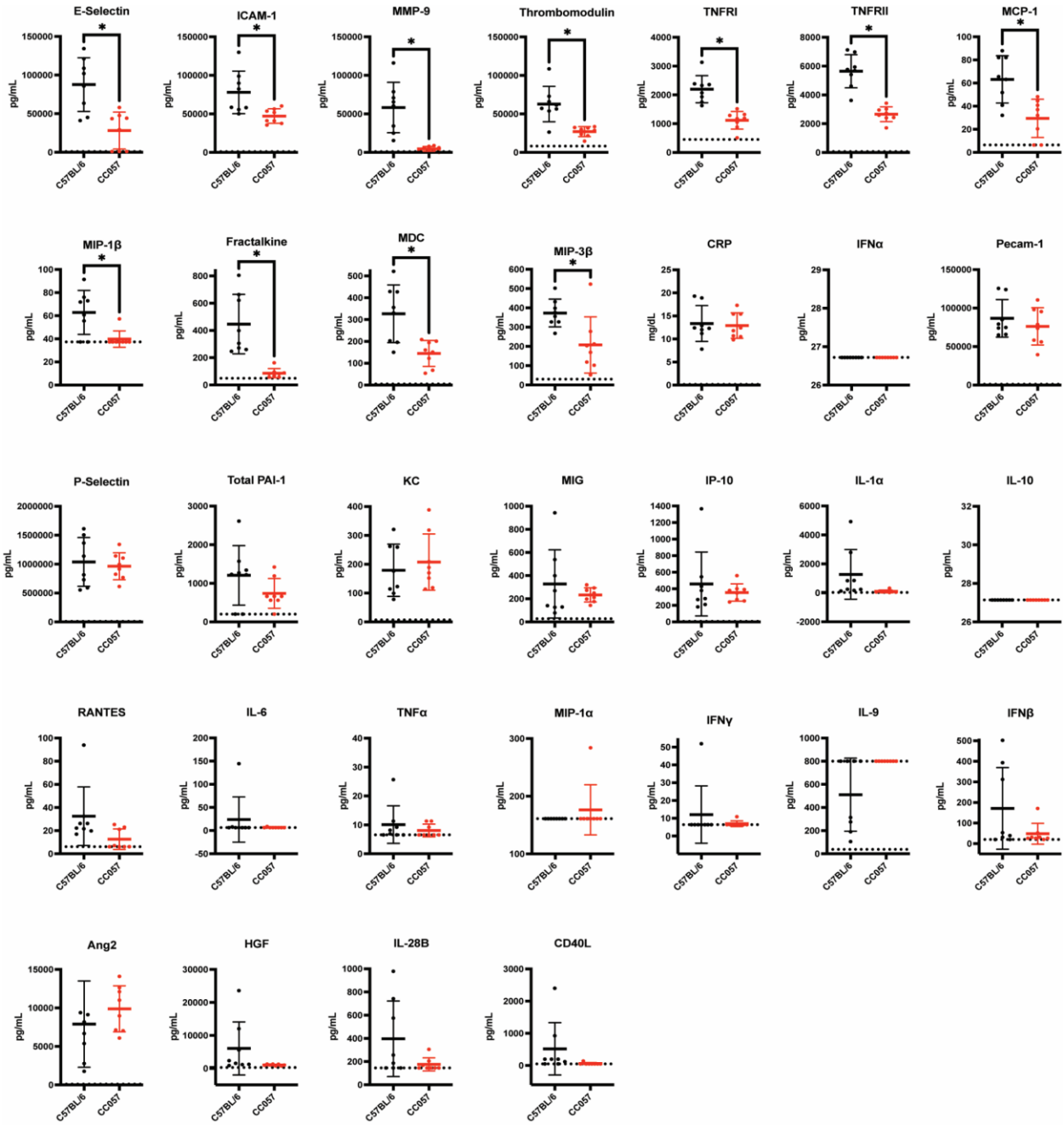

Figure 20 Baseline inflammatory environment is lower in CC057 mice

Analyte concentrations in uninfected C57BL/6 and CC057 mice. Data shown as mean ± SD (n=8/strain). Comparison of baselines for each analyte was performed by Mann-Whitney (E-Selectin p=0.0045; ICAM-1 p=0.0104; MMP-9 p=0.0002; Thrombomodulin p=0.003; TNFRI p=0.0002; TNFRII p=0.0002; MCP-1 p=0.0065; MIP-1β p=0.0126; Fractalkine p=0.0002; MDC p=0.0104; MIP-3β p=0.0134). Lower LOD for assays noted by horizontal dotted line. IL-9 is the only analyte with an upper LOD. E-Selectin LOD: 1000pg/mL; ICAM-1 LOD: 200pg/mL; MMP-9 LOD:

1000pg/mL; Thrombomodulin LOD: 8200pg/mL; TNFRI LOD: 450.95pg/mL; TNFRII LOD: 62pg/mL; MCP-1 LOD: 6.4pg/mL; MIP-1β LOD: 37.32pg/mL; Fractalkine LOD: 48.48pg/mL; MDC LOD: 4.74pg/mL; MIP-3β LOD: 29.96pg/mL; CRP LOD: 0.000004mg/dL; IFN-a LOD: 26.72pg/mL; Pecam-1 LOD: 600pg/mL; P-Selectin LOD: 8800pg/mL; Total PAI-1 LOD: 200pg/mL; KC LOD: 6.96pg/mL; MIG LOD: 27.3pg/mL; IP-10 LOD: 6.26pg/mL; IL-1α LOD: 28.88pg/mL; IL-10 LOD: 27.14pg/mL; RANTES LOD: 6.1pg/mL; IL-6 LOD: 6.42pg/mL; TNF-a LOD: 6.56pg/mL; MIP-1-a LOD: 161.08pg/mL; IFN-γ LOD: 6.46pg/mL; IL-9 lower LOD: 37.82pg/mL; IL9 upper LOD: 800pg/mL; IFNβ LOD: 20.18pg/mL; Ang2 LOD: 59.3pg/mL; HGF LOD: 273.68pg/mL; IL-28B LOD: 145.39pg/mL; CD40L LOD: 48.83pg/mL.

Table 1 C57BL/6 and CC057 analyte mean + 95% Confidence Interval (CI) at 3 dpi as a function of difference from the uninfected mean

Analyte (pg/mL)	Mean C57BL/6 difference from uninfected	C57BL/6 95% CI	Mean CC057 difference from uninfected	CC057 95% CI	Significance by Mann-Whitney (C57BL/6 verses CC057)
CRP	-61,633,583	[-80746132, -42521035]	-9,429,167	[-60072281, 41213948]	P=0.0270
IFN-α	2,621	[586.8, 4656]	282.6	[-350.9, 916.1]	ns
E-Selectin	303,293	[216118, 390467]	-4,646	[-101714, 92422]	P=0.0257
ICAM-1	59,309	[33804, 84814]	12,759	[-18375, 43892]	ns
Pecam-1	132,361	[76664, 188059]	-1,357	[-56773, 54059]	ns
P-Selectin	4,667,448	[-63667, 9398563]	166,311	[-874149, 1206772]	P=0.0098
Total PAI-1	83,365	[54090, 112640]	3,236	[-859.5, 7332]	P=0.0025
MMP-9	344,725	[242434, 447015]	9,459	[-10451, 29369]	ns
Thrombomodulin	759,107	[441391, 1076822]	2,588	[-14486, 19662]	P=0.0270
TNFRI	23,949	[11392, 36506]	492.6	[-288.4, 1274]	P=0.0172
TNFRII	49,081	[30699, 67464]	3,476	[-4250, 11203]	P=0.0172
KC	11,823	[7659, 15987]	188.3	[-11.73, 388.4]	P=0.0012
MIG	12,486	[8424, 16548]	1,286	[15, 2557]	P=0.0049
MCP-1	14,664	[10604, 18725]	511.2	[-217.6, 1240]	P=0.0086
IP-10	5,742	[3577, 7906]	2,800	[1650, 3950]	P=0.0392
IL-1a	-882.3	[-973.7, -791]	26.31	[-75.23, 127.9]	P=0.0025
IL-10	75.04	[53.16, 96.92]	19.12	[5.764, 32.47]	P=0.0098
RANTES	164.6	[118.1, 211]	-0.5971	[-13.44, 12.25]	P=0.0098

Table 1 continued

IL-6	16131	[11722, 20540]	45.53	[-46.25, 137.3]	P=0.0012
TNFα	256	[169.1, 342.8]	2.335	[-8.975, 13.64]	P=0.0049
MIP-1α	215.9	[155.3, 276.5]	-15.52	[-15.52, -15.52]	P=0.0025
MIP-1β	1,077	[684.9, 1469]	181.9	[-34.32, 398.2]	ns
IFN-γ	30.47	[19.75, 41.18]	-0.56 (undetectable)	[-0.56, -0.56]	P=0.0025
IFN-β	3,057	[264.6, 5849]	219.5	[51.59, 387.5]	P=0.0049
Fractalkine	1,518	[897, 2138]	-23.64	[-83.38, 36.09]	ns
MDC	1,106	[384.7, 1826]	60.72	[-105.6, 227]	P=0.0172
MIP-3β	2,694	[1881, 3508]	-19.38	[-223.3, 184.5]	P=0.0098
Ang2	16,248	[10387, 22110]	649.2	[-6846, 8144]	P=0.0159
HGF	49,599	[36548, 62650]	-272.1	[-524.8, -19.29]	P=0.0184
IL-28B	482.1	[264.8, 699.5]	-28.05	[-334.2, 278.1]	ns

3.2.3 CC057 mice are a novel model of RVF encephalitic disease

To characterize disease course in the novel CC057 encephalitis mouse model, viral RNA titers were assessed at timepoints throughout disease progression. Some mice were viremic at 2 dpi (**Figure 21A**). CC057 liver viral RNA titers peaked at 3 dpi but viral RNA levels in the liver decreased to below the LOD by 7 dpi before increasing slightly at the 10-11 dpi terminal timepoints. CC057 brain viral RNA load peaked at 7 dpi and remained high for the remainder of the disease course until euthanasia or death. Interestingly, viral RNA titers did not peak first in the left sciatic nerve as would be expected if RVFV trafficked to the brain via the sciatic nerve, but

rather both left and right sciatic nerve viral RNA loads increased after viral RNA was detectable in the brain. Viral RNA was sporadically present in spinal cord sections as early as 3 dpi, with peak spinal cord titers coinciding with peak brain titers at 7 dpi.

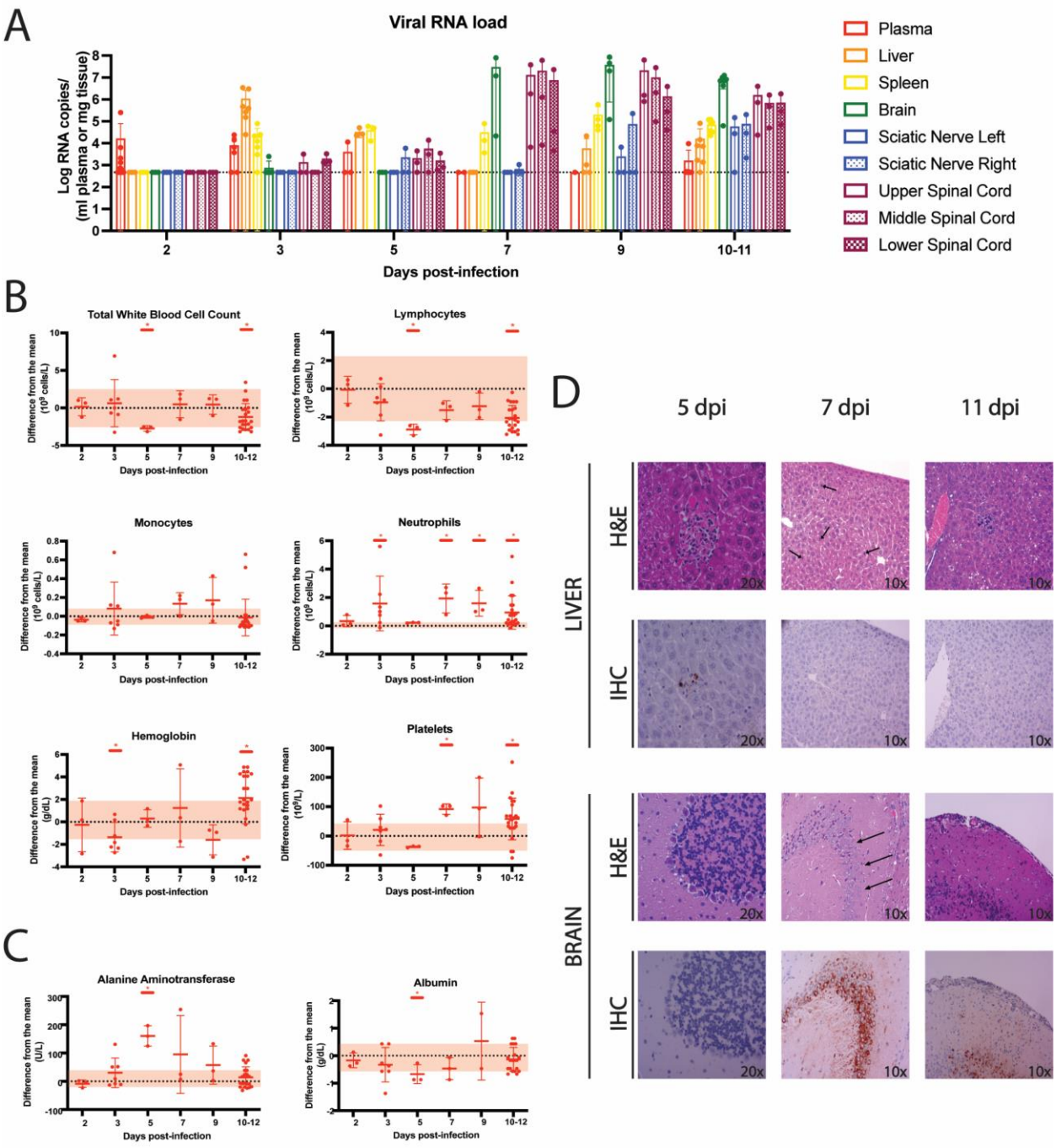

Figure 21 CC057/Unc mice control acute hepatitis and progress on to late-onset encephalitis

(A) qRT-PCR assessment of viral RNA loads in CC057 plasma and tissues over time. Data shown as mean ± SD (N=1-16/tissue type). LOD of assay noted by dotted line. (B) CBC and (C) CHEM over time with data presented as a function of difference from the uninfected mean, shown as mean ± SD (n=3-23/time point). 2 and 3 dpi data previously presented in Figure 18A, B. Pink horizontal shading represents uninfected normal ranges for CC057 mice.

Comparisons of CBC data were performed at each timepoint by Mann-Whitney to compare RVFV-infected samples to uninfected control samples (Total white blood cells 5 dpi p=0.0485, 10-12 dpi p=0.0274; Lymphocytes 5 dpi p=0.0121, 10-12 dpi p=0.0021; Neutrophils 3 dpi p=0.0098, 7 dpi p=0.0121, 9 dpi p=0.0031, 10-12 dpi p=0.0004; Hemoglobin 3 dpi p=0.0499, 10-12 dpi p=0.0065; Platelets 7 dpi p=0.0121, 10-12 dpi p=0.0103). Comparisons of CHEM data were performed at each timepoint by Mann-Whitney to compare RVFV-infected samples to uninfected control samples (ALT 5 dpi p=0.0091; Albumin 5 dpi p=0.0182). (D) Representative H&E-stained sections of formalin-fixed paraffin-embedded livers and brains from RVFV-infected mice at different times post-infection. Liver arrows point to active hepatocellular mitotic events while brain arrows point to neuronal dropout. IHC of RVFV antigen (brown) in representative sections of formalin-fixed paraffin-embedded RVFV-infected livers and brains at different times post-infection.(A) qRT-PCR assessment of viral RNA loads in CC057 plasma and tissues over time. Data shown as mean ± SD (N=1-16/tissue type). LOD of assay noted by dotted line. (B) CBC and (C) CHEM over time with data presented as a function of difference from the uninfected mean, shown as mean ± SD (n=3-23/time point). 2 and 3 dpi data previously presented in Figure 18A, B. Pink horizontal shading represents uninfected normal ranges for CC057 mice. Comparisons of CBC data were performed at each timepoint by Mann-Whitney to compare RVFV-infected samples to uninfected control samples (Total white blood cells 5 dpi p=0.0485, 10-12 dpi p=0.0274; Lymphocytes 5 dpi p=0.0121, 10-12 dpi p=0.0021; Neutrophils 3 dpi p=0.0098, 7 dpi p=0.0121, 9 dpi p=0.0031, 10-12 dpi p=0.0004; Hemoglobin 3 dpi p=0.0499, 10-12 dpi p=0.0065; Platelets 7 dpi p=0.0121, 10-12 dpi p=0.0103). Comparisons of CHEM data were performed at each timepoint by Mann-Whitney to compare RVFV-infected samples to uninfected control samples (ALT 5 dpi p=0.0091; Albumin 5 dpi p=0.0182). (D) Representative H&E-stained sections of formalin-fixed paraffin-embedded livers and brains from RVFV-infected mice at different times post-infection. Liver arrows point to active hepatocellular mitotic events while brain arrows point to neuronal dropout. IHC of RVFV antigen (brown) in representative sections of formalin-fixed paraffin-embedded RVFV-infected livers and brains at different times post-infection.

CBC and CHEM data supported a biphasic disease course in CC057 mice with mice displaying leukopenia and lymphopenia at 5 dpi and 10-11 dpi (**Figure 21B**). CC057 mice also exhibited neutrophilia at all timepoints except early at 2 dpi and immediately after liver insult at 5

dpi. CC057 mice presented with anemia during the acute hepatic phase of infection then progressed on to hemoconcentration with accompanying thrombocytosis at the later timepoints during encephalitic disease. Levels of the hepatic indicators of liver damage (ALT) and synthetic function (albumin), also differed significantly from baseline at 5 dpi immediately following the liver infection phase (**Figure 21C**). CHEM data with no physiologically relevant changes are included in the supplementary material (**Figure 22**).

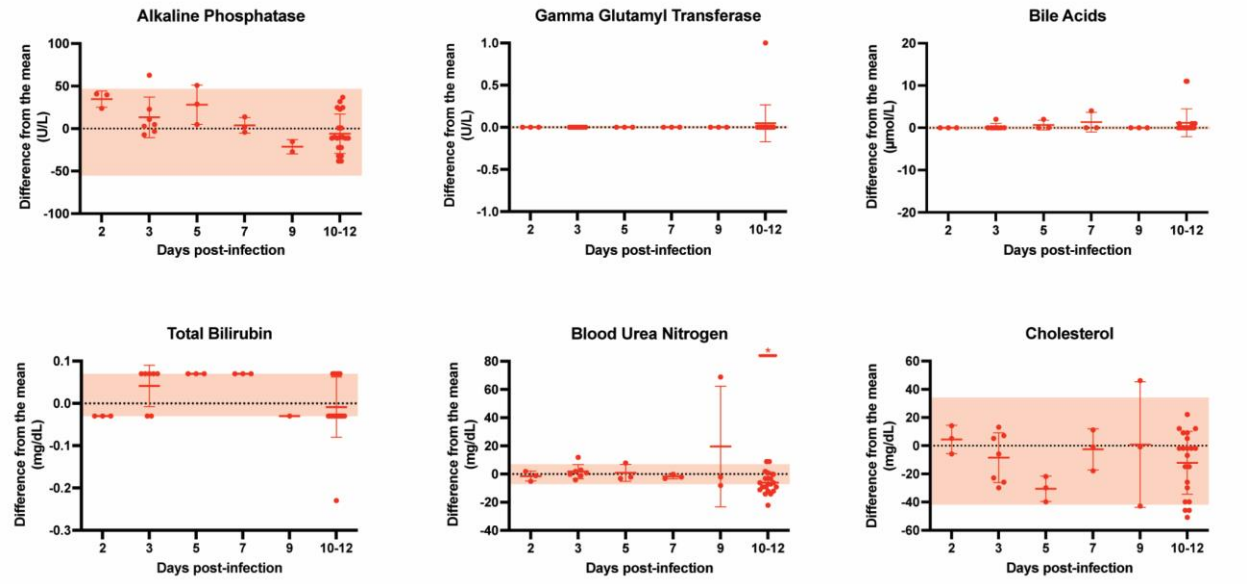

Figure 22 Additional CHEM data presented over the course of disease in CC057 mice

Data presented as a function of difference from the uninfected mean, shown as mean ± SD (N=3-23/time point). Pink horizontal bars represent uninfected normal ranges for CC057 mice. Comparisons of CHEM data were performed at each timepoint by Mann-Whitney to compare RVFV-infected samples to uninfected control samples for each mouse strain separately (Blood Urea Nitrogen 10-12 dpi p=0.0192).

After the initial manifestation of liver cytopathology at 3 dpi, CC057 mice continued to display focal areas of inflammation and necrosis at 5 dpi, although more sparsely distributed (3 of 3 mice) (**Figure 21D**). CC057 livers had very low levels of antigen staining by 5 dpi (3 of 3 mice). By 7 dpi, the livers of CC057 mice lacked antigen staining altogether (3 of 3 mice) and displayed

signs of regenerative activity post-insult including a marked increase in hepatocellular mitotic rate by 7 dpi and eventual hepatocellular mineralization at 11 dpi (1 of 3 mice). The late-encephalitic phase of infection in CC057 mice was marked by the appearance of lesions in the brain at 7 dpi (1 of 3 mice) and high levels of viral antigen (3 of 3 mice). Noted brain pathology from 7-11 dpi included patchy to focally extensive acute cortical neuronal necrosis, neuronal dropout, perivascular inflammatory infiltrates, patchy meningeal perivascular cuffing, and infrequent focal meningeal thrombosis.

To further characterize the later course of disease in CC057 mice, multiplex immune assays were run at various timepoints after hepatic recovery to assess plasma analyte concentrations. Of the 32 assessed analytes, 9 were found to be both statistically significant and deemed to play a physiologically plausible role in clinical disease (**Figure 23A, B**). Significant elevation in five inflammatory cytokines and chemokines were found between 5 and 7 dpi, peaking concurrent to the time of viral entry into the central nervous system (CNS) (IL-10, IP-10, IL-6, MIG, MCP-1) (**Figure 23A**). Of the analytes related to endothelial function, ICAM-1, PAI-1, and thrombomodulin were elevated at 5 dpi, while PAI-1, MMP-9, and thrombomodulin peaked at 9 dpi (**Figure 23B**). Remaining analyte data are included in the supplementary material (**Figure 24**). IFN-α, CD40L, and IL-9 are not included in the supplement due to a lack of data points above the limit of detection.

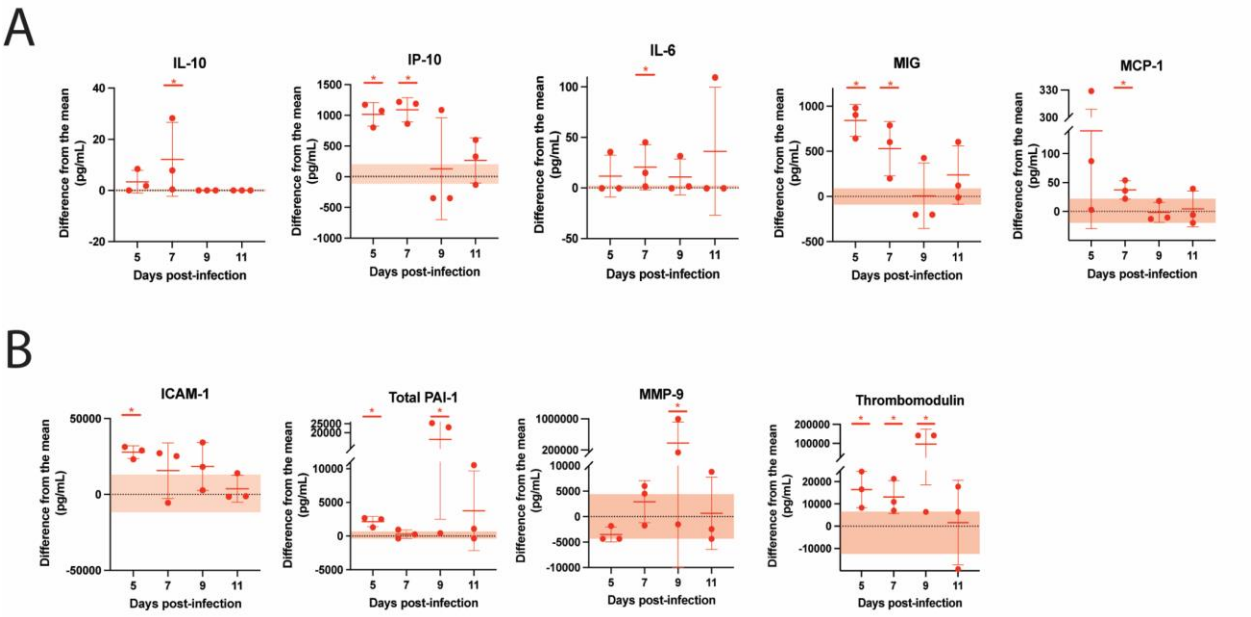

Figure 23 Cytokine signaling and markers of endothelial activation in CC057 mice

Analyte concentrations in the plasma over the course of late-onset disease with data presented as a function of difference from the uninfected mean, shown as mean ± SD (n=3/time point). Pink horizontal shading represents uninfected normal ranges for CC057 mice. For each analyte, comparisons were performed at each timepoint by Mann-Whitney to compare RVFV-infected samples to uninfected control samples. (A) Cytokines and chemokines: IL-10 (7 dpi p=0.0061); IP-10 (5 dpi 0.0121; 7 dpi 0.0121); IL-6 (7 dpi p=0.0121); MIG (5 dpi p=0.0121; 7 dpi p=0.0121); MCP-1 (7 dpi p=0.0182). (B) Tissue barriers: ICAM (5 dpi p=0.0424); Total PAI (5 dpi p=0.0121; 9 dpi p=0.0242); MMP-9 9 dpi (p=0.0121); Thrombomodulin (5 dpi p=0.0121; 7 dpi p=0.0121; 9 dpi p=0.0242).

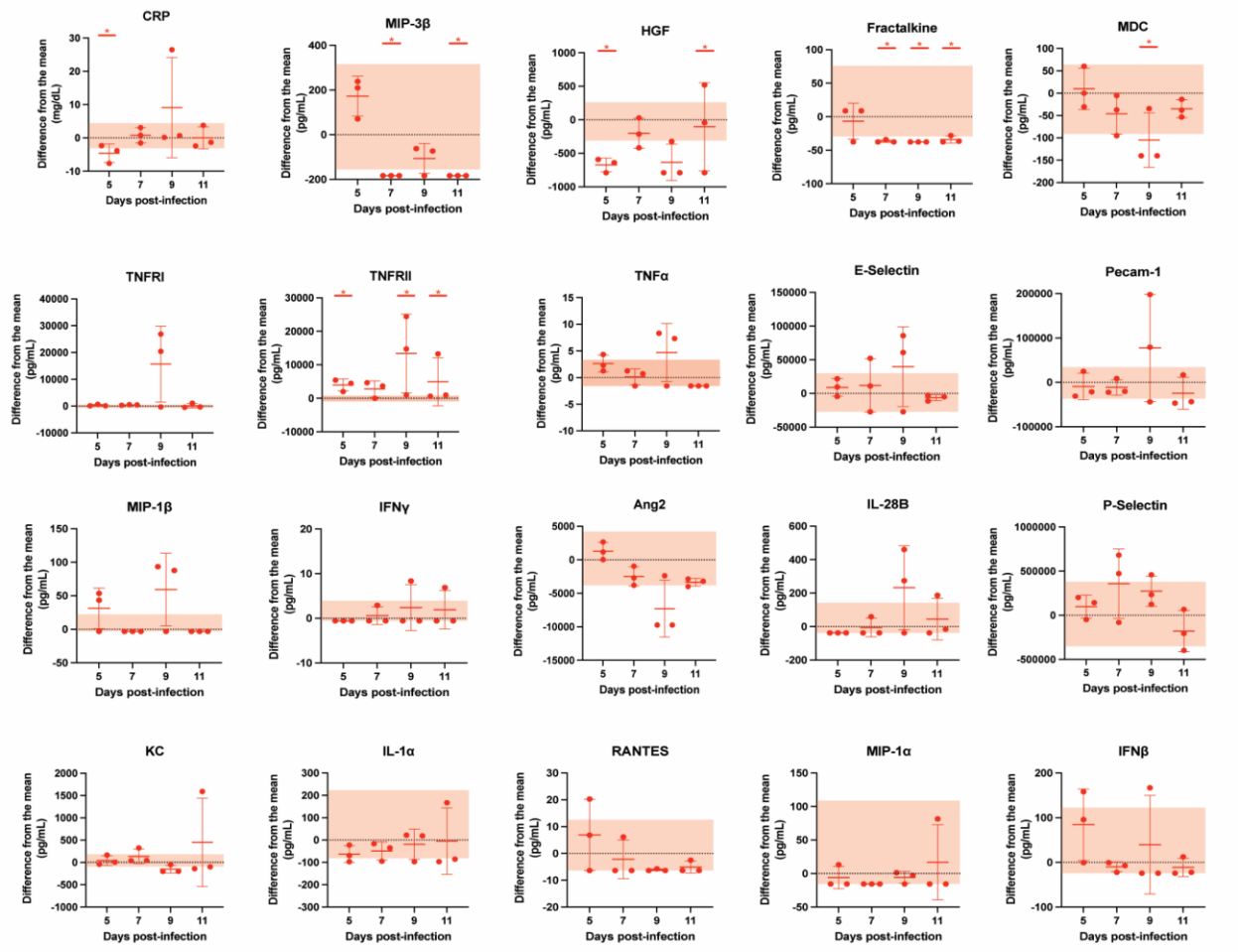

Figure 24 Remaining CC057 analyte concentrations in the plasma over the course of late-onset disease

Data presented as a function of difference from the uninfected mean, shown as mean ± SD (N=3/time point). Pink horizontal bars represent uninfected normal ranges for CC057 mice. For each analyte, comparisons were performed at each timepoint by Mann-Whitney to compare RVFV-infected samples to uninfected control samples. CRP (5 dpi p=0.0424); MIP-3b (7 dpi p=0.0121; 11 dpi p=0.0121); HGF (5 dpi p=0.0121; 11 dpi p=0.0121); Fractalkine (7 dpi p=0.0121; 9 dpi p=0.0121; 11 dpi p=0.0424); MDC (9 dpi p=0.0424); TNFRII (5 dpi p=0.0121; 9 dpi p=0.0121; 11 dpi p=0.0242).Data presented as a function of difference from the uninfected mean, shown as mean ± SD (N=3/time point). Pink horizontal bars represent uninfected normal ranges for CC057 mice. For each analyte, comparisons were performed at each timepoint by Mann-Whitney to compare RVFV-infected samples to uninfected control samples. CRP (5 dpi p=0.0424); MIP-3b (7 dpi p=0.0121; 11 dpi p=0.0121); HGF (5 dpi p=0.0121; 11 dpi p=0.0121); Fractalkine (7 dpi p=0.0121; 9 dpi p=0.0121; 11 dpi p=0.0424); MDC (9 dpi p=0.0424); TNFRII (5 dpi p=0.0121; 9 dpi p=0.0121; 11 dpi p=0.0242).

3.3 Discussion

Inbred mice almost uniformly succumb to acute hepatitis following WT RVFV infection (94-98). Given the usefulness of murine models for host genetics and immunity studies as well as high-throughput pre-clinical evaluation of vaccines and therapeutics, murine models for other forms of RVF disease are needed. In this study, we utilized the CC resource with the goal of identifying additional RVF disease phenotypes. A comprehensive analysis of RVF disease manifestations in 20 genetically diverse CC strains identified a novel immunocompetent murine model of consistent late-onset RVF encephalitis. Importantly, this model uses a footpad administration of virus which mimics a peripheral route of exposure, as might be seen during infection via mosquito bite.

This model provides a critical tool for elucidating factors that control viral infection in the liver and provides a tractable murine model in which the route of virus entry into the brain can be dissected. Moreover, future studies using additional CC strains, will permit quantitative trait locus (QTL) mapping of the genetic loci that dictate these divergent clinical outcomes following RVFV infection. However, even without genetic loci mapping, this study illuminates multiple aspects of RVF disease.

3.3.1 The host factor Mx1 is not responsible for RVFV susceptibility in mice

All CC strains, regardless of disease phenotype, succumbed to RVFV infection despite all possessing a functional Mx1 locus. Wild-derived, i.e., functional, Mx1 has been associated with increased Influenza A virus resistance in mice and is also known to inhibit its replication (177, 198). With most inbred mice containing a non-functional Mx1 locus, we hypothesized that CC

strains containing wild-derived Mx1 would show increased survival after RVFV challenge (182, 199). However, the universal lethality of RVFV in the 20 CC strains eliminates Mx1 as the main host genetic factor responsible for mouse susceptibility to RVFV.

3.3.2 CC mouse phenotypes share similarities to those observed in humans and other animal models

CC mice classified as hepatic presented with gross liver pathology, high liver viral RNA loads, viremia, and elevated ALP, ALT, and bile acids. These disease characteristics match previously established RVF hepatitis models and human cases (58, 62, 68, 94-98). Intermediate phenotype CC mouse strains paralleled the disease course in BALB/c mice, dying at a median of 5-8 dpi with earlier deaths caused by hepatic disease and later deaths manifesting as encephalitis (98). Encephalitic CC mice presented with CNS symptoms, high viral brain RNA titers with clearance of viral RNA from the periphery, and an absence of clinical markers of liver involvement. These findings correlated with previously described rat and NHP models of encephalitis and human cases (58, 62, 75, 82, 89, 91, 200).

3.3.3 CC057 mice are resistant to severe hepatitis caused by RVFV

Surprisingly, no tissue viral RNA titers, liver damage, or liver antigen staining were found in either C57BL/6 or CC057 mice mouse models until 3 dpi. This signals an extremely rapid progression of disease in C57BL/6 mice for they succumbed consistently between 3-4 dpi with 8-9 logs of viral RNA in their liver. At 3 dpi, unique signatures were seen between C57BL/6 and CC057 models in the levels of viral replication, hepatocellular damage and infection, immune

response to infection, and liver disfunction. The encephalitic CC057 model displayed significantly lower levels of organ viral RNA titers, liver damage, and hepatocellular infection and was able to overcome hepatic disease. C57BL/6 mice were extremely sick at 3 dpi and exhibited common markers of severe viral hepatic infection often seen in fatal human cases including leukopenia, lymphopenia, thrombocytopenia, and elevated ALT and ALP (58, 62, 68). Contrastingly, CC057 mice displayed a notable absence of severe hematological change. CC057 mice also failed to show major elevation in most immunologic analyte concentrations during hepatic insult. This was juxtaposed with the total immunologic disfunction seen in late-stage disease in C57BL/6 mice and which is characteristic of fatal RVF disease in mice (95). These distinctive signatures indicate a much milder course of liver disease in the CC057 model.

3.3.4 Factors that control RVF hepatitis do not necessarily prevent RVF encephalitis.

Despite the ability to bypass severe liver damage, CC057 mice were unable to prevent progression to CNS invasion and death. This phenomenon of CNS disease progression has been documented by others but not in an immunocompetent mouse model that faithfully develops late-onset encephalitis (72, 92, 98, 200). In the CC057 model, progression on to late-stage disease was marked by simultaneous clearance of viral RNA from the liver and viral invasion into the CNS by 7 dpi. High viral RNA loads in the brain at 7 dpi and onward were accompanied by cortical lesions and high brain antigen staining. The method that RVFV employs to invade the CNS has been elucidated for some models of RVF disease. In animals challenged by intranasal or aerosol RVFV inoculation RVFV has been shown to first infect the olfactory bulb then spread caudally into the cerebrum and cerebellum (78, 99, 201). However, the method of entry into the CNS is unknown for challenge that begins at the periphery such as infection by mosquito bite or FP injection. One

possible route of brain entry from an initial peripheral challenge is retrograde neuronal transport, as is known to occur with Rabies virus (202-204). However, in CC057 mice, viral RNA appeared earliest at very low levels in spinal cord sections at 3 and 5 dpi. At 7 dpi, brain and spinal cord sections peaked with high viral RNA titers while the sciatic nerves remained near the LOD for viral RNA until 9-11 dpi. These data suggest that trafficking via the sciatic nerve is not the mode of viral entry into the CNS for the CC057 encephalitis model.

3.3.5 Biomarkers of clinical outcome

Serum viral titers taken at 2 dpi did not clearly correlate with disease outcome or time to death among the CC strains. Although a general trend can be seen between the three disease categorizations, the difference in titer is not large and outlier strains such as CC071 and CC058 prevent identifying a direct correlation between titer at 2 dpi and time to death.

Despite the presence of neutralizing antibody levels, no CC mice were able to prevent or overcome CNS disease, likely due to the timing of the humoral response. Neutralizing antibody titers against RVFV did not appear in terminal mice until 8 dpi while virus was present at high levels in the brains of CC057 mice by 7 dpi as assessed by qRT-PCR and IHC. It is therefore possible that brain damage is too severe by the time a humoral response is mounted or that antibodies are not able to effectively clear virus from the brain once RVFV has already crossed the blood brain barrier (BBB).

A prominent feature of the post-hepatic phase of disease in CC057 mice was a sustained neutrophilia from 3 dpi to the point of death with the only drop occurring at 5 dpi. The decrease in circulating neutrophils at 5 dpi could be due to liver infiltration during the hepatic disease phase. During the end stage of disease, CC057 mice present with significant leukopenia and lymphopenia

suggestive of brain infiltration or cellular death from severe disease. As has been seen in other animal models of RVF encephalitis, increases in cytokine, chemokine, and endothelial-related blood markers were seen in the CC057 model late in the course of disease between 5-11 dpi (92, 200). Important increases in inflammatory and chemoattractant markers were seen in IP-10, IL-6, MIG, and MCP-1 with an accompanying increase in the anti-inflammatory cytokine IL-10. All five of these markers have been shown to be elevated in human RVF cases (68, 77). IL-6 and MCP-1 elevation has also been shown in lethal intranasally infected mice (78). Intriguingly MIG was the most elevated at 5 dpi, two days before viral entry into the brain, which indicates IFN-γ elevation prior to the time of brain viral invasion. There is also evidence of T-cell and monocyte recruitment at 5 and 7 dpi due to elevation of IP-10 and MCP-1 at these timepoints. However, these increases in cytokine and chemokine production are likely too late in the course of disease to offer mice protection and it is also possible that elevated analyte levels are simply cytokine dysregulation in severely sick animals near death.

While the significance of analyte increases in this model are not yet completely understood, we speculate that they could signal brain endothelial infection or breach of the CNS by RVFV. ICAM-1 peaked the earliest of the endothelial-related markers at 5 dpi in the blood, signaling it has been shed by an activated endothelium. This increase in ICAM-1 before detectable viral entry into the brain could serve as an early biomarker of CNS invasion. The lack of overwhelming increases in measured blood inflammatory markers before virus is detected in the brain at 7 dpi suggests that RVFV gains entry to the brain without the need for BBB breakdown. Peaks in markers signaling potential BBB breakdown such as Total PAI-1, MMP-9, and thrombomodulin do not occur until 9 dpi during the endpoint of disease (205). These findings are supported by work in various animal models detailing that BBB breakdown is not required for RVFV entry into the

brain and often only occurs late in the course of disease after the virus has already caused severe brain damage (78, 206). Further study into the route of viral brain invasion upon peripheral infection is an essential next step and can be accomplished by using the novel CCO57 mouse model.

3.3.6 Conclusion

In conclusion, we describe here a comprehensive analysis of RVF disease manifestations in 20 CC mouse strains resulting in the characterization of three distinct phenotypes: hepatitis, intermediate phenotype, and encephalitis. Large differences in viral load kinetics, pathologies, CBC, CHEM, and blood analytes were found between hepatic and encephalitic clinical outcomes. Of the challenged CC strains, the CC057 strain was identified as a novel immunocompetent model of late-onset RVF encephalitis, and a detailed analysis of phenotype was performed by virologic, pathologic, hematologic, histologic, and immunologic assessment. Our data suggest that host factors play a critical role in determining RVF disease manifestation and we demonstrate that the genetic diversity provided by the CC resource enables the identification of novel mouse models of human disease manifestations. The CC resource allows us to link identified outcome to host genotype, therefore future work should focus on identifying genes of protection and susceptibility from various RVF clinical outcomes. The CC057 model described in this paper will enable immediate investigation into the pathogenesis of RVF CNS disease, identification of the genetic basis for disease variation, and evaluation of therapeutic strategies that have direct human implications.

4.0 Fc Effector Functions Enhance Antibody-Mediated Rift Valley Fever Virus Protection In Vivo

Rift Valley fever virus (RVFV) is a mosquito-borne virus found throughout Africa and into the Middle East. It has a substantial disease burden; in areas of endemicity, up to 60% of adults are seropositive. With a case fatality rate of up to 3% and the ability to cause hemorrhagic fever and encephalitis, RVFV poses a serious threat to human health. Despite the known human disease burden and the fact that it is a NIAID category A priority pathogen and a WHO priority disease for research and development, there are no vaccines or therapeutics available for RVF. Given the recent advances in the use of monoclonal antibodies (mAbs) for treating infectious disease, in this study, we developed and characterized a panel of monoclonal antibodies against the RVFV surface glycoprotein, Gn. RVFV mAbs spanned a range of neutralizing abilities and mapped to distinct epitopes along Gn. We then demonstrated therapeutic efficacy in the prevention of RVF in vivo in an otherwise lethal mouse model. Finally, we revealed a role for Fc-mediated function in augmenting the protection provided by these antibodies. IgG2a version mAbs had increased capacity to induce effector functions and conferred better protection from RVFV challenge than IgG1 version MAbs. Overall, this study shows that Fc-mediated functions are a critical component of humoral protection from RVFV. The data presented in this chapter have been previously published in the American Society for Microbiology journal mSphere. Manuscript information: Cartwright HN, Barbeau DJ, McElroy AK. Isotype-Specific Fc Effector Functions Enhance Antibody-Mediated Rift Valley Fever Virus Protection In Vivo. mSphere. 2021 6(5):e0055621. doi: 10.1128/mSphere.00556-21. PMID: 34494884; PMCID: PMC8550229.etc (207).

4.1 Introduction

Rift Valley fever virus (RVFV) is a zoonotic arbovirus of the family Phenuviridae first identified in 1931 in Kenya (1). RVFV is endemic throughout Africa and the Arabian Peninsula (174), with recent outbreaks across many countries since 2018 (208-211). There is significant risk of spread due to widespread competent mosquito vectors (2, 3, 212). Given its potential to cause a public health emergency as well as the absence of human therapeutics or vaccines, WHO has listed Rift Valley fever (RVF) as a priority disease for research and development (213). RVF displays a variety of clinical manifestations, ranging from acute flu-like illness to severe and sometimes lethal hemorrhagic disease or encephalitis (4). Approximately 4,500 cases of severe RVF disease were reported to WHO between 2000 and 2016 (214), although this greatly underestimates the true burden of disease. Serosurveys have revealed widespread seropositivity in humans and animals across Africa (16-20).

Monoclonal antibodies (mAbs) have already shown efficacy in the treatment of multiple infectious diseases, with many in clinical development (133). To date, RVFV mAb research has focused on the development and evaluation of neutralizing mAbs. Neutralization is mediated by the Fab region, which directly contacts a viral surface glycoprotein, blocking entry into host cells. Rabbit, human, monkey, and mouse mAbs directed against the two RVFV glycoproteins—Gn and Gc—have been recently developed and demonstrated protective efficacy in mice (166, 168-171). Gn- and Gc-neutralizing mAbs have demonstrated protection in vivo by blocking attachment, entry, or fusion of RVFV (168-171).

In addition to neutralization, antibodies (Abs) provide protection through a variety of mechanisms via their ability to interact with Fc gamma receptors (FcγRs) on innate immune cells. Abs bind FcγRs through their Fc domain to mediate functions, including antibody-dependent

cellular cytotoxicity (ADCC), antibody-dependent cellular phagocytosis (ADCP), antibody-dependent neutrophil phagocytosis (ADNP), and complement-dependent cytotoxicity (CDC) (137, 138). The essential role of Fc-mediated immune effector functions in providing protection from viral disease has been reported for Ebola virus, human immunodeficiency virus, influenza A virus, and chikungunya virus (139-144). This suggests the potential for Fc effector functions to be an essential component of mAb-mediated protection from RVFV, a role that has yet to be investigated.

We report the development of a panel of six mouse mAbs against the RVFV Gn glycoprotein. To investigate the contribution of Fc effector functions in antibody-mediated RVFV protection, mAbs were subclass switched to produce IgG1 and IgG2a versions. IgG1 subclass mAbs provided incomplete protection from RVFV disease in vivo. However, administration of IgG2a subclass mAbs increased protection to 100% for the three most promising candidates. These results indicate that Fc-effector mechanisms are key components of humoral protection from RVF.

4.2 Results

4.2.1 Generation and characterization of anti-Gn RVFV mAbs

A panel of eight RVFV Gn-specific mouse mAbs were generated. These mAbs were selected to span a range of neutralizing and Gn binding abilities based on initial hybridoma cell supernatant enzyme-linked immunosorbent assay (ELISA) and foci reduction neutralization test (FRNT) screening. Antibody variable domain sequencing found mAb-2, -2.2, and -2.3 to be identical, and so six unique mAbs were used throughout the study. Variable domains were cloned

into heavy and light chain expression plasmids, and Abs were purified to produce mAb-1, -2, -3, -4, -5, and -6.

MAbs displayed a range of RVFV neutralization abilities (**Figure 25A**). Three mAbs showed no neutralization ability, even at 500 µg/ml. The half maximal inhibitory concentration (IC_{50}) was calculated for each of the three neutralizing mAbs. MAb-1 was the most potently neutralizing, with an IC_{50} of 28 ng/ml followed by mAb-2 (1,532 ng/ml) and MAb-3 (12,260 ng/ml) (**Table 2**).

In an RVFV lysate ELISA, all six mAbs were able to bind Gn with varied affinities (**Figure 25B**). The lower maximal binding values for mAb-4, -5, and -6 suggest that fewer of these mAbs were able to bind RVFV at saturation than mAb-1, -2, and -3. Fifty percent effective concentration (EC_{50}) values ranged from 3.97 to 327.8 ng/ml with mAb-1, -2, and -3 having the lowest values (**Table 2**).

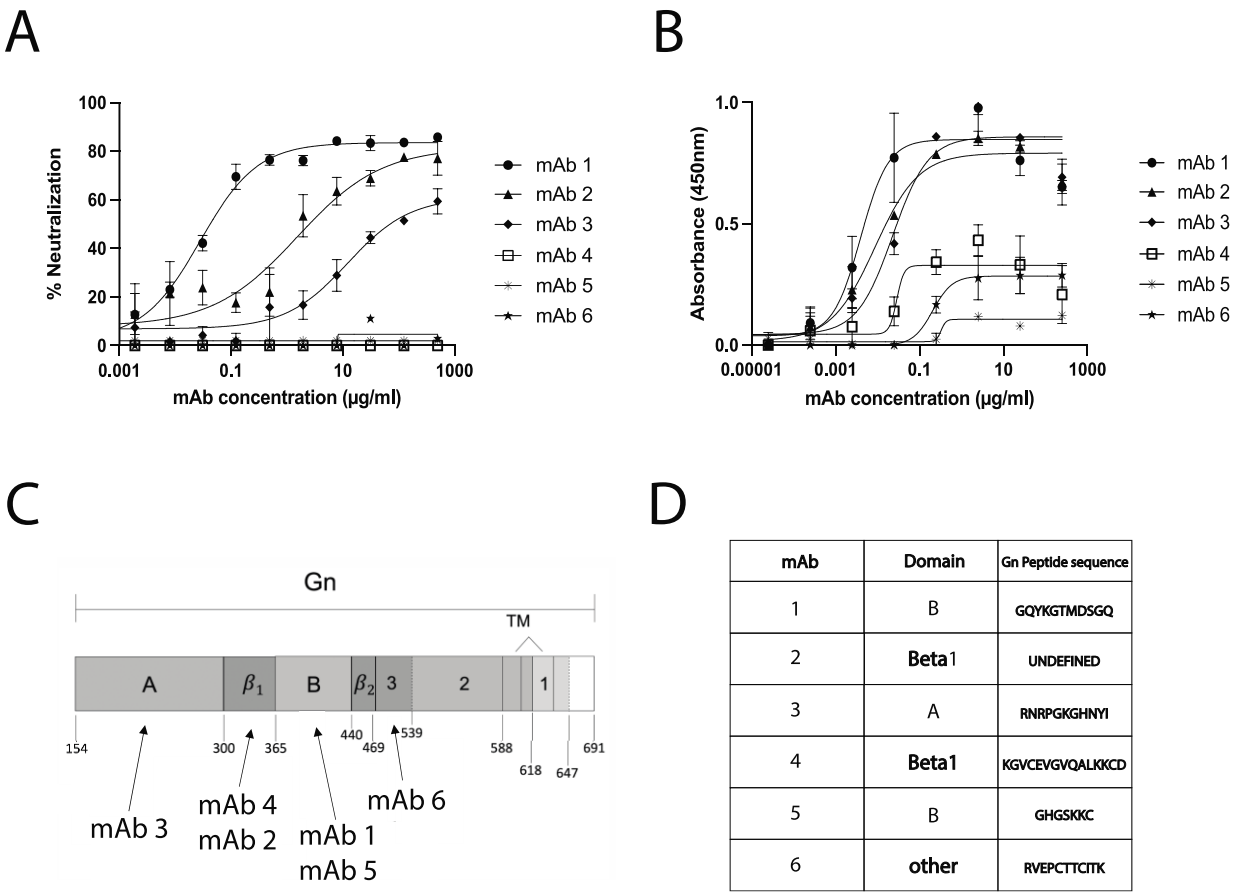

mAb	Domain	Gn Peptide sequence
1	B	GQYKGTMDSGQ
2	Beta1	UNDEFINED
3	A	RNRPGKGHNYI
4	Beta1	KGVCEVGVQALKKCD
5	B	GHGSKKC
6	other	RVEPCTTCITK

Figure 25 RVFV mAbs display a range of binding and neutralization activities and target domains throughout Gn

(A) The ability of mAbs to neutralize RVFV was assessed by serial dilution of mAbs in an FRNT assay. (B) MAbs were also tested for their ability to bind Gn by RVFV-infected lysate ELISA. Means and standard deviations (SDs) from triplicates are reported for both FRNT and ELISA data. (C) Schematic of the RVFV Gn protein with mAbs mapped to the domain required for binding, as determined through Western blot analysis of truncated Gn constructs. (D) MAbs were mapped to specific epitopes by Gn peptide ELISA.

Table 2 Characterization of anti-Gn mAb neutralization and binding

mAb	IC50 for neutralizing RVFV (ng/ml)	EC50 for binding Gn (ng/ml)
1	28.06	3.97
2	1,532	8.77
3	12,260	23.04
4	N/A	28.73
5	N/A	327.8
6	N/A	206.8

4.2.2 Domain and epitope mapping of anti-Gn RVFV mAbs

Gn truncations were made based on three previously identified structural domains of Gn: A (amino acids [aa] 154 to 300), B (aa 366 to 440), and beta (beta$_1$ aa 301 to 365 and beta$_2$ 441 to 469) (**Figure 25C**) (155, 215). Truncations were also made outside these three domains to split up Gn between the beta$_2$ domain and the transmembrane (TM) domain (denoted 1, 2, and 3) (**Figure 26A**). Using these seven Gn truncations (**Figure 26A**), the domain required for binding of each MAb (**Figure 26B**) was identified. MAbs mapped to different domains along Gn, with mAb-6 binding closest to the TM, outside the previously defined A, B, and beta domains (**Figure 25C**; **Figure 26B**). Interestingly, the highest neutralizers (mAb-1, -2, and -3) bound different domains of Gn. All mAbs were found to recognize denatured forms of Gn, suggesting linear epitopes. Peptide ELISA was performed to map the epitope recognized by each mAb. All mAbs strongly bound at least one peptide except for mAb-2 (**Figure 25D**). Some mAbs bound multiple adjacent

and overlapping peptides, which enabled the identification of shorter binding epitopes. All identified binding epitopes were within the domain to which that mAb had previously been mapped by Western blotting. Successful binding to 15-mer peptides by mAbs confirmed that most of these mAbs bound linear epitopes.

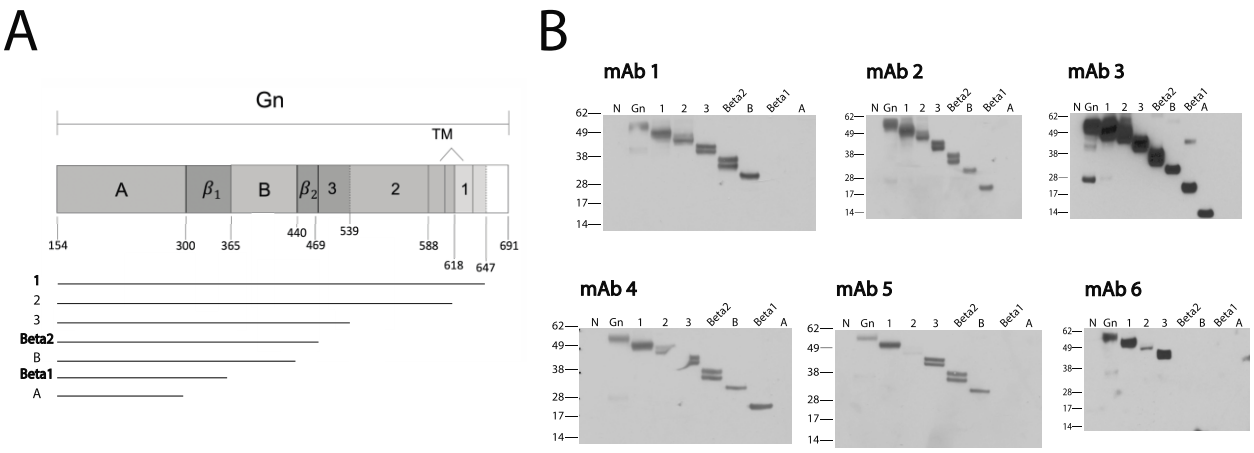

Figure 26 RVFV mAbs target various domains along the length of Gn

(A) Schematic of the RVFV Gn protein with representations of the truncated versions of Gn proteins that were generated for domain mapping. (B) Required domains for binding were mapped by Western Blot analysis.

4.2.3 Anti-Gn mAbs increased survival following lethal RVFV challenge

C57BL/6 mice are an RVFV lethal challenge model, succumbing to infection within 4 days (94). To determine the protective potential of these anti-Gn mAbs, 400 µg of each IgG1 mAb was administered via intraperitoneal (i.p.) injection 48 h pre-challenge with 200 times the 50% tissue culture infective dose ($TCID_{50}$) of wild-type (WT) RVFV (**Figure 27A**). Serum FRNT and ELISA at 24 h post-injection (**Figure 27B**) confirmed mAb administration in all mice.

IgG1 isotype control-treated mice succumbed to disease within 3 days of challenge, while positive-control mice given RVFV-vaccinated immune serum survived to the end of the

experiment (**Figure 27C**). MAb-1 and -2 protected mice significantly better than the isotype control, with only one mouse per experimental group succumbing to disease. Although mAb 3-treated mice all succumbed to disease, their survival curve was different from that of the isotype control, with a significantly increased time to death. Mice treated with non-neutralizing mAb-4, -5, or -6 all succumbed to disease with no significant delay in time to death. Weight loss was appreciated in all mice that succumbed to acute hepatic death (**Figure 28**). At the point of euthanasia, tissues and serum were assessed for RVFV RNA loads. Elevated viral RNA throughout the tissues and serum confirmed that mice succumbed due to RVFV infection (**Figure 27D**). Notably, although mice treated with mAb-3 all succumbed, decreased levels of viral RNA suggest some level of mAb-mediated viral control (**Figure 27D**). In survivor mice, RNA levels were at or near the limit of detection (LOD) by day 28 post-challenge, suggesting overall control of the virus (**Figure 27D**).

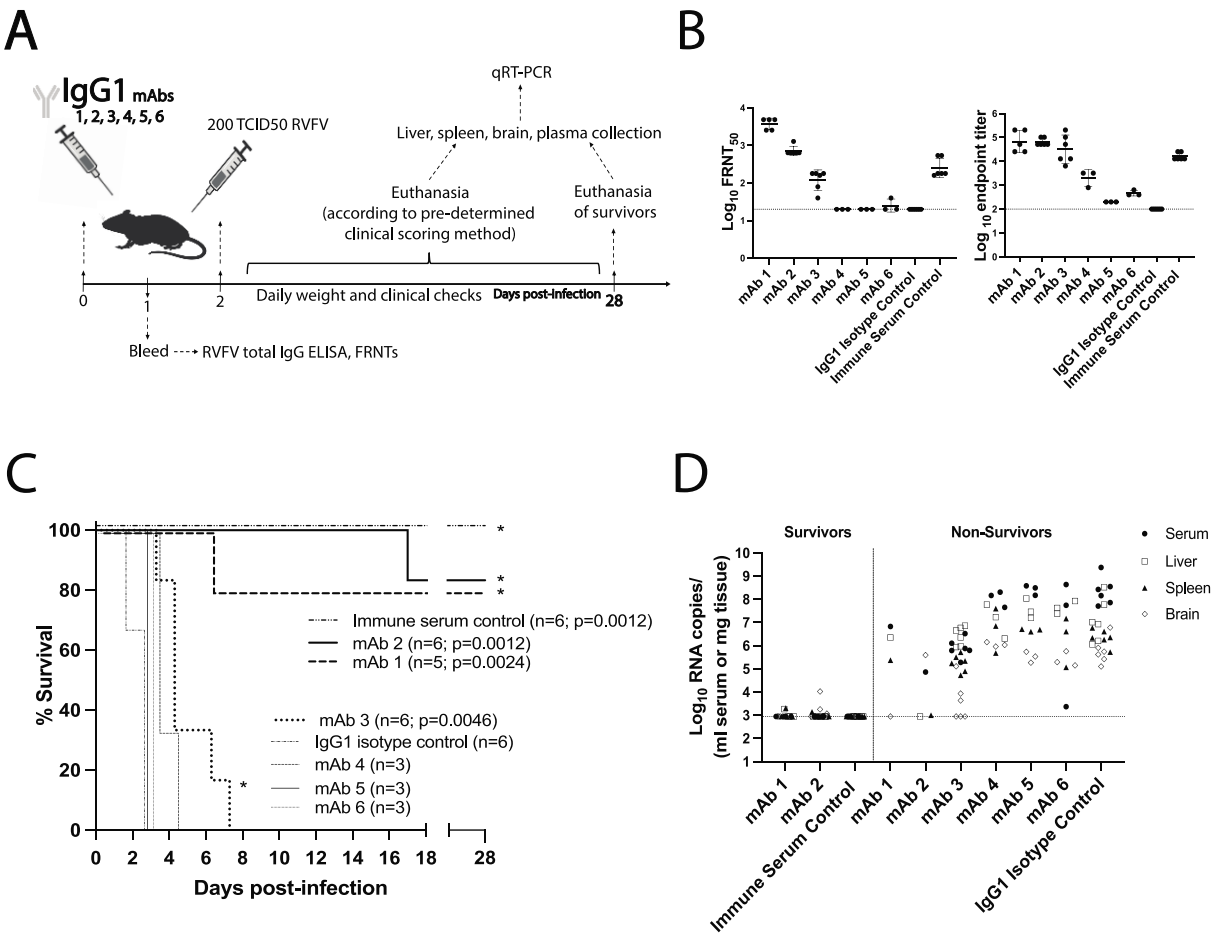

Figure 27 Anti-Gn mAbs increase survival against lethal RVFV challenge

(A) Schematic of the IgG1 mAb-treated mouse survival experiment. (B) FRNT and ELISA of serum collected 24 h after mAb injection. Geometric mean titers are shown with a horizontal line, and error bars represent the geometric SD for each mAb treatment group. LOD of each assay is noted by dotted line. (C) Survival curve of mice following challenge. Positive-control mice injected with RVFV immune serum all survived challenge and exhibited a statistically significant difference in survival compared to that of IgG1 isotype control-treated mice (Mantel-Cox test; P = 0.0012). mAb-1 and -2 also showed equally significant differences in survival compared to that of IgG1 isotype control-treated mice, although there was not 100% protection from lethal RVFV challenge (Mantel-Cox test; mAb-1 P = 0.0024; mAb-2 P = 0.0012). *, significance in survival compared to IgG1 isotype control survival. (D) qRT-PCR based assessment of viral RNA loads in tissues and serum at time of euthanasia. Surviving mice were euthanized 28 days post-infection (dpi). The LOD for this assay is reported as a horizontal dashed line at 887 RNA copies.

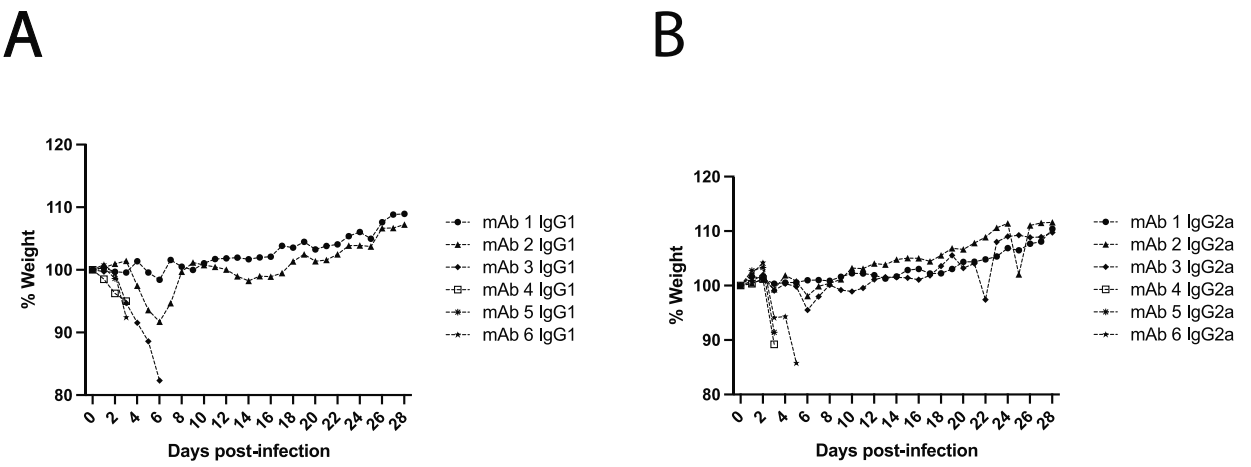

Figure 28 Weight loss of IgG1 and IgG2a mAb-treated mice

Percent change in mouse daily weight from baseline in either (A) IgG1 or (B) IgG2a mAb-treated mice. Weight loss curves represent six female mice for a given mAb treatment group.

4.2.4 Subclass switching of anti-Gn RVFV mAbs

To test the hypothesis that protection delivered by the three partially protective mAbs could be enhanced by increasing their ability to induce Fc effector functions, the inherent differential abilities of murine IgGs to interact with FcγRs on innate immune cells was utilized. In mice, IgG2a Abs induce high effector function strength by binding the high-affinity activating receptors FcγRIV and FcγRI and the low-affinity receptor FcγRIII. IgG1 Abs signal through FcγRIII but not FcγRIV or FcγRI and are thus classically thought to affect lower levels of Fc-mediated defense (216-219). Therefore, to increase the ability of the RVFV-Gn IgG1 mAbs to induce Fc-mediated immune effector functions, they were subclass switched to IgG2a.

Functionality of IgG2a version mAbs that had shown some level of protection in vivo was assessed by FRNT and ELISA. Subclass-switched mAbs exhibited an RVFV neutralization capacity similar to that of their IgG1 counterparts (**Figure 29A**). Subclass-switched mAbs also

bound Gn with affinities resembling those of their IgG1 versions, confirmed by ELISA (**Figure 29B**). To confirm that IgG2a version mAbs successfully induced higher effector functions, their ability to induce Gn/mAb interaction-dependent activation of NK cells was assessed by NK cell degranulation (% $CD107a^+$ NK cells) (**Figure 29C; Figure 30**). The IgG2a version of all three mAbs showed significantly higher NK cell degranulation (**Figure 29C**).

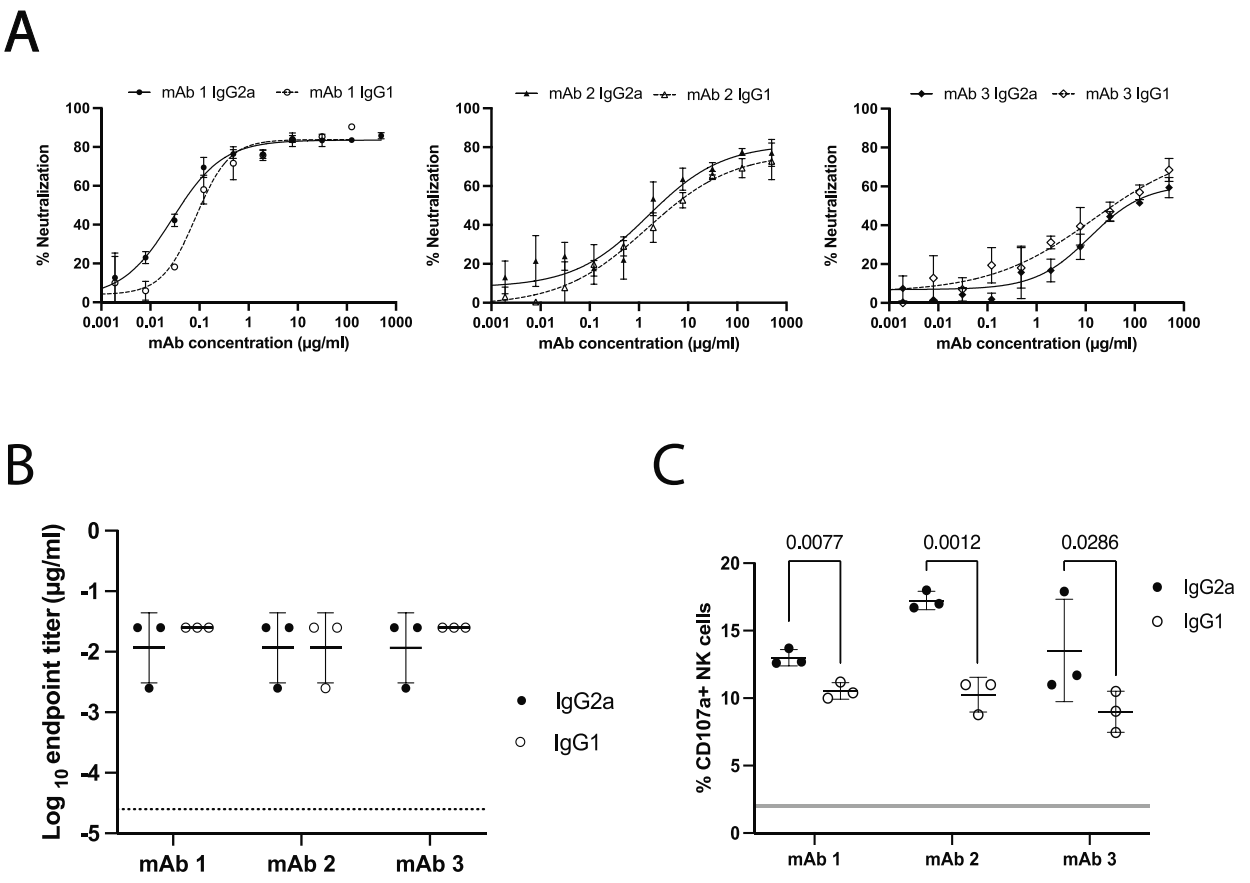

Figure 29 Subclass-switched mAbs display similar binding and neutralization but increased ability to activate effector functions

(A) Subclass-switched mAbs had similar neutralizing ability as assessed by FRNT. Mean and SD in triplicate are reported. (B) Subclass-switched mAbs had similar Gn binding as tested by ELISA of RVFV-infected lysates. Geometric means are shown with a horizontal line, and error bars represent the geometric SD for each mAb. The horizontal dashed line represents the LOD of this assay. (C) Assessment of mAb ADCC by NK cell degranulation assay. Each point represents an independent replicate, with means shown by a horizontal line and SD by the error bars. The gray horizontal line indicates the range of degranulation induced by IgG1 and IgG2a isotype control Abs. Statistical significance in the ability of mAbs to induce degranulation in NK cells was assessed by unpaired Student's t tests. (mAb-1, P = 0.0077; mAb-2, P = 0.0012; mAb-3, P = 0.0286).

(A) Subclass-switched mAbs had similar neutralizing ability as assessed by FRNT. Mean and SD in triplicate are reported. (B) Subclass-switched mAbs had similar Gn binding as tested by ELISA of RVFV-infected lysates. Geometric means are shown with a horizontal line, and error bars represent the geometric SD for each mAb. The

horizontal dashed line represents the LOD of this assay. (C) Assessment of mAb ADCC by NK cell degranulation assay. Each point represents an independent replicate, with means shown by a horizontal line and SD by the error bars. The gray horizontal line indicates the range of degranulation induced by IgG1 and IgG2a isotype control Abs. Statistical significance in the ability of mAbs to induce degranulation in NK cells was assessed by unpaired Student's t tests. (mAb-1, P = 0.0077; mAb-2, P = 0.0012; mAb-3, P = 0.0286).

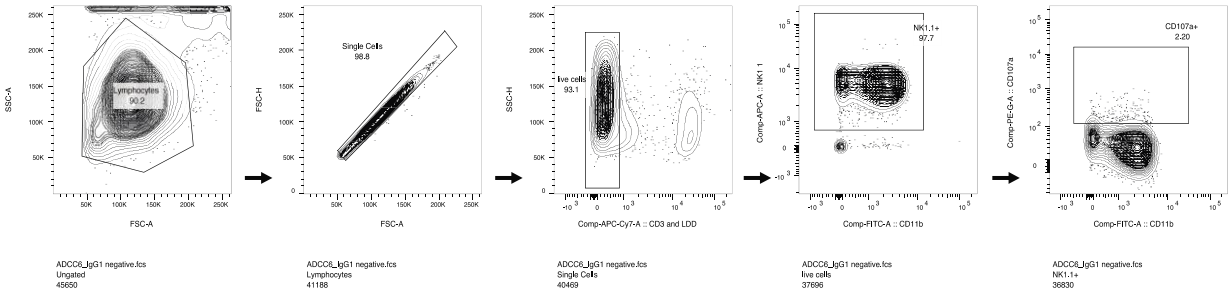

Figure 30 Identification and characterization of NK cells

Flow cytometry gating strategy used in the identification of NK cells and the quantification of CD107a+ NK cells. Doublets and dead cells were excluded from total selected lymphocytes. NK cells were discriminated from any remaining cells as NK1.1+ and from this population the percentage of NK cells positive for CD107a was quantified. A negative control sample is shown.

4.2.5 Protection in vivo was enhanced by Fc effector function

To test whether Fc effector functions were important for RVFV protection in vivo, IgG2a version mAbs were administered to C57BL/6 mice pre-challenge as before (**Figure 31A**). FRNT and ELISA of mouse bleed serum 24 h post-injection revealed appropriate levels and functionality of the administered IgG2a mAbs (**Figure 31B**).

IgG2a isotype control-treated mice succumbed to lethal RVFV challenge similarly to the IgG1 isotype controls, while all positive-control mice survived (**Figure 31C**). IgG2a mAb- 1, -2, and -3 fully protected mice from lethal challenge, with their survival curves being significant

compared to those of IgG2a isotype control-treated mice. All mice administered a non-neutralizing IgG2a (mAb-4, -5, or -6) still succumbed to disease. Viral RNA loads were high in all mice that succumbed and were at or below the LOD in surviving mice (**Figure 31D**).

To determine if protection provided by mAb-1, -2, and -3, was sterilizing, results from ELISA and FRNT on terminal survivor mouse serum were compared to bleed antibody titers measured at 24 h pre-challenge (**Figure 32**). These data showed an overall increase in total antibody titers and neutralization in the serum of mice treated with mAbs that survived RVFV infection (**Figure 32A**). RVFV N protein-specific ELISA was performed on terminal survivor serum to confirm that antibody titer increases were due to de novo production of antibody within the mice in response to infection (**Figure 32B**). The presence of anti-N antibody titers in all survivor mAb-treated mice, regardless of subclass, confirmed that protection by these anti-Gn mAbs was not sterilizing.

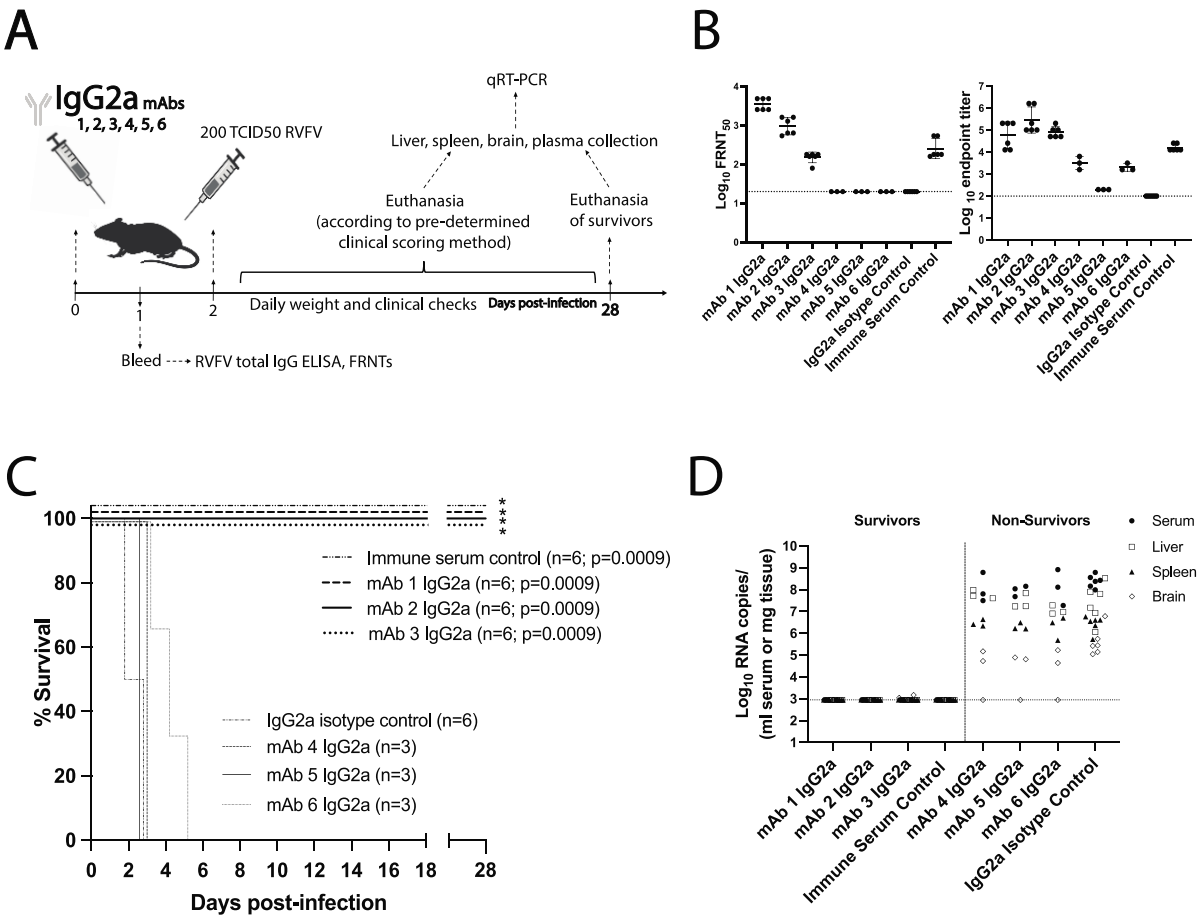

Figure 31 IgG2a mAbs confer increased protection against lethal RVFV challenge

(A) Schematic of the IgG2a mAb-treated mouse survival experiment. (B) FRNT and ELISA of bleed serum taken 24 h after mAb injection. Geometric means are shown with a horizontal line, and error bars represent the geometric SD for each mAb treatment group. LOD of each assay is noted by the dotted line. (C) Survival curve of mice following challenge. Positive-control mice injected with RVFV immune serum all survived challenge and exhibited a statistically significant difference in survival compared to IgG2a isotype control-treated mice (Mantel-Cox test; P = 0.0009). The IgG2a version of mAb-1, -2, and -3 all displayed complete protection from lethal challenge, and the survival curves were significant compared to those of IgG2a isotype control-treated mice (Mantel-Cox test, mAb-1, -2, and -3, P = 0.0009). *, significance in survival compared to IgG2a isotype control survival. (D) qRT-PCR based assessment of viral RNA loads in tissues and serum at time of euthanasia. Surviving mice were euthanized 28 dpi. The LOD for this assay is reported as a horizontal dashed line at 887 RNA copies.

(A) Schematic of the IgG2a mAb-treated mouse survival experiment. (B) FRNT and ELISA of bleed serum taken 24 h after mAb injection. Geometric means are shown with a horizontal line, and error bars represent the geometric SD for each mAb treatment group. LOD of each assay is noted by the dotted line. (C) Survival curve of mice following challenge. Positive-control mice injected with RVFV immune serum all survived challenge and exhibited a statistically significant difference in survival compared to IgG2a isotype control-treated mice (Mantel-Cox test; P = 0.0009). The IgG2a version of mAb-1, -2, and -3 all displayed complete protection from lethal challenge, and the survival curves were significant compared to those of IgG2a isotype control-treated mice (Mantel-Cox test, mAb-1, -2, and -3, P = 0.0009). *, significance in survival compared to IgG2a isotype control survival. (D) qRT-PCR based assessment of viral RNA loads in tissues and serum at time of euthanasia. Surviving mice were euthanized 28 dpi. The LOD for this assay is reported as a horizontal dashed line at 887 RNA copies.

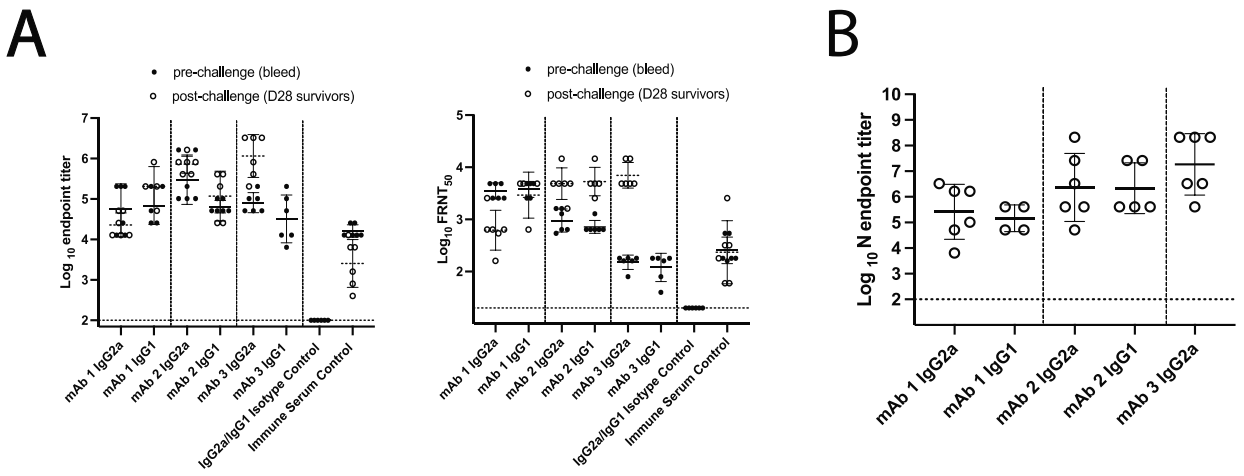

Figure 32 Anti-Gn mAbs confer non-sterilizing protection from lethal RVFV challenge regardless of subclass

(A) Comparison of FRNT and ELISA data at 24 hours post administration (pre-challenge bleed, black circles) with terminal bleed from all surviving animals (28 days post challenge, open circles). There are no terminal data for mAb-3 IgG1 due to all mice succumbing to disease before day 28. Geometric mean titers are shown with a horizontal line and error bars represent the geometric SD for each mAb treatment group either pre- (solid) or post-challenge (dotted). The horizontal dashed lines represent the LOD of these assays. (B) All mice that survived RVFV challenge developed anti-N antibody titers. Geometric means are shown with a horizontal line and error bars represent the geometric SD for each mAb treatment group. The horizontal dashed line represents the LOD of this assay.

4.3 Discussion

Previous studies have investigated the importance of neutralizing mAbs in protection from lethal RVFV disease. Neutralizing mAbs raised against Gn or Gc protect by various mechanisms of virus neutralization, including the blocking of attachment, entry, or fusion (168-171). When each mAb described in this study was mapped to its Gn binding domain, all except mAb-2 were found to bind linear epitopes. This overwhelming recognition of linear epitopes was not surprising,

as the immunogen was produced in bacteria and may not have had its native confirmation. The mAbs in this study bound to epitopes across the three domains of Gn, with the highest neutralizer (mAb-1) binding a new site of vulnerability in domain B. This domain has been suggested as an immunodominant region of Gn, with others having mapped protective mAbs to this region (168). Other work has identified domain A as a hot spot for binding of highly neutralizing mAbs (169, 171). The lowest of the three neutralizers, mAb-3, bound a new site of vulnerability in domain A distinct from those for previously identified mAbs. These novel protective epitopes point to the probability that the entire outward facing surface of Gn can be targeted by mAbs to elicit protection in vivo.

Despite published work regarding RVFV-neutralizing Abs providing protection from disease, the reliance on Fc effector function for delivering said protection was not previously assessed. This study investigated the role of Fc effector functions in mAb-mediated RVFV protection using the divergent effector function strengths of IgG subclass mAbs. A panel of mAbs was developed against the RVFV Gn glycoprotein, and each mAb was cloned to be both IgG1 and IgG2a subclass. When administered to mice pre-challenge, protection from RVFV disease was enhanced by IgG2a subclass mAbs.

Indeed, protection from lethal RVFV challenge was dependent on the functions provided by the IgG2a Fc domain, as mAb-1, -2, and -3 only afforded complete protection when administered as the IgG2a subclass. A significant difference in survival was seen between mAb-3 IgG2a- and IgG1-treated groups (Mantel-Cox test P = 0.0005) (**Figure 27C, 31C**). mAb-1 and -2 did not show a statistically significant difference in survival between subclasses, but IgG2a-administered mice were provided a clear survival advantage. Lack of statistical significance between subclasses for mAb-1 and -2 was likely due to relatively small sample sizes. MAb-3

provided the greatest increase in protection when the subclass was switched to IgG2a, with survival outcomes changing from 0% to 100%. This large increase was ostensibly due to mAb-3 being the lowest level neutralizer, as all three partially protective IgG1 mAbs elicited similar levels of NK cell degranulation. This suggests that humoral protection from RVFV likely requires a level of contribution from non-neutralizing mechanisms that changes depending on the neutralizing strength of the response.

The protective capacity of each mAb was unequally enhanced, however, when given as the IgG2a version. MAb-4, -5, and -6 failed to protect mice from death regardless of antibody subclass. This difference in protection between mAbs could be due to the lower binding affinity of mAb-4, -5, and -6. Binding with high enough affinity to the antigen to induce immune complex formation is known to be crucial for the activation of Fc effector functions (220, 221). The inability of mAb-4, -5, and -6 to protect mice could alternatively be due to their non-neutralizing status. Optimal protection from RVFV may require both neutralization and Fc-dependent effector functions, as seen for other viruses (139, 141, 222). Future work is required to test whether non-neutralizing mAbs with strong Gn binding affinity can protect from RVFV in vivo.

In addition to increasing survival, IgG2a mAbs also seemed to control viral infection more efficiently. Viral RNA was detected at day 28 at low levels in IgG1 mAb-1 and -2 surviving mice. Contrastingly, RNA levels were below the LOD for survivor mice treated with the IgG2a version. Decreased viral titers were also seen in the brains of mice treated with the nonprotective, non-neutralizing IgG2a version of mAbs-4, -5, and -6. This might suggest increased control of viral replication and/or spread to the brain by IgG2a mAbs. This accelerated viral clearance by IgG2a mAbs may mitigate the development potential of late-onset encephalitis. Individuals presenting for care with RVF are typically well into the disease course. Therefore, it will be important to

determine if mAb therapy can prevent progression to late-onset encephalitis and the role of Fc effector functions therein, as this is where mAbs have the most human promise. Recent work in humans found that the antibody response to naturally acquired infection preferentially targets Gn, with neutralizing anti-Gn IgG responses lasting decades (223). Future investigation into the contribution of Fc effector functions in the human humoral response could further increase understanding of how antibody-mediated immunity protects against RVFV disease.

5.0 Materials and Methods

5.1 Ethics Statement and Biosafety Information

All research in this study was conducted under the oversight of the University of Pittsburgh IACUC (protocol 19044158). All experiments with wild-type RVFV ZH501 strain were performed in the University of Pittsburgh Regional Biocontainment Laboratory (RBL) Biosafety Level 3 (BSL-3) and Animal Biosafety Level 3 (ABSL-3) facilities.

5.2 Virus Generation, Growth, and Titer

The WT ZH501 strain of RVFV was originally isolated from a febrile human during the 1977 Egyptian epidemic (71). For these studies, recombinant WT, DelNSs, and DelNSs/DelNSm RVFV was generated using reverse genetics based on the ZH501 strain background (224, 225). Virus stocks were grown to passage 2 and fully sequence confirmed using next-generation sequencing prior to use. Viral titer of the passage 2 stock was determined using a standard tissue culture infective dose 50 ($TCID_{50}$) assay. Briefly, viral stocks were serially diluted in Dulbecco's Modified Eagle Medium (DMEM) then added to 96-well plates containing 1×10^4 Vero-E6 cells/well (eight replicates per viral dilution). Titers were determined through visualization by indirect fluorescent antibody assay (IFA) using a 1:500 dilution of a custom RVFV anti-N polyclonal #5584 (Genscript) as primary antibody and a 1:500 dilution of anti-rabbit 488

(Invitrogen) as secondary antibody. $TCID_{50}$ titers were calculated using the Reed and Muench calculations (226).

5.3 Collaborative Cross Founder Strains Mouse Study Design

Six to eight-week-old female and male A/J (stock #000646), C57BL/6J (stock #000664), 129S1/SvlmJ (stock #002448), NOD/ShiLtJ (stock #001976), and NZO/HILtJ (stock #002105) inbred mice were purchased from Jackson Laboratories. All mice were housed in HEPA filtration racks in the RBL's ABSL-3 facility and provided ad lib access to food and water. All mice were infected with recombinant wild-type RVFV ZH501 strain under isoflurane anesthesia via left rear footpad (FP) injection to imitate a mosquito bite. Viral infection doses in these studies ranged from 0.2 to 2,000 $TCID_{50}$ per animal, which equates to doses ranging from 0.138 to 1,380 PFU per animal (0.69 $TCID_{50}$ = 1 PFU; Poisson distribution based upon (226)). Mice received a 20 µl injection of virus diluted in sterile phosphate buffered saline (PBS). For all experiments, daily weights were recorded, and mice were evaluated at least once daily for clinical signs of disease. Mice were euthanized according to a predetermined clinical scoring method (**Table 3**). At the time of euthanasia, mice were anesthetized with isoflurane and blood was collected via cardiac puncture. Following cervical dislocation, liver, spleen, brain, and testes (where applicable) were collected for subsequent RNA extraction and viral RNA load quantitation.

Table 3 RVFV-specific mouse clinical scoring system

Clinical Symptom	**Score** *Scores ≥ 10 will result in immediate euthanasia
• Hunched back • Ruffled coat/piloerection • Huddling	2 points each
• Ataxia • Circling • Weakness • Shaking • Tremors • Dehydration (eye recession)	3 points each
• Anemia (pale mucous membranes, pale footpads) • Abnormal breathing (dyspnea, tachypnea, rales/audible breaths)	5 points each
• Hemorrhage/bleeding • Paralysis • Moribund • Unresponsive	10 points each
• >20% weight loss	Immediate euthanasia

5.4 Collaborative Cross Mouse Strain Screening

All Collaborative Cross mice used in this study were obtained from the Systems Genetics Core Facility at the University of North Carolina (227). Previous to their relocation to UNC, CC lines were generated and bred at Tel Aviv University in Israel (228), Geniad in Australia (229) and Oak Ridge National Laboratory in the US (230). Mice used in this study: 4- to 12-week-old female CC001/Unc, CC005/TauUnc, CC011/Unc, CC013/GeniUnc, CC023/GeniUnc, CC027/GeniUnc, CC028/GeniUnc, CC030/GeniUnc, CC031/GeniUnc, CC035/Unc, CC039/Unc, CC042/GeniUnc, CC044/Unc, CC058/Unc, CC060/Unc, CC062/Unc, CC068/TauUnc, CC071/TauUnc,

CC078/TauUnc, and female and male CC057/Unc. All mice were housed in HEPA filtration racks with ad lib access to food and water. Mice were infected with 2 $TCID_{50}$ recombinant WT RVFV ZH501 strain diluted in PBS under isoflurane anesthesia via left rear FP injection to model a mosquito bite. For all experiments, mice were weighed and evaluated daily for clinical signs of disease and euthanized according to a predetermined clinical scoring method (**Table 3**). At 2 dpi, blood was drawn via lateral saphenous bleed for quantification of viral RNA. At the time of euthanasia, mice were anesthetized with isoflurane and blood was collected via cardiac puncture for qRT-PCR, ELISA, FRNT, CBC, and CHEM. CBC and CHEM data were analyzed using a VETSCAN HM5 hematology analyzer (Abaxis) and a VETSCAN VS2 chemistry analyzer (Abaxis) using the Mammalian Liver Profile reagent rotor, respectively. Following cervical dislocation, liver, spleen, kidney, small intestine, eye, and brain were collected in PBS supplemented with antibiotics and antimycotic (Invitrogen).

5.5 Serial Euthanasia of C57BL/6 and CC057 mice

4- to 12-week-old female and male C57BL/6J (stock #000664) mice, purchased from Jackson Laboratories, and 4- to 12-week-old female and male CC057/Unc mice were infected with 2 $TCID_{50}$ recombinant WT RVFV ZH501 strain as above or mock-infected with PBS to serve as negative controls. C57BL/6J mice were euthanized at 0.5, 1, 2, and 3 dpi. CC057/Unc mice were euthanized at 0.5, 1, 2, 3, 5, 7, 9, 10, and 11 dpi. At each timepoint, blood, tissue samples, and whole organs were collected from both infected and mock-infected animals. Blood was taken for qRT-PCR, CBC, CHEM, and multiplex assays. Tissue samples were taken for quantification of viral RNA in order (liver, spleen, right sciatic nerve, left sciatic nerve, upper spinal cord section,

middle spinal cord section, and lower spinal cord section, brain) with instruments cleaned in ethanol between each harvest. Whole organ tissue sampling order: liver, spleen, and brain whole organs were collected and fixed in 10% formalin for pathological analysis.

5.6 RNA Extraction and Quantitative PT-PCR

Mouse tissue samples were weighed and then homogenized in sterile PBS with 1X Antibiotic- Antimycotic (Gibco) using a D2400 Homogenizer (Benchmark Scientific). RNA was extracted from tissue, serum, and plasma samples with TRIzol reagent (Ambion) following the Direct-zol RNA purification protocol (Zymo Research). Quantitative RT-PCR (qRT-PCR) targeting the L segment of RVFV (231) was performed using the SuperScript III Platinum One-Step qRT-PCR kit (Thermofisher). T7 driven RVFV L RNA template of known quantity was serially diluted to generate a RVFV RNA standard curve. This template RNA was made by In-Fusion cloning (Takara Bio), a fragment of the ZH501 RVFV L segment into pET-9a (Millipore Sigma). To generate linear pET-9a primers 5'-AATCCTCAAACTTCT GGGAAACCGTTGTGGTC-3' and 5'-TTCAAAGCTTATCATT CTAGAAATAATTTTGTTTAACTTTAAGAAGGA-3' were used. To prepare the RVFV L segment fragment primers 5'-AA AATTATTTCTAGAATGATAAGCTTTGAAGAGATCCAT-3' and 5'-CCACAACGGTTTCCCAGAAGTTTGAGGATTGTATGA GG-3' were used. The resultant plasmid, pLquant, was gel purified and linearized with XbaI (New England Biolabs), and then used as template in a TranscriptAid T7 High Yield in vitro transcription reaction (Thermo Scientific). Product RNA was purified using the GeneJET RNA Purification kit (Thermo Scientific), and then diluted to known copies/ml in RNase-free water for use as qRT-PCR standard

curve template. The assay was performed using a C1000 Touch Thermo Cycler/CFX96 Real-Time System (Bio-Rad) under the following reaction conditions: 50°C for 15 min, 95°C for 3 min, and then 40 cycles of 95°C for 15 s and 55°C for 1 min. RNA copies for each unknown sample were normalized by tissue weight and are reported as log viral RNA copies per milligram of tissue or ml or serum/plasma. The LOD was calculated as the highest threshold cycle (CT) value detected in the standard curve multiplied by 50, to account for dilutions, and divided by the average sampled tissue weight.

5.7 Enzyme-Linked Immunosorbent Assay

For total anti-RVFV ELISA, MaxiSorp plates (Thermo Scientific) were coated with lysate, diluted 1:1,000 in PBS, from RVFV-infected Vero-E6 cells or with lysate from uninfected Vero-E6 cells to act as a negative control (232). For anti-RVFV N and Gn protein ELISA, MaxiSorp plates (Thermo Scientific) were coated with 200 ng/well of purified RVFV N or Gn protein (custom; GenScript). Plates were left at 4°C overnight, and then blocked in blocking buffer (5% non-fat milk in PBS-0.1% Tween 20) at 37°C for 1 h. Terminal mouse serum/plasma samples were serially diluted in blocking buffer, and then incubated on blocked plates at 37°C for 2 h. All serum/plasma samples were assayed in duplicate alongside normal mouse serum as a negative control. After incubation with sera/plasma, plates were washed three times with PBS-0.1% Tween 20 (PBST), and then incubated for 1 h at 37°C in anti-mouse IgG-HRP (Jackson ImmunoResearch) diluted 1:5,000 in blocking buffer. Following three PBST washes, the plates were incubated in tetramethylbenzidine (TMB) substrate, and then stopped with TMB stop solution. Plates were read at 450 nm and the raw data were analyzed in Excel by subtracting the negative control absolute

values from those of the RVFV lysate plate. Endpoint ELISA titers for lysate and anti-N protein ELISAs were defined as the highest dilution of serum/plasma that resulted in an OD value at least two standard deviations above the average obtained from all negative mouse serum control wells. EC_{50}s were calculated by fitting raw OD ELISA data, in triplicates, with a nonlinear least-squares regression best fit curve.

5.8 Foci Reduction Neutralization Test

Mouse serum/plasma or mAb was serially diluted, in duplicates, and incubated with 200 foci-forming units of DelNSs/DelNSm RVFV as described previously (233). Foci were detected using Moss TMB-H peroxidase substrate (MossBio) and counted using an immunospot reader (CTL). Percent neutralization was calculated by comparing sample wells to wells containing virus but no serum/plasma/antibody. The concentration of mAb or dilution of serum/plasma at which 50% of foci were neutralized is reported as $FRNT_{50}$.

5.9 Histopathology

Fixed liver, spleen, and brain tissues were processed, paraffin embedded, and sectioned using standard methods. Tissues were stained with hematoxylin and eosin (H&E) for visualization. IHC assays were performed through the Pitt Biospecimen Core. Tissues were evaluated for anti-RVFV immunoreactivity using a polyclonal anti-N protein rabbit antibody (1:200, Genscript,

custom). Appropriate negative control tissues were included at each timepoint for each mouse strain.

5.10 Multiplex Assays

Plasma samples collected during the CC057 versus C57BL/6 serial euthanasia experiment, from both mock-infected and RVFV-infected mice, were analyzed using commercial multiplex assays according to the manufacturer's instructions. 32 analytes were assessed in 8 commercially available assays. Millipore assays: thirteen-plex assay for keratinocyte chemoattractant (KC), monokine induced by gamma interferon (MIG, CXCL-9), monocyte chemoattractant protein 1 (MCP-1, CCL2), interferon gamma-induced protein 10 (IP-10, CXCL-10), interleukin 1 alpha (IL-1α), interleukin 10 (IL-10), regulated on activation normal T-cell-expressed and secreted (RANTES, CCL-5), interleukin 6 (IL-6), tumor necrosis factor alpha (TNFα), macrophage inflammatory protein-1 alpha (MIP-1α, CCL3), macrophage inflammatory protein-1 beta (MIP-1β, CCL4), interferon gamma (IFN-γ), and interleukin 9 (IL-9); seven-plex assay for E-Selectin, intercellular adhesion molecule (ICAM), platelet endothelial cell adhesion molecule (Pecam-1), P-Selectin, plasminogen activator inhibitor-1 (PAI-1), matrix metallopeptidase 9 (MMP-9), and Thrombomodulin; four-plex assay for interferon beta (IFN-β), Fractalkine, macrophage-derived chemokine (MDC, CCL22), and macrophage inflammatory protein-3 (MIP-3β, CCL19); two-plex assay for angiopoietin-2 (Ang-2) and hepatocyte growth factor (HGF); two-plex assay for tumor necrosis factor receptor I (TNFRI) and tumor necrosis factor receptor II (TNFRII); two-plex assay for interleukin 28 (IL-28B) and CD40L. ThermoFisher assays: single-plex assays for C-reactive protein (CRP) and interferon alpha (IFN-α). Data were collected on a Bio-Plex 200 (Bio-Rad)

instrument. All assay results were reported either as raw data or as the difference from the mean of mouse strain-specific mock infected samples (shown as either pg/mL or mg/dL).

5.11 Monoclonal Antibody Generation

Custom mouse hybridomas were generated commercially by GenScript. Briefly, 5 BALB/c and 5 C57BL/6 mice were immunized 3 times with bacterially produced RVFV Gn protein. Splenocytes from three mice with the highest RVFV Gn-specific ELISA titers were fused to SP/0 myeloma cells to generate hybridomas. Hybridoma supernatants were screened for antibody reactivity via ELISA and FRNT. Six hybridoma clones, naturally derived as 1 IgG2a and 5 IgG1, spanning a range of neutralization and binding abilities were selected for antibody production and purification. Antibody variable domains were sequenced and cloned into heavy and light chain expression plasmids pFUSEss-CHIg- mG1/pFUSEss-CHIg-mG2a and pFUSE2ss-CLIg-mk (InvivoGen). Heavy and light chain plasmids were cotransfected into FreeStyle 293-F suspension cells using 293fectin. Cells were cultured in FreeStyle 293 expression medium (Thermo Fisher) for 4 days. Secreted Abs were purified by protein G affinity chromatography from cell supernatants (Thermo Fisher).

5.12 Monoclonal Antibody Domain Mapping

Gn truncations (**Figure 26**) were cloned into pcDNA3.1 under the cytomegalovirus (CMV) promoter and then transfected into Vero-E6 cells. Lysates were harvested at 48 h in 50 mM

dithiothreitol LDS buffer (Thermo Fisher). Samples were heated at 70°C and then loaded into 4 to 12% bis-Tris gels (Thermo Fisher). Proteins were transferred to nitrocellulose membranes using a Mini Blot module wet transfer system (Thermo Fisher). Membranes were blocked in 5% nonfat dry milk (NFDM) in phosphate-buffered saline with 0.1% Tween 20 (PBST) for 1 h and then probed with each anti-Gn MAb, diluted 1:1,000. Bound MAbs were detected using anti-mouse IgG conjugated to horseradish peroxidase (HRP) (Jackson ImmunoResearch), diluted 1:15,000. Membranes were incubated in SuperSignal West Dura extended duration substrate (Thermo Fisher) for 2 min before exposure to CL-XPosure Film (Thermo Fisher) and developed using an SRX-101A film processor (Konica Minolta).

5.13 Monoclonal Antibody Epitope Mapping

Overlapping peptides with >70% purity (15-mers with 11-aa overlaps) were generated to span RVFV Gn (GenScript). MaxiSorp plates (Thermo Fisher) were coated one peptide per well with 1 mM each Gn peptide. Plates were incubated at 4°C overnight and then blocked in 1% bovine serum albumin (BSA) in PBST (0.01%) at 37°C for 1 h. After washing in 0.05% PBST, 0.25 µg/ml of each MAb was incubated on blocked plates at 37°C for 2 h. Plates were washed and then incubated for 1 h at 37°C in anti-mouse IgG-HRP (Jackson ImmunoResearch) diluted 1:5,000. Plates were developed in tetramethylbenzidine (TMB) and stopped with TMB stop solution (Seracare). Plates were read at 450 nm, and wells were considered positive if the raw optical density (OD) was >1.

5.14 Monoclonal Antibody Treatment Mouse Study Design

Six- to 8-week-old female C57BL/6J (stock number 000664) mice were purchased from Jackson Laboratories. Mice were housed in HEPA filtration racks with ad lib access to food and water. Mice were administered 400 µg of MAb or 200 µl of RVFV immune serum (derived from mice vaccinated with either DelNSs or DelNSs/DelNSm RVFV) by intraperitoneal (i.p.) injection 48 h pre-challenge. Isotype control MAbs were InVivoPlus mouse isotype control, unknown specificity (IgG1 clone MOPC-21, IgG2a clone C1.18.4; BioXcell). Twenty-four hours post-MAb administration, serum was obtained via lateral saphenous bleed. Following infection by footpad injection with 200 $TCID_{50}$ recombinant WT RVFV, mice were evaluated for clinical signs of disease and weighed daily (**Table 3**).

5.15 Antibody-dependent Cellular Cytotoxicity

Three micrograms per milliliter RVFV Gn protein (custom; GenScript)-coated MaxiSorp plates (Thermo Fisher) were blocked with 5% BSA in PBST (0.01%) for 1 h at 37°C. MAbs were added to wells at 5 µg/ml and incubated for 2 h at 37°C. NK cells were isolated by negative selection from C57BL/6 mouse spleens using EasySep mouse NK cell isolation kit (StemCell Technologies). Purified NK cells were added at $2x10^5$ cells/well in the presence of brefeldin A (Sigma-Aldrich), GolgiStop (BD), and anti-CD107a conjugated to phycoerythrin (PE) (BioLegend clone 1D4B) to wells already containing Gn/MAb. NK cells were incubated for 5 h at 37°C. Cells were then washed and stained with near-infrared (IR) fluorescent reactive dye (Thermo Fisher). Cells were stained for cell surface markers CD3 allophycocyanin (APC)-Cy7 (BioLegend clone

17A2), CD11b fluorescein isothiocyanate (FITC) (BioLegend clone M1/70), and NK1.1 APC (BioLegend clone PK136). The purity of NK cells was confirmed by CD3 APC (BioLegend clone 17A2), CD19 BV421 (BioLegend clone 6D5), NKp46 PE-Cy7 (Biolegend clone 29A1.4), and CD14 APC-Cy7 (BioLegend clone Sa14-2) staining. All cells were fixed in BD Cytofix/Cytoperm and then analyzed by flow cytometry on a BD LSRFortessa flow cytometer. All flow cytometric data were analyzed using FlowJo 10.7.1.

5.16 Statistical Analysis

All data were entered into GraphPad Prism 8 or 9 for statistical analysis and generation of graphs. qRT-PCR data were analyzed in Excel. Specific statistical tests for each data set are indicated in the figure legends. A $p \leq 0.05$ was considered statistically significant.

6.0 Summary and Future Directions

RVFV is a global public health concern for its ability to cause severe disease in both humans and livestock, its ability to disrupt global economies, and its potential for introduction into naïve populations. To combat the threat posed by this virus, we must fill key gaps in our understanding of viral pathogenesis while simultaneously developing and understanding the mechanisms behind novel therapeutics. Therefore, in this dissertation I aimed to add to the RVFV field by pursuing two independent but related arms of study: 1) furthering our understanding of RVFV pathogenesis by discovering and characterizing a novel model of RVF encephalitis and 2) developing and characterizing novel therapeutic monoclonal antibodies.

In Chapter 2, I began my work by evaluating the pathogenesis and severity of RVFV in 5 common inbred mouse strains, concluding that RVFV is overwhelmingly lethal in inbred mice. I investigated mouse strain, viral dose, sex, weight loss, and viral load following challenge with the wild-type ZH501 strain of RVFV. All 5 mouse strains (C57BL/6J, 129S1/SvlmJ, NOD/ShiLtJ, A/J, and NZO/HILtJ) developed severe early hepatitis with complete lethality observed down to a dose of 2 $TCID_{50}$. This is consistent with other published studies using different strains of inbred mice (95-97).

The Chapter 2 study and all other work presented in this dissertation used a recombinant reverse genetics-generated strain of RVFV. Sequence confirmed, early passage recombinant RVFV (rRVFV) made by reverse genetics offers far greater reproducibility (224, 225). This is especially essential when evaluating novel mouse strains for their susceptibility to RVFV (179). Reverse genetics-derived stocks that exclude the possibility of distinct viral subpopulations being present are essential to obtain reliable lethality in mouse challenge studies, such as the ones

presented here. However, future experiments could benefit from the development of a reverse genetics-derived RVFV strain based directly on a human isolate. Although the original ZH501 RVFV strain was isolated from a human patient in 1977, it was passaged hundreds of times in animals and cell lines in the decades following isolation before being sequenced. Therefore, the ZH501 WT virus used in this study, produced via reverse genetics using the recent viral sequence, does not represent the most clinically relevant human isolate. To develop a more clinically relevant RVFV strain, RVFV should be immediately sequenced when isolated from a patient. My lab is currently undertaking the sequencing of a RVFV strain recently isolated from a patient in Uganda. This sequence will be used to develop a reverse genetics system for production of a clinically relevant RVFV viral stock for use in future studies.

Sex significantly influences infectious disease pathogenesis and severity for some microbes (184, 185). Males and females of numerous species differ in disease severity to various viral pathogens due to differences in their immune response potentials and general hormone environments (186, 187). The influences of sex on the severity of viral disease are complex and thus must be investigated for each individual pathogen. Little data exist on the importance of sex in the context of RVFV infection in mice. Historic RVFV studies have used both sexes of mice, but few have directly compared females and males in the same study. In the study in Chapter 2, both females and males of the five inbred mouse strains were challenged with the same doses of RVFV. There was no significant difference in survival curves or time to death between female and male mice.

These data differed from that presented by Tokuda et al. who found that sex influenced susceptibility to RVFV in MBT and BALB/c mice (191). Differences in the amount of influence attributable to sex between ours and other's research could be caused by a variety of factors. These

include the mouse strains used, the RVFV challenge strain, the age of the mice, the power of the study, and whether reverse-genetics derived virus or passaged isolate is used for challenge. Additionally, the mouse microbiome could differ between research sites due to environmental factors. This could skew results, as the mouse microbiome has been shown to influence severity of various infectious diseases (192-194). The five mice per group used in the studies in Chapter 2 are not of sufficient power to conclude a total absence of sex differences in RVFV infection. However, even with small sample sizes, the uniform lethality seen in both sexes suggests that it would be a reasonable approach to use only one sex for initial survival studies in future experiments. Therefore, in Chapter 3, I decided to only assess RVFV susceptibility in female mice for the initial 20 CC strain challenge experiment, saving both time and resources. However, I did investigate potential sex differences within the CC057 encephalitis strain and did not find any relevant differences. In the context of future vaccine and therapeutic studies, it would still be reasonable to evaluate both sexes for potential subtle variation in responses that could be revealed with a more highly powered study.

From the work presented in Chapter 2, it is clear that the five inbred mouse strains used in that study do not contain adequate genetic diversity to elicit increased resistance to RVFV infection or a skewing toward different manifestations of RVF disease. It is for this reason that I next assessed RVFV pathogenicity in the CC mouse resource (Chapter 3). CC mice are derived from 8 founder strains, 3 of which are wild-derived (PWK/EiJ, CAST/EiJ, and WSB/EiJ), and therefore contain more genetic diversity than commonly used laboratory mice. Infection with RVFV in 20 recombinant inbred CC mice revealed novel manifestations of RVF in multiple strains. All 20 CC strains were characterized through clinical, virologic, immunologic, hematologic, and metabolic readouts. After this initial assessment, an in-depth characterization of the novel CC057 RVF

encephalitis model was completed demonstrating resistance to liver disease but susceptibility to CNS disease within this mouse strain. The CC resource allows us to link identified outcome to host genotype, therefore future work should focus on identifying genes associated with various RVF clinical outcomes. The CC057 model described in Chapter 3 will enable immediate investigation into the identification of the genetic basis for disease variation, the pathogenesis of RVF CNS disease, and evaluation of therapeutic strategies targeted towards prevention or treatment of RVFV encephalitis.

In Chapter 3, all CC strains, regardless of disease phenotype, succumbed to RVFV infection despite all containing a functional Mx1 locus. Wild-derived, thus functional, Mx1 has been correlated with increased resistance to influenza A virus in mice and is also known to inhibit viral replication (177, 198). Additionally, the human homologue MxA has been shown to inhibit Bunyaviruses in vitro including RVFV (181). Knowing that most inbred mice contain a non-functional Mx1 locus, we hypothesized that CC strains containing functional Mx1 would show increased resistance to RVFV challenge (182, 199). However, the universal lethality of RVFV in the 20 CC strains eliminates Mx1 as the main host genetic factor responsible for mouse susceptibility to RVFV. As Mx1 was found to also not be responsible for RVFV divergence between hepatitis and encephalitis, it is possible that I missed CC strains containing important genetic contributions to RVF disease phenotypes. Therefore, immediate future work should focus on the evaluation of RVF disease in additional CC strains with the goal of identifying novel RVF phenotypes.

Following phenotyping of additional CC strains, genetic mapping should be performed to identify quantitative trait loci (QTL). QTL mapping would be performed using established methods with the goal of identifying polymorphic genome regions associated with the observed

divergent clinical outcomes following RVFV infection (182, 234). Future linkage disequilibrium mapping studies will be performed in collaboration with our collaborators at the University of North Carolina. Upon identification of loci associated with RVF phenotypes, genes within the loci should be studied for their potential contribution to RVF clinical phenotypes. I hypothesize that genes involved in innate immunity or RNA sensing pathways will be identified from QTL studies comparing hepatic and encephalitic CC mouse strains. Upon the identification of candidate genes responsible for the divergence between hepatic and encephalitic manifestations, a myriad of experiments could be performed to confirm their importance in defining RVF phenotype in the mouse. Important first experiments with genes of interest could include the assessment of transcript and protein level differences between CC057 and C57BL/6 mouse livers. Protein overexpression and knockout experiments could also be performed in liver cell lines to assess each gene of interest's anti-RVFV properties.

The CC057 model identified and detailed in Chapter 3 provides a critical tool for elucidating factors that control viral infection in the liver and provides a tractable murine model in which the route of virus entry into the brain can be dissected. Despite the ability to bypass severe liver damage, CC057 mice were unable to prevent progression to CNS invasion and subsequent death. In the CC057 model, progression to late-stage disease was marked by simultaneous clearance of viral RNA from the liver and viral invasion into the CNS by 7 dpi. High viral RNA loads in the brain at 7 dpi and onward were accompanied by cortical lesions and high brain antigen staining. The method of CNS invasion by RVFV has been elucidated for some models of RVF disease. In animals given RVFV by intranasal or aerosol challenge, RVFV first infects the olfactory bulb and then spreads caudally into the cerebrum and cerebellum (78, 99, 201). However, the method of viral entry into the brain is unknown for infection that begins at the periphery such

as a mosquito bite or FP injection. One possible route of brain entry from an initial peripheral challenge is retrograde neuronal transport. Viral trafficking up a peripheral nerve is known to be a main method of CNS entry for rabies virus (202-204). However, in CC057 mice, viral RNA appeared earliest at very low levels in spinal cord sections at 3 and 5 dpi. At 7 dpi, brain and spinal cord sections peaked with high viral RNA titers while the sciatic nerves remained near the LOD for viral RNA until 9-11 dpi. These data suggest that trafficking via the sciatic nerve is not the mode of viral entry into the CNS for the CC057 encephalitis model.

To confirm that RVFV does not traffic from the site of infection via a peripheral nerve to invade the CNS, sciatic nerve dissection experiments could be performed in the novel CC057 model. If nerve ligation prior to RVFV challenge resulted in a lack of viral brain invasion, it could be concluded that the means of RVFV entry into the brain is via the sciatic nerve. However, if virus was still able to invade the CNS in a nerve ligated mouse, other methods of CNS viral entry should be investigated. The lack of overwhelming increases in measured blood inflammatory markers before virus is detected in the brain at 7 dpi in CC057 mice suggests that RVFV gains entry to the brain without the need for BBB breakdown. Peaks in markers signaling potential BBB breakdown such as total PAI-1, MMP-9, and thrombomodulin do not occur until 9 dpi during the endpoint of disease (205). These findings are supported by work in various animal models detailing that BBB breakdown is not required for RVFV entry into the brain and often only occurs late in the course of disease after the virus has already caused severe brain damage (78, 206). Therefore, the likely alternative routes of RVFV entry into the brain are infection of brain microvascular endothelial cells (BMECs) or infection of leukocytes with subsequent trafficking into the brain. WNV, Japanese encephalitis virus, and alphaviruses are all able to cross BMECs to invade the brain (235-237). Leukocytes are known targets of RVFV infection and have been shown to carry

other viruses into the brain (238). A BMEC in vitro model could be used to determine if RVFV can infect and/or transcytose across BMECs. To assess the reliance on leukocyte infection for access to the CNS, CC057 mice could be depleted of their neutrophils via anti-Ly6G treatment, depleted of their mononuclear phagocytic cells via clodronate liposome treatment, or depleted of both via combination treatment (239, 240).

In Chapter 3, none of the 20 challenged CC mouse strains were able to prevent or overcome CNS disease despite their ability to produce anti-RVFV neutralizing antibodies by their time of death. This is likely due to the timing of the humoral response. Neutralizing antibody titers against RVFV did not appear in terminal mice until 8 dpi while virus was present at high levels in the brains of CC057 mice by 7 dpi as assessed by qRT-PCR and IHC. It is therefore possible that brain damage is too severe by the time a humoral response is mounted or that antibodies are not able to effectively clear virus from the brain once RVFV has reached the brain parenchyma. It is known that passively transferred humoral immunity can prevent RVFV hepatitis in multiple mouse models when administered pre-challenge. What is unknown is whether pre-challenge or post-challenge transfer of RVFV immune serum or monoclonal antibodies could prevent CNS disease development. CNS disease prevention is a difficult task given the challenges of accessing the CNS through the BBB. It is therefore possible that passively transferred humoral immunity will only be effective pre-challenge or very early in disease. Our development of the CC057 mouse strain as a late-onset encephalitis model enables testing of the protective efficacy of humoral immunity against CNS disease. Future work should therefore assess the protection afforded by immune serum or monoclonal antibody transfer both pre- and post-RVFV challenge. Studies should aim to determine both the lowest doses necessary for protection and the latest timepoint post-infection where treatments can be delivered to elicit effective protection.

Finally, in Chapter 4 I developed 6 monoclonal antibodies against RVFV Gn with three showing therapeutic potential. To investigate the contribution of Fc effector functions in antibody mediated RVFV protection, mAbs were subclass switched to produce IgG1 and IgG2a versions. IgG1 subclass mAbs provided incomplete protection from RVFV disease in vivo. However, administration of IgG2a subclass mAbs increased protection to 100% for the three most promising candidates. These results indicate that Fc-effector mechanisms are key components of humoral protection from RVF.

The work in Chapter 4 demonstrated a dependence on the functions provided by the IgG2a Fc domain for eliciting protection from lethal RVFV challenge. For the three most promising mAbs developed in this study, mAb-1, -2, and -3, only afforded complete protection when administered as the IgG2a subclass. A significant difference in survival was seen between mAb-3 IgG2a- and IgG1-treated groups. Although mAb-1 and -2 did not show a statistically significant difference in survival between subclasses, IgG2a-administered mice were provided a clear survival advantage. The relatively small sample sizes were likely responsible for the lack of statistical significance between subclasses for mAb-1 and -2. MAb-3 provided the greatest increase in protection when the subclass was switched to IgG2a, with survival outcomes changing from 0% to 100%. This large increase was ostensibly due to mAb-3 being the lowest level neutralizer, as all three partially protective IgG1 mAbs elicited similar levels of NK cell degranulation. This suggests that humoral protection from RVFV likely requires a level of contribution from non-neutralizing mechanisms that changes depending on the neutralizing strength of the response.

Although IgG2a versions enhanced protection for mAbs -1, -2, and -3, mAbs -4, -5, and -6 failed to protect mice from death regardless of antibody subclass. This difference in protection between mAbs could be due to the lower binding affinity of mAb-4, -5, and -6. The induction of

immune complex formation through high affinity antigen binding is known to be crucial for the activation of Fc effector functions (220, 221). The inability of mAb-4, -5, and -6 to protect mice could alternatively be due to their non-neutralizing status. Optimal protection from RVFV may require both Fc-dependent effector functions and neutralization, as has been seen for other viruses (139, 141, 222). Future work is required to test whether non-neutralizing mAbs with strong Gn binding affinity could offer protection from RVFV in vivo. To test this, anti-Gn mAbs should be developed to bind Gn with high affinity and be non-neutralizing. If, upon administration of these non-neutralizing antibodies, mice survive challenge it could be concluded that neutralization is not necessary for antibody mediated RVFV protection. This is a distinct possibility as completely non-neutralizing mAbs have been found to be protective for other viruses including EBOV and alphaviruses (139, 241). However, it is also possible that antibody mediated RVFV protection depends on some level of neutralization. Future work should also utilize the newly developed CC057 encephalitis model to test the efficacy of various cocktails of antibodies at preventing CNS disease. Combining neutralizing and non-neutralizing mAbs is a classic way of eliciting increased protection; therefore, it is possible that a cocktail therapeutic approach would enable successful treatment later in the course of infection.

Individuals presenting for care with RVF are typically well into the disease course. Therefore, it will be important to determine if mAb therapy can prevent progression to late-onset encephalitis and the role of Fc effector functions therein, as this is where mAbs have the most human promise. Recent work in humans found that the antibody response to naturally acquired infection preferentially targets Gn, with neutralizing anti-Gn IgG responses lasting decades (223). Future investigation into the contribution of Fc effector functions in the human humoral response

could further increase understanding of how antibody-mediated immunity protects against RVFV disease.

The results from my dissertation serve as a launching point for future work, providing both a novel mouse model and newly developed therapeutics. Future studies should use the CC057 mouse model to uncover the genetic basis for RVF disease variation, to increase our understanding of RVFV pathogenesis, and to test the efficacy of promising therapeutics against RVF encephalitic disease. Overall, my research answers many questions about the pathogenesis of RVFV in the mouse, but more importantly, this work has produced both a novel model of RVF encephalitis and multiple monoclonal antibody therapeutic candidates.

Bibliography

1.Daubney R HJ. Enzootic hepatitis or Rift Valley Fever: an undescribed virus disease of sheep, cattle, and man from east Africa. J Path Bact. 1931;34:545–579.

2.Weaver SC, Reisen WK. Present and future arboviral threats. Antiviral Research. 2010;85(2):328-45.

3.Hartley DM, Rinderknecht JL, Nipp TL, Clarke NP, Snowder GD. Potential effects of Rift Valley fever in the United States. Emerg Infect Dis. 2011 Aug;17(8):e1.

4.Laughlin LW, Meegan JM, Strausbaugh LJ, Morens DM, Watten RH. Epidemic Rift Valley fever in Egypt: observations of the spectrum of human illness. Trans R Soc Trop Med Hyg. 1979;73(6):630-3.

5.Laughlin LW, Girgis NI, Meegan JM, Strausbaugh LJ, Yassin MW, Watten RH. Clinical studies on Rift Valley fever. Part 2: Ophthalmologic and central nervous system complications. J Egypt Public Health Assoc. 1978;53(3-4):183-4.

6.Strausbaugh LJ, Laughlin LW, Meegan JM, Watten RH. Clinical studies on Rift Valley fever, Part I: Acute febrile and hemorrhagic-like diseases. J Egypt Public Health Assoc. 1978;53(3-4):181-2.

7.Blitvich BJ, Beaty BJ, Blair CD, Brault AC, Dobler G, Drebot MA, et al. Bunyavirus Taxonomy: Limitations and Misconceptions Associated with the Current ICTV Criteria Used for Species Demarcation. Am J Trop Med Hyg. 2018 Jul;99(1):11-6.

8.Smithburn KC, Haddow AJ, Mahaffy AF. A neurotropic virus isolated from Aedes mosquitoes caught in the Semliki forest. Am J Trop Med Hyg. 1946 Mar;26:189-208.

9.Abudurexiti A, Adkins S, Alioto D, Alkhovsky SV, Avšič-Županc T, Ballinger MJ, et al. Taxonomy of the order Bunyavirales: update 2019. Archives of Virology. 2019;164(7):1949-65.

10.Leventhal SS, Wilson D, Feldmann H, Hawman DW. A Look into Bunyavirales Genomes: Functions of Non-Structural (NS) Proteins. Viruses. 2021;13(2):314.

11.Davies FG. The Historical and Recent Impact of Rift Valley Fever in Africa. The American Journal of Tropical Medicine and Hygiene. 2010;83(2_Suppl):73-4.

12.Morvan J, Rollin PE, Roux J. [Rift Valley fever in Madagascar in 1991. Sero-epidemiological studies in cattle]. Rev Elev Med Vet Pays Trop. 1992;45(2):121-7.

13.Morvan J, Rollin PE, Laventure S, Rakotoarivony I, Roux J. Rift Valley fever epizootic in the central highlands of Madagascar. Res Virol. 1992 Nov-Dec;143(6):407-15.

14.Ahmad K. More deaths from Rift Valley fever in Saudi Arabia and Yemen. The Lancet. 2000;356(9239):1422.

15.LaBeaud AD, Muchiri EM, Ndzovu M, Mwanje MT, Muiruri S, Peters CJ, et al. Interepidemic Rift Valley fever virus seropositivity, northeastern Kenya. Emerg Infect Dis. 2008 Aug;14(8):1240-6.

16.Clark MHA, Warimwe GM, Di Nardo A, Lyons NA, Gubbins S. Systematic literature review of Rift Valley fever virus seroprevalence in livestock, wildlife and humans in Africa from 1968 to 2016. PLOS Neglected Tropical Diseases. 2018;12(7):e0006627.

17.Endale A, Michlmayr D, Abegaz WE, Geda B, Asebe G, Medhin G, et al. Sero-prevalence of West Nile virus and Rift Valley fever virus infections among cattle under extensive production system in South Omo area, southern Ethiopia. Tropical Animal Health and Production. 2021;53(1).

18.Muturi M, Akoko J, Nthiwa D, Chege B, Nyamota R, Mutiiria M, et al. Serological evidence of single and mixed infections of Rift Valley fever virus, Brucella spp. and Coxiella burnetii in dromedary camels in Kenya. PLOS Neglected Tropical Diseases. 2021;15(3):e0009275.

19.Ndumu DB, Bakamutumaho B, Miller E, Nakayima J, Downing R, Balinandi S, et al. Serological evidence of Rift Valley fever virus infection among domestic ruminant herds in Uganda. BMC Veterinary Research. 2021;17(1).

20.Ushijima Y, Abe H, Nguema Ondo G, Bikangui R, Massinga Loembé M, Zadeh VR, et al. Surveillance of the major pathogenic arboviruses of public health concern in Gabon, Central Africa: increased risk of West Nile virus and dengue virus infections. BMC Infectious Diseases. 2021;21(1).

21.Javelle E, Lesueur A, Pommier De Santi V, De Laval F, Lefebvre T, Holweck G, et al. The challenging management of Rift Valley Fever in humans: literature review of the clinical disease and algorithm proposal. Annals of Clinical Microbiology and Antimicrobials. 2020;19(1).

22.Hornak KE, Lanchy JM, Lodmell JS. RNA Encapsidation and Packaging in the Phleboviruses. Viruses. 2016 Jul 15;8(7).

23.Pepin M, Bouloy M, Bird BH, Kemp A, Paweska J. Rift Valley fever virus (Bunyaviridae: Phlebovirus): an update on pathogenesis, molecular epidemiology, vectors, diagnostics and prevention. Veterinary Research. 2010;41(6):61.

24.Gaudreault NN, Indran SV, Balaraman V, Wilson WC, Richt JA. Molecular aspects of Rift Valley fever virus and the emergence of reassortants. Virus Genes. 2019 Feb;55(1):1-11.

25.Kakach LT, Suzich JA, Collett MS. Rift Valley fever virus M segment: phlebovirus expression strategy and protein glycosylation. Virology. 1989 Jun;170(2):505-10.

26.Ganaie SS, Schwarz MM, McMillen CM, Price DA, Feng AX, Albe JR, et al. Lrp1 is a host entry factor for Rift Valley fever virus. Cell. 2021;184(20):5163-78.e24.

27.Odendaal L, Clift SJ, Fosgate GT, Davis AS. Lesions and Cellular Tropism of Natural Rift Valley Fever Virus Infection in Adult Sheep. Vet Pathol. 2019 Jan;56(1):61-77.

28.Gommet C, Billecocq A, Jouvion G, Hasan M, Zaverucha Do Valle T, Guillemot L, et al. Tissue Tropism and Target Cells of NSs-Deleted Rift Valley Fever Virus in Live Immunodeficient Mice. PLoS Neglected Tropical Diseases. 2011;5(12):e1421.

29.Scharton D, Van Wettere AJ, Bailey KW, Vest Z, Westover JB, Siddharthan V, et al. Rift Valley fever virus infection in golden Syrian hamsters. PLoS One. 2015;10(1):e0116722.

30.McMillen CM, Hartman AL. Rift Valley fever in animals and humans: Current perspectives. Antiviral Research. 2018;156:29-37.

31.Barr JN. Bunyavirus mRNA synthesis is coupled to translation to prevent premature transcription termination. Rna. 2007 May;13(5):731-6.

32.Ikegami T, Won S, Peters CJ, Makino S. Rift Valley fever virus NSs mRNA is transcribed from an incoming anti-viral-sense S RNA segment. J Virol. 2005 Sep;79(18):12106-11.

33.Elliott RM. The Bunyaviridae: Plenum Press, New York and London; 1996.

34.Gerrard SR, Nichol ST. Characterization of the Golgi Retention Motif of Rift Valley Fever Virus G N Glycoprotein. Journal of Virology. 2002;76(23):12200-10.

35.Gerrard SR, Nichol ST. Synthesis, proteolytic processing and complex formation of N-terminally nested precursor proteins of the Rift Valley fever virus glycoproteins. Virology. 2007 Jan 20;357(2):124-33.

36.Wasmoen TL, Kakach LT, Collett MS. Rift Valley fever virus M segment: cellular localization of M segment-encoded proteins. Virology. 1988 Sep;166(1):275-80.

37.Suzich JA, Collett MS. Rift Valley fever virus M segment: cell-free transcription and translation of virus-complementary RNA. Virology. 1988 Jun;164(2):478-86.

38.Carnec X, Ermonval M, Kreher F, Flamand M, Bouloy M. Role of the cytosolic tails of Rift Valley fever virus envelope glycoproteins in viral morphogenesis. Virology. 2014 Jan 5;448:1-14.

39.Wichgers Schreur PJ, Kortekaas J. Single-Molecule FISH Reveals Non-selective Packaging of Rift Valley Fever Virus Genome Segments. PLoS Pathog. 2016 Aug;12(8):e1005800.

40.Ratovonjato J, Olive MM, Tantely LM, Andrianaivolambo L, Tata E, Razainirina J, et al. Detection, isolation, and genetic characterization of Rift Valley fever virus from Anopheles (Anopheles) coustani, Anopheles (Anopheles) squamosus, and Culex (Culex) antennatus of the Haute Matsiatra region, Madagascar. Vector Borne Zoonotic Dis. 2011 Jun;11(6):753-9.

41.Rostal MK, Evans AL, Sang R, Gikundi S, Wakhule L, Munyua P, et al. Identification of potential vectors of and detection of antibodies against Rift Valley fever virus in livestock during interepizootic periods. Am J Vet Res. 2010 May;71(5):522-6.

42.Sang R, Kioko E, Lutomiah J, Warigia M, Ochieng C, O'Guinn M, et al. Rift Valley fever virus epidemic in Kenya, 2006/2007: the entomologic investigations. Am J Trop Med Hyg. 2010 Aug;83(2 Suppl):28-37.

43.Turell MJ, Lee JS, Richardson JH, Sang RC, Kioko EN, Agawo MO, et al. Vector competence of Kenyan Culex zombaensis and Culex quinquefasciatus mosquitoes for Rift Valley fever virus. J Am Mosq Control Assoc. 2007 Dec;23(4):378-82.

44.Linthicum KJ, Bailey CL, Davies FG, Kairo A, Logan TM. The horizontal distribution of Aedes pupae and their subsequent adults within a flooded dambo in Kenya: implications for Rift Valley fever virus control. J Am Mosq Control Assoc. 1988 Dec;4(4):551-4.

45.Bird BH, McElroy AK. Rift Valley fever virus: Unanswered questions. Antiviral Research. 2016;132:274-80.

46.Linthicum KJ, Davies FG, Kairo A, Bailey CL. Rift Valley fever virus (family Bunyaviridae, genus Phlebovirus). Isolations from Diptera collected during an inter-epizootic period in Kenya. J Hyg (Lond). 1985 Aug;95(1):197-209.

47.Gora D, Yaya T, Jocelyn T, Didier F, Maoulouth D, Amadou S, et al. The potential role of rodents in the enzootic cycle of Rift Valley fever virus in Senegal. Microbes Infect. 2000 Apr;2(4):343-6.

48.Manore CA, Beechler BR. Inter-epidemic and between-season persistence of rift valley fever: vertical transmission or cryptic cycling? Transbound Emerg Dis. 2015 Feb;62(1):13-23.

49.Ahmed Kamal S. Observations on rift valley fever virus and vaccines in Egypt. Virology Journal. 2011;8(1):532.

50.Sissoko D, Giry C, Gabrie P, Tarantola A, Pettinelli F, Collet L, et al. Rift Valley Fever, Mayotte, 2007–2008. Emerging Infectious Diseases. 2009;15(4):568-70.

51.Liu J, Sun Y, Shi W, Tan S, Pan Y, Cui S, et al. The first imported case of Rift Valley fever in China reveals a genetic reassortment of different viral lineages. Emerg Microbes Infect. 2017 Jan 18;6(1):e4.

52.De St. Maurice A, Harmon J, Nyakarahuka L, Balinandi S, Tumusiime A, Kyondo J, et al. Rift valley fever viral load correlates with the human inflammatory response and coagulation pathway abnormalities in humans with hemorrhagic manifestations. PLOS Neglected Tropical Diseases. 2018;12(5):e0006460.

53.Memish ZA, Masri MA, Anderson BD, Heil GL, Merrill HR, Khan SU, et al. Elevated antibodies against Rift Valley fever virus among humans with exposure to ruminants in Saudi Arabia. Am J Trop Med Hyg. 2015 Apr;92(4):739-43.

54.Ng'Ang'A CM, Bukachi SA, Bett BK. Lay perceptions of risk factors for Rift Valley fever in a pastoral community in northeastern Kenya. BMC Public Health. 2015;16(1).

55.Nicholas DE, Jacobsen KH, Waters NM. Risk factors associated with human Rift Valley fever infection: systematic review and meta-analysis. Trop Med Int Health. 2014 Dec;19(12):1420-9.

56.LaBeaud AD, Pfeil S, Muiruri S, Dahir S, Sutherland LJ, Traylor Z, et al. Factors associated with severe human Rift Valley fever in Sangailu, Garissa County, Kenya. PLoS Negl Trop Dis. 2015 Mar;9(3):e0003548.

57.Anyangu AS, Njenga MK, Paweska JT, Lederman ER, Mutonga D, Sharif SK, et al. Risk Factors for Severe Rift Valley Fever Infection in Kenya, 2007. The American Journal of Tropical Medicine and Hygiene. 2010;83(2_Suppl):14-21.

58.van Velden DJ, Meyer JD, Olivier J, Gear JH, McIntosh B. Rift Valley fever affecting humans in South Africa: a clinicopathological study. S Afr Med J. 1977 Jun 11;51(24):867-71.

59.Al-Hamdan NA, Panackal AA, Al Bassam TH, Alrabea A, Al Hazmi M, Al Mazroa Y, et al. The Risk of Nosocomial Transmission of Rift Valley Fever. PLoS Negl Trop Dis. 2015 Dec;9(12):e0004314.

60.Cook EAJ, Grossi-Soyster EN, De Glanville WA, Thomas LF, Kariuki S, Bronsvoort BMDC, et al. The sero-epidemiology of Rift Valley fever in people in the Lake Victoria Basin of western Kenya. PLOS Neglected Tropical Diseases. 2017;11(7):e0005731.

61.Findlay GM. Rift valley fever or enzootic hepatitis. Transactions of the Royal Society of Tropical Medicine and Hygiene. 1932 1932/01/30/;25(4):229-IN11.

62.Madani TA, Al-Mazrou YY, Al-Jeffri MH, Mishkhas AA, Al-Rabeah AM, Turkistani AM, et al. Rift Valley Fever Epidemic in Saudi Arabia: Epidemiological, Clinical, and Laboratory Characteristics. Clinical Infectious Diseases. 2003;37(8):1084-92.

63.Baba M, Masiga DK, Sang R, Villinger J. Has Rift Valley fever virus evolved with increasing severity in human populations in East Africa? Emerg Microbes Infect. 2016 Jun 22;5(6):e58.

64.Saluzzo JF, Digoutte JP, Chartier C, Martinez D, Bada R. Focus of Rift Valley fever virus transmission in southern Mauritania. Lancet. 1987 Feb 28;1(8531):504.

65.Zeller HG, Fontenille D, Traore-Lamizana M, Thiongane Y, Digoutte JP. Enzootic activity of Rift Valley fever virus in Senegal. Am J Trop Med Hyg. 1997 Mar;56(3):265-72.

66.Kahlon SS, Muiruri S, Peters CJ, Clinton White A, Leduc J, King CH, et al. Severe Rift Valley Fever May Present with a Characteristic Clinical Syndrome. The American Journal of Tropical Medicine and Hygiene. 2010;82(3):371-5.

67.Woods CW, Karpati AM, Grein T, McCarthy N, Gaturuku P, Muchiri E, et al. An Outbreak of Rift Valley Fever in Northeastern Kenya, 1997-98. Emerging Infectious Diseases. 2002;8(2):138-44.

68.McElroy AK, Nichol ST. Rift Valley fever virus inhibits a pro-inflammatory response in experimentally infected human monocyte derived macrophages and a pro-inflammatory cytokine

response may be associated with patient survival during natural infection. Virology. 2012 Jan 5;422(1):6-12.

69.McElroy AK, Harmon JR, Flietstra T, Nichol ST, Spiropoulou CF. Human Biomarkers of Outcome Following Rift Valley Fever Virus Infection. The Journal of Infectious Diseases. 2018;218(11):1847-51.

70.Shieh W-J, Breiman RF, Mosha F, Bloland P, Rao CY, Njenga MK, et al. Pathologic Studies on Suspect Animal and Human Cases of Rift Valley Fever from an Outbreak in Eastern Africa, 2006–2007. The American Journal of Tropical Medicine and Hygiene. 2010;83(2_Suppl):38-42.

71.Meegan JM. The Rift Valley fever epizootic in Egypt 1977-78. 1. Description of the epizzotic and virological studies. Trans R Soc Trop Med Hyg. 1979;73(6):618-23.

72.Alrajhi AA, Al-Semari A, Al-Watban J. Rift Valley Fever Encephalitis. Emerging Infectious Diseases. 2004;10(3):554-5.

73.Gear J, De Meillon B, Measroch V, Davis DH, Harwin H. Rift valley fever in South Africa. 2. The occurrence of human cases in the Orange Free State, the North-Western Cape Province, the Western and Southern Transvaal. B. Field and laboratory investigation. S Afr Med J. 1951 Dec 8;25(49):908-12.

74.Al-Hazmi A, Al-Rajhi AA, Abboud EB, Ayoola EA, Al-Hazmi M, Saadi R, et al. Ocular complications of Rift Valley fever outbreak in Saudi Arabia. Ophthalmology. 2005 Feb;112(2):313-8.

75.Hise AG, Traylor Z, Hall NB, Sutherland LJ, Dahir S, Ermler ME, et al. Association of symptoms and severity of rift valley fever with genetic polymorphisms in human innate immune pathways. PLoS Negl Trop Dis. 2015 Mar;9(3):e0003584.

76.Mohamed M, Bloland P, Paweska J, Omulo S, Zeidner N, Njenga MK, et al. Epidemiologic and Clinical Aspects of a Rift Valley Fever Outbreak in Humans in Tanzania, 2007. The American Journal of Tropical Medicine and Hygiene. 2010;83(2_Suppl):22-7.

77.Jansen Van Vuren P, Shalekoff S, Grobbelaar AA, Archer BN, Thomas J, Tiemessen CT, et al. Serum levels of inflammatory cytokines in Rift Valley fever patients are indicative of severe disease. 2015;12(1).

78.Dodd KA, McElroy AK, Jones TL, Zaki SR, Nichol ST, Spiropoulou CF. Rift valley Fever virus encephalitis is associated with an ineffective systemic immune response and activated T cell infiltration into the CNS in an immunocompetent mouse model. PLoS Negl Trop Dis. 2014 Jun;8(6):e2874.

79.Peters CJ, Linthicum KJ. Rift Valley Fever. Boca Raton, FL: CRC Press; 1994.

80.Davenport FM, Hennessy AV, Francis T, Jr. Epidemiologic and immunologic significance of age distribution of antibody to antigenic variants of influenza virus. J Exp Med. 1953 Dec;98(6):641-56.

81.Jensen KE, Francis T, Jr. The antigenic composition of influenza virus measured by antibody-absorption. J Exp Med. 1953 Dec;98(6):619-39.

82.Hartman AL, Powell DS, Bethel LM, Caroline AL, Schmid RJ, Oury T, et al. Aerosolized rift valley fever virus causes fatal encephalitis in african green monkeys and common marmosets. J Virol. 2014 Feb;88(4):2235-45.

83.Smith DR, Bird BH, Lewis B, Johnston SC, McCarthy S, Keeney A, et al. Development of a novel nonhuman primate model for Rift Valley fever. J Virol. 2012 Feb;86(4):2109-20.

84.Francis T, Magill TP. RIFT VALLEY FEVER : A REPORT OF THREE CASES OF LABORATORY INFECTION AND THE EXPERIMENTAL TRANSMISSION OF THE DISEASE TO FERRETS. J Exp Med. 1935 Aug 31;62(3):433-48.

85.Barbeau DJ, Albe JR, Nambulli S, Tilston-Lunel NL, Hartman AL, Lakdawala SS, et al. Rift Valley Fever Virus Infection Causes Acute Encephalitis in the Ferret. mSphere. 2020;5(5):e00798-20.

86.Peters CJ, Anderson GW, Jr. Pathogenesis of Rift Valley fever. Contr Epidem Biostatist. 1981(3):21-41.

87.Anderson GW, Jr., Rosebrock JA, Johnson AJ, Jennings GB, Peters CJ. Infection of inbred rat strains with Rift Valley fever virus: development of a congenic resistant strain and observations on age-dependence of resistance. Am J Trop Med Hyg. 1991 May;44(5):475-80.

88.Peters CJ, Slone TW. Inbred rat strains mimic the disparate human response to Rift Valley fever virus infection. J Med Virol. 1982;10(1):45-54.

89.T.J. Bucci IMM, O.L. Wood. Experimental Rift Valley Fever Encephalitis in ACI Rats. Contr Epidem Biostatist. 1981;3:60-7.

90.Anderson GW, Jr., Slone TW, Jr., Peters CJ. Pathogenesis of Rift Valley fever virus (RVFV) in inbred rats. Microb Pathog. 1987 Apr;2(4):283-93.

91.Bales JM, Powell DS, Bethel LM, Reed DS, Hartman AL. Choice of inbred rat strain impacts lethality and disease course after respiratory infection with Rift Valley Fever Virus. Front Cell Infect Microbiol. 2012;2:105.

92.Caroline AL, Kujawa MR, Oury TD, Reed DS, Hartman AL. Inflammatory Biomarkers Associated with Lethal Rift Valley Fever Encephalitis in the Lewis Rat Model. Front Microbiol. 2015;6:1509.

93.Ross TM, Bhardwaj N, Bissel SJ, Hartman AL, Smith DR. Animal models of Rift Valley fever virus infection. 2012;163(2):417-23.

94.Cartwright HN, Barbeau DJ, McElroy AK. Rift Valley Fever Virus Is Lethal in Different Inbred Mouse Strains Independent of Sex. Frontiers in Microbiology. 2020;11.

95.Gray KK, Worthy MN, Juelich TL, Agar SL, Poussard A, Ragland D, et al. Chemotactic and inflammatory responses in the liver and brain are associated with pathogenesis of Rift Valley fever virus infection in the mouse. PLoS Negl Trop Dis. 2012;6(2):e1529.

96.do Valle TZ, Billecocq A, Guillemot L, Alberts R, Gommet C, Geffers R, et al. A new mouse model reveals a critical role for host innate immunity in resistance to Rift Valley fever. J Immunol. 2010 Nov 15;185(10):6146-56.

97.Lathan R, Simon-Chazottes D, Jouvion G, Godon O, Malissen M, Flamand M, et al. Innate Immune Basis for Rift Valley Fever Susceptibility in Mouse Models. Sci Rep. 2017 Aug 2;7(1):7096.

98.Smith DR, Steele KE, Shamblin J, Honko A, Johnson J, Reed C, et al. The pathogenesis of Rift Valley fever virus in the mouse model. Virology. 2010 Nov 25;407(2):256-67.

99.Reed C, Lin K, Wilhelmsen C, Friedrich B, Nalca A, Keeney A, et al. Aerosol exposure to Rift Valley fever virus causes earlier and more severe neuropathology in the murine model, which has important implications for therapeutic development. PLoS Negl Trop Dis. 2013;7(4):e2156.

100.Brown JL, Dominik JW, Morrissey RL. Respiratory infectivity of a recently isolated Egyptian strain of Rift Valley fever virus. Infect Immun. 1981 Sep;33(3):848-53.

101.Dodd KA, McElroy AK, Jones ME, Nichol ST, Spiropoulou CF. Rift Valley fever virus clearance and protection from neurologic disease are dependent on CD4+ T cell and virus-specific antibody responses. J Virol. 2013 Jun;87(11):6161-71.

102.Harmon JR, Spengler JR, Coleman-McCray JD, Nichol ST, Spiropoulou CF, McElroy AK. CD4 T Cells, CD8 T Cells, and Monocytes Coordinate To Prevent Rift Valley Fever Virus Encephalitis. J Virol. 2018 Dec 15;92(24).

103.Barbeau DJ, Cartwright HN, Harmon JR, Spengler JR, Spiropoulou CF, Sidney J, et al. Identification and characterization of Rift Valley fever virus-specific T cells reveals a dependence on CD40/CD40L interactions for prevention of encephalitis. J Virol. 2021 Sep 8:Jvi0150621.

104.Mansfield KL, Banyard AC, McElhinney L, Johnson N, Horton DL, Hernández-Triana LM, et al. Rift Valley fever virus: A review of diagnosis and vaccination, and implications for emergence in Europe. Vaccine. 2015;33(42):5520-31.

105.Bird BH, Khristova ML, Rollin PE, Ksiazek TG, Nichol ST. Complete genome analysis of 33 ecologically and biologically diverse Rift Valley fever virus strains reveals widespread virus movement and low genetic diversity due to recent common ancestry. J Virol. 2007 Mar;81(6):2805-16.

106.Randall R, Gibbs CJ, Jr., Aulisio CG, Binn LN, Harrison VR. The development of a formalin-killed Rift Valley fever virus vaccine for use in man. J Immunol. 1962 Nov;89:660-71.

107.Faburay B, LaBeaud AD, McVey DS, Wilson WC, Richt JA. Current Status of Rift Valley Fever Vaccine Development. Vaccines (Basel). 2017 Sep 19;5(3).

108.Fawzy M, Helmy YA. The One Health Approach is Necessary for the Control of Rift Valley Fever Infections in Egypt: A Comprehensive Review. Viruses. 2019;11(2):139.

109.Botros B, Omar A, Elian K, Mohamed G, Soliman A, Salib A, et al. Adverse response of non-indigenous cattle of European breeds to live attenuated Smithburn Rift Valley fever vaccine. J Med Virol. 2006 Jun;78(6):787-91.

110.Kamal SA. Pathological studies on postvaccinal reactions of Rift Valley fever in goats. Virol J. 2009 Jul 6;6:94.

111.Caplen H, Peters CJ, Bishop DH. Mutagen-directed attenuation of Rift Valley fever virus as a method for vaccine development. J Gen Virol. 1985 Oct;66 (Pt 10):2271-7.

112.Wilson WC, Bawa B, Drolet BS, Lehiy C, Faburay B, Jasperson DC, et al. Evaluation of lamb and calf responses to Rift Valley fever MP-12 vaccination. Vet Microbiol. 2014 Aug 6;172(1-2):44-50.

113.Lokugamage N, Ikegami T. Genetic stability of Rift Valley fever virus MP-12 vaccine during serial passages in culture cells. NPJ Vaccines. 2017;2.

114.Smith DR, Johnston SC, Piper A, Botto M, Donnelly G, Shamblin J, et al. Attenuation and efficacy of live-attenuated Rift Valley fever virus vaccine candidates in non-human primates. PLoS Negl Trop Dis. 2018 May;12(5):e0006474.

115.Pittman PR, Norris SL, Brown ES, Ranadive MV, Schibly BA, Bettinger GE, et al. Rift Valley fever MP-12 vaccine Phase 2 clinical trial: Safety, immunogenicity, and genetic characterization of virus isolates. Vaccine. 2016 Jan 20;34(4):523-30.

116.Kortekaas J, Zingeser J, de Leeuw P, de La Rocque S, Unger H, Moormann RJ. Rift Valley Fever Vaccine Development, Progress and Constraints. Emerg Infect Dis. 2011 Sep;17(9):e1.

117.Muller R, Saluzzo JF, Lopez N, Dreier T, Turell M, Smith J, et al. Characterization of clone 13, a naturally attenuated avirulent isolate of Rift Valley fever virus, which is altered in the small segment. Am J Trop Med Hyg. 1995 Oct;53(4):405-11.

118.Njenga MK, Njagi L, Thumbi SM, Kahariri S, Githinji J, Omondi E, et al. Randomized controlled field trial to assess the immunogenicity and safety of rift valley fever clone 13 vaccine in livestock. PLoS Negl Trop Dis. 2015 Mar;9(3):e0003550.

119.Makoschey B, van Kilsdonk E, Hubers WR, Vrijenhoek MP, Smit M, Wichgers Schreur PJ, et al. Rift Valley Fever Vaccine Virus Clone 13 Is Able to Cross the Ovine Placental Barrier Associated with Foetal Infections, Malformations, and Stillbirths. PLoS Negl Trop Dis. 2016 Mar;10(3):e0004550.

120.Dungu B, Lubisi BA, Ikegami T. Rift Valley fever vaccines: current and future needs. Current Opinion in Virology. 2018;29:8-15.

121.Kirsi JJ, North JA, McKernan PA, Murray BK, Canonico PG, Huggins JW, et al. Broad-spectrum antiviral activity of 2-beta-D-ribofuranosylselenazole-4-carboxamide, a new antiviral agent. Antimicrobial Agents and Chemotherapy. 1983;24(3):353-61.

122.Kende M, Lupton HW, Rill WL, Gibbs P, Levy HB, Canonico PG. Ranking of prophylactic efficacy of poly(ICLC) against Rift Valley fever virus infection in mice by incremental relative risk of death. Antimicrob Agents Chemother. 1987 Aug;31(8):1194-8.

123.Hartman A. Rift Valley Fever. Clinics in Laboratory Medicine. 2017;37(2):285-301.

124.Scharton D, Bailey KW, Vest Z, Westover JB, Kumaki Y, Van Wettere A, et al. Favipiravir (T-705) protects against peracute Rift Valley fever virus infection and reduces delayed-onset neurologic disease observed with ribavirin treatment. Antiviral Research. 2014;104:84-92.

125.Caroline AL, Powell DS, Bethel LM, Oury TD, Reed DS, Hartman AL. Broad Spectrum Antiviral Activity of Favipiravir (T-705): Protection from Highly Lethal Inhalational Rift Valley Fever. PLoS Neglected Tropical Diseases. 2014;8(4):e2790.

126.Atkins C, Freiberg AN. Recent advances in the development of antiviral therapeutics for Rift Valley fever virus infection. Future Virology. 2017;12(11):651-65.

127.Wolf MC, Freiberg AN, Zhang T, Akyol-Ataman Z, Grock A, Hong PW, et al. A broad-spectrum antiviral targeting entry of enveloped viruses. Proc Natl Acad Sci U S A. 2010 Feb 16;107(7):3157-62.

128.Panchal RG, Reid SP, Tran JP, Bergeron AA, Wells J, Kota KP, et al. Identification of an antioxidant small-molecule with broad-spectrum antiviral activity. Antiviral Res. 2012 Jan;93(1):23-9.

129.Warren TK, Wells J, Panchal RG, Stuthman KS, Garza NL, Van Tongeren SA, et al. Protection against filovirus diseases by a novel broad-spectrum nucleoside analogue BCX4430. Nature. 2014 Apr 17;508(7496):402-5.

130.Benedict A, Bansal N, Senina S, Hooper I, Lundberg L, de la Fuente C, et al. Repurposing FDA-approved drugs as therapeutics to treat Rift Valley fever virus infection. Front Microbiol. 2015;6:676.

131.Bell TM, Espina V, Senina S, Woodson C, Brahms A, Carey B, et al. Rapamycin modulation of p70 S6 kinase signaling inhibits Rift Valley fever virus pathogenesis. Antiviral Res. 2017 Jul;143:162-75.

132.Burton DR, Saphire EO. Swift antibodies to counter emerging viruses. Proc Natl Acad Sci U S A. 2015 Aug 18;112(33):10082-3.

133.Sparrow E, Friede M, Sheikh M, Torvaldsen S. Therapeutic antibodies for infectious diseases. Bulletin of the World Health Organization. 2017;95(3):235-7.

134.Qiu X, Wong G, Audet J, Bello A, Fernando L, Alimonti JB, et al. Reversion of advanced Ebola virus disease in nonhuman primates with ZMapp. Nature. 2014 Oct 2;514(7520):47-53.

135.Barouch DH, Whitney JB, Moldt B, Klein F, Oliveira TY, Liu J, et al. Therapeutic efficacy of potent neutralizing HIV-1-specific monoclonal antibodies in SHIV-infected rhesus monkeys. Nature. 2013 Nov 14;503(7475):224-8.

136.de Jong YP, Dorner M, Mommersteeg MC, Xiao JW, Balazs AB, Robbins JB, et al. Broadly neutralizing antibodies abrogate established hepatitis C virus infection. Sci Transl Med. 2014 Sep 17;6(254):254ra129.

137.Pincetic A, Bournazos S, Dilillo DJ, Maamary J, Wang TT, Dahan R, et al. Type I and type II Fc receptors regulate innate and adaptive immunity. Nature Immunology. 2014;15(8):707-16.

138.Bournazos S, Wang TT, Dahan R, Maamary J, Ravetch JV. Signaling by Antibodies: Recent Progress. Annual Review of Immunology. 2017;35(1):285-311.

139.Gunn BM, Yu WH, Karim MM, Brannan JM, Herbert AS, Wec AZ, et al. A Role for Fc Function in Therapeutic Monoclonal Antibody-Mediated Protection against Ebola Virus. Cell Host Microbe. 2018 Aug 8;24(2):221-33.e5.

140.Saphire EO, Schendel SL, Gunn BM, Milligan JC, Alter G. Antibody-mediated protection against Ebola virus. Nat Immunol. 2018 Nov;19(11):1169-78.

141.Fox JM, Roy V, Gunn BM, Huang L, Edeling MA, Mack M, et al. Optimal therapeutic activity of monoclonal antibodies against chikungunya virus requires Fc-FcγR interaction on monocytes. Sci Immunol. 2019 Feb 22;4(32).

142.Lofano G, Gorman MJ, Yousif AS, Yu WH, Fox JM, Dugast AS, et al. Antigen-specific antibody Fc glycosylation enhances humoral immunity via the recruitment of complement. Sci Immunol. 2018 Aug 17;3(26).

143.DiLillo DJ, Tan GS, Palese P, Ravetch JV. Broadly neutralizing hemagglutinin stalk-specific antibodies require FcγR interactions for protection against influenza virus in vivo. Nat Med. 2014 Feb;20(2):143-51.

144.DiLillo DJ, Palese P, Wilson PC, Ravetch JV. Broadly neutralizing anti-influenza antibodies require Fc receptor engagement for in vivo protection. J Clin Invest. 2016 Feb;126(2):605-10.

145.Bonsignori M, Pollara J, Moody MA, Alpert MD, Chen X, Hwang KK, et al. Antibody-dependent cellular cytotoxicity-mediating antibodies from an HIV-1 vaccine efficacy trial target multiple epitopes and preferentially use the VH1 gene family. J Virol. 2012 Nov;86(21):11521-32.

146.Lambotte O, Ferrari G, Moog C, Yates NL, Liao H-X, Parks RJ, et al. Heterogeneous neutralizing antibody and antibody-dependent cell cytotoxicity responses in HIV-1 elite controllers. AIDS. 2009;23(8):897-906.

147.Jegaskanda S, Luke C, Hickman HD, Sangster MY, Wieland-Alter WF, McBride JM, et al. Generation and Protective Ability of Influenza Virus-Specific Antibody-Dependent Cellular Cytotoxicity in Humans Elicited by Vaccination, Natural Infection, and Experimental Challenge. J Infect Dis. 2016 Sep 15;214(6):945-52.

148.Vogt MR, Dowd KA, Engle M, Tesh RB, Johnson S, Pierson TC, et al. Poorly neutralizing cross-reactive antibodies against the fusion loop of West Nile virus envelope protein protect in vivo via Fcgamma receptor and complement-dependent effector mechanisms. J Virol. 2011 Nov;85(22):11567-80.

149.Barouch DH, Stephenson KE, Borducchi EN, Smith K, Stanley K, McNally AG, et al. Protective efficacy of a global HIV-1 mosaic vaccine against heterologous SHIV challenges in rhesus monkeys. Cell. 2013 Oct 24;155(3):531-9.

150.He W, Chen CJ, Mullarkey CE, Hamilton JR, Wong CK, Leon PE, et al. Alveolar macrophages are critical for broadly-reactive antibody-mediated protection against influenza A virus in mice. Nat Commun. 2017 Oct 10;8(1):846.

151.Mehlhop E, Nelson S, Jost CA, Gorlatov S, Johnson S, Fremont DH, et al. Complement protein C1q reduces the stoichiometric threshold for antibody-mediated neutralization of West Nile virus. Cell Host Microbe. 2009 Oct 22;6(4):381-91.

152.Li F, Freed DC, Tang A, Rustandi RR, Troutman MC, Espeseth AS, et al. Complement enhances in vitro neutralizing potency of antibodies to human cytomegalovirus glycoprotein B (gB) and immune sera induced by gB/MF59 vaccination. NPJ Vaccines. 2017;2:36.

153.Huiskonen JT, ÖVerby AK, Weber F, GrüNewald K. Electron Cryo-Microscopy and Single-Particle Averaging of Rift Valley Fever Virus: Evidence for GN-GC Glycoprotein Heterodimers. Journal of Virology. 2009;83(8):3762-9.

154.Freiberg AN, Sherman MB, Morais MC, Holbrook MR, Watowich SJ. Three-dimensional organization of Rift Valley fever virus revealed by cryoelectron tomography. J Virol. 2008 Nov;82(21):10341-8.

155.Halldorsson S, Li S, Li M, Harlos K, Bowden TA, Huiskonen JT. Shielding and activation of a viral membrane fusion protein. Nat Commun. 2018 Jan 24;9(1):349.

156.Besselaar TG, Blackburn NK. The synergistic neutralization of Rift Valley fever virus by monoclonal antibodies to the envelope glycoproteins. Arch Virol. 1992;125(1-4):239-50.

157.Faburay B, Lebedev M, McVey DS, Wilson W, Morozov I, Young A, et al. A Glycoprotein Subunit Vaccine Elicits a Strong Rift Valley Fever Virus Neutralizing Antibody Response in Sheep. Vector-Borne and Zoonotic Diseases. 2014;14(10):746-56.

158.Bird BH, Maartens LH, Campbell S, Erasmus BJ, Erickson BR, Dodd KA, et al. Rift Valley fever virus vaccine lacking the NSs and NSm genes is safe, nonteratogenic, and confers protection from viremia, pyrexia, and abortion following challenge in adult and pregnant sheep. J Virol. 2011 Dec;85(24):12901-9.

159.Dodd KA, Bird BH, Metcalfe MG, Nichol ST, Albariño CG. Single-Dose Immunization with Virus Replicon Particles Confers Rapid Robust Protection against Rift Valley Fever Virus Challenge. Journal of Virology. 2012;86(8):4204-12.

160.Morrill JC, Ikegami T, Yoshikawa-Iwata N, Lokugamage N, Won S, Terasaki K, et al. Rapid Accumulation of Virulent Rift Valley Fever Virus in Mice from an Attenuated Virus Carrying a Single Nucleotide Substitution in the M RNA. 2010;5(4):e9986.

161.Peters CJ, Reynolds JA, Slone TW, Jones DE, Stephen EL. Prophylaxis of Rift Valley fever with antiviral drugs, immune serum, an interferon inducer, and a macrophage activator. Antiviral Res. 1986 Aug;6(5):285-97.

162.Peters CJ, Jones D, Trotter R, Donaldson J, White J, Stephen E, et al. Experimental Rift Valley fever in rhesus macaques. Arch Virol. 1988;99(1-2):31-44.

163.Labeaud D. Towards a safe, effective vaccine for Rift Valley fever virus. Future Virol. 2010 Nov;5(6):675-8.

164.Jansen Van Vuren P, Tiemessen CT, Paweska JT. Anti-Nucleocapsid Protein Immune Responses Counteract Pathogenic Effects of Rift Valley Fever Virus Infection in Mice. PLoS ONE. 2011;6(9):e25027.

165.López-Gil E, Lorenzo G, Hevia E, Borrego B, Eiden M, Groschup M, et al. A Single Immunization with MVA Expressing GnGc Glycoproteins Promotes Epitope-specific CD8+-T Cell Activation and Protects Immune-competent Mice against a Lethal RVFV Infection. PLoS Neglected Tropical Diseases. 2013;7(7):e2309.

166.Gutjahr B, Keller M, Rissmann M, von Arnim F, Jäckel S, Reiche S, et al. Two monoclonal antibodies against glycoprotein Gn protect mice from Rift Valley Fever challenge by cooperative effects. PLoS Negl Trop Dis. 2020 Mar;14(3):e0008143.

167.Bhardwaj N, Heise MT, Ross TM. Vaccination with DNA plasmids expressing Gn coupled to C3d or alphavirus replicons expressing gn protects mice against Rift Valley fever virus. PLoS Negl Trop Dis. 2010 Jun 22;4(6):e725.

168.Allen ER, Krumm SA, Raghwani J, Halldorsson S, Elliott A, Graham VA, et al. A Protective Monoclonal Antibody Targets a Site of Vulnerability on the Surface of Rift Valley Fever Virus. Cell Rep. 2018 Dec 26;25(13):3750-8.e4.

169.Wang Q, Ma T, Wu Y, Chen Z, Zeng H, Tong Z, et al. Neutralization mechanism of human monoclonal antibodies against Rift Valley fever virus. Nat Microbiol. 2019 Jul;4(7):1231-41.

170.Hao M, Zhang G, Zhang S, Chen Z, Chi X, Dong Y, et al. Characterization of Two Neutralizing Antibodies against Rift Valley Fever Virus Gn Protein. Viruses. 2020 Feb 27;12(3).

171.Chapman NS, Zhao H, Kose N, Westover JB, Kalveram B, Bombardi R, et al. Potent neutralization of Rift Valley fever virus by human monoclonal antibodies through fusion inhibition. Proceedings of the National Academy of Sciences. 2021;118(14):e2025642118.

172.LaBeaud AD, Ochiai Y, Peters CJ, Muchiri EM, King CH. Spectrum of Rift Valley fever virus transmission in Kenya: insights from three distinct regions. Am J Trop Med Hyg. 2007 May;76(5):795-800.

173.LaBeaud AD, Muiruri S, Sutherland LJ, Dahir S, Gildengorin G, Morrill J, et al. Postepidemic analysis of Rift Valley fever virus transmission in northeastern kenya: a village cohort study. PLoS Negl Trop Dis. 2011 Aug;5(8):e1265.

174.Nanyingi MO, Munyua P, Kiama SG, Muchemi GM, Thumbi SM, Bitek AO, et al. A systematic review of Rift Valley Fever epidemiology 1931–2014. Infection Ecology & Epidemiology. 2015;5(1):28024.

175.Lorenzo G, López-Gil E, Warimwe GM, Brun A. Understanding Rift Valley fever: contributions of animal models to disease characterization and control. Mol Immunol. 2015 Jul;66(1):78-88.

176.Keane TM, Goodstadt L, Danecek P, White MA, Wong K, Yalcin B, et al. Mouse genomic variation and its effect on phenotypes and gene regulation. Nature. 2011;477(7364):289-94.

177.Leist SR, Pilzner C, Van Den Brand JMA, Dengler L, Geffers R, Kuiken T, et al. Influenza H3N2 infection of the collaborative cross founder strains reveals highly divergent host responses and identifies a unique phenotype in CAST/EiJ mice. 2016;17(1).

178.Gralinski LE, Ferris MT, Aylor DL, Whitmore AC, Green R, Frieman MB, et al. Genome Wide Identification of SARS-CoV Susceptibility Loci Using the Collaborative Cross. PLOS Genetics. 2015;11(10):e1005504.

179.Ikegami T, Balogh A, Nishiyama S, Lokugamage N, Saito TB, Morrill JC, et al. Distinct virulence of Rift Valley fever phlebovirus strains from different genetic lineages in a mouse model. PLOS ONE. 2017;12(12):e0189250.

180.Staeheli P, Grob R, Meier E, Sutcliffe JG, Haller O. Influenza virus-susceptible mice carry Mx genes with a large deletion or a nonsense mutation. Molecular and Cellular Biology. 1988;8(10):4518-23.

181.Frese M, Kochs G, Feldmann H, Hertkorn C, Haller O. Inhibition of bunyaviruses, phleboviruses, and hantaviruses by human MxA protein. Journal of virology. 1996;70(2):915-23.

182.Ferris MT, Aylor DL, Bottomly D, Whitmore AC, Aicher LD, Bell TA, et al. Modeling Host Genetic Regulation of Influenza Pathogenesis in the Collaborative Cross. PLoS Pathogens. 2013;9(2):e1003196.

183.Verhelst J, Hulpiau P, Saelens X. Mx Proteins: Antiviral Gatekeepers That Restrain the Uninvited. Microbiology and Molecular Biology Reviews. 2013;77(4):551-66.

184.vom Steeg LG, Klein SL. SeXX Matters in Infectious Disease Pathogenesis. PLoS Pathog. 2016 Feb;12(2):e1005374.

185.Vom Steeg LG, Klein SL. Sex Steroids Mediate Bidirectional Interactions Between Hosts and Microbes. Horm Behav. 2017 Feb;88:45-51.

186.Klein SL, Roberts CW. Sex hormones and immunity to infection. Berlin: Springer-Verlag; 2010.

187.Klein SL, Roberts CW. Sex and gender differences in infection and treatments for infectious diseases. Switzerland: Springer International Publishing; 2015.

188.Chan WK, Klock G, Bernard HU. Progesterone and glucocorticoid response elements occur in the long control regions of several human papillomaviruses involved in anogenital neoplasia. J Virol. 1989 Aug;63(8):3261-9.

189.Lorenzo ME, Hodgson A, Robinson DP, Kaplan JB, Pekosz A, Klein SL. Antibody responses and cross protection against lethal influenza A viruses differ between the sexes in C57BL/6 mice. Vaccine. 2011 Nov 15;29(49):9246-55.

190.Hoffmann J, Otte A, Thiele S, Lotter H, Shu Y, Gabriel G. Sex differences in H7N9 influenza A virus pathogenesis. Vaccine. 2015 Dec 8;33(49):6949-54.

191.Tokuda S, Do Valle TZ, Batista L, Simon-Chazottes D, Guillemot L, Bouloy M, et al. The genetic basis for susceptibility to Rift Valley fever disease in MBT/Pas mice. Genes Immun. 2015 Apr-May;16(3):206-12.

192.Villarino NF, LeCleir GR, Denny JE, Dearth SP, Harding CL, Sloan SS, et al. Composition of the gut microbiota modulates the severity of malaria. Proc Natl Acad Sci U S A. 2016 Feb 23;113(8):2235-40.

193.Li S, Zhu X, Guan Z, Huang W, Zhang Y, Kortekaas J, et al. NSs Filament Formation Is Important but Not Sufficient for RVFV Virulence In Vivo. Viruses. 2019 Sep 8;11(9).

194.Robinson CM, Woods Acevedo MA, McCune BT, Pfeiffer JK. Related Enteric Viruses Have Different Requirements for Host Microbiota in Mice. J Virol. 2019 Dec 1;93(23).

195.The Genome Architecture of the Collaborative Cross Mouse Genetic Reference Population. Genetics. 2012;190(2):389-401.

196.The Collaborative Cross, a community resource for the genetic analysis of complex traits. Nature Genetics. 2004;36(11):1133-7.

197.Roberts A, Pardo-Manuel De Villena F, Wang W, McMillan L, Threadgill DW. The polymorphism architecture of mouse genetic resources elucidated using genome-wide resequencing data: implications for QTL discovery and systems genetics. Mammalian Genome. 2007;18(6-7):473-81.

198.Patzina C, Haller O, Kochs G. Structural requirements for the antiviral activity of the human MxA protein against Thogoto and influenza A virus. J Biol Chem. 2014 Feb 28;289(9):6020-7.

199.Lindenmann J, Lane CA, Hobson D. The Resistance of A2G Mice to Myxoviruses. The Journal of Immunology. 1963;90(6):942-51.

200.Wonderlich ER, Caroline AL, McMillen CM, Walters AW, Reed DS, Barratt-Boyes SM, et al. Peripheral Blood Biomarkers of Disease Outcome in a Monkey Model of Rift Valley Fever Encephalitis. Journal of Virology. 2017;92(3).

201.Boyles DA, Schwarz MM, Albe JR, McMillen CM, O'Malley KJ, Reed DS, et al. Development of Rift valley fever encephalitis in rats is mediated by early infection of olfactory epithelium and neuroinvasion across the cribriform plate. Journal of General Virology. 2021;102(2).

202.Finke S, Conzelmann KK. Replication strategies of rabies virus. Virus Res. 2005 Aug;111(2):120-31.

203.Jacob Y, Badrane H, Ceccaldi PE, Tordo N. Cytoplasmic dynein LC8 interacts with lyssavirus phosphoprotein. J Virol. 2000 Nov;74(21):10217-22.

204.Raux H, Flamand A, Blondel D. Interaction of the rabies virus P protein with the LC8 dynein light chain. J Virol. 2000 Nov;74(21):10212-6.

205.Wang P, Dai J, Bai F, Kong K-F, Wong SJ, Montgomery RR, et al. Matrix Metalloproteinase 9 Facilitates West Nile Virus Entry into the Brain. Journal of Virology. 2008;82(18):8978-85.

206.Albe JR, Boyles DA, Walters AW, Kujawa MR, McMillen CM, Reed DS, et al. Neutrophil and macrophage influx into the central nervous system are inflammatory components of lethal Rift Valley fever encephalitis in rats. PLoS Pathog. 2019 Jun;15(6):e1007833.

207.Cartwright HN, Barbeau DJ, McElroy AK. Isotype-Specific Fc Effector Functions Enhance Antibody-Mediated Rift Valley Fever Virus Protection In Vivo. mSphere. 2021 Sep 8:e0055621.

208.Rift Valley fever – Kenya. [cited; Available from: www.who.int/csr/don/18-june-2018-rift-valley-fever-kenya/en/

209.Rift Valley fever – Gambia. [cited; Available from: www.who.int/csr/don/26-february-2018-rift-valley-fever-gambia/en/

210.South Sudan declares Rift Valley fever outbreak in parts of Eastern Lakes State. [cited; Available from: https://www.afro.who.int/news/south-sudan-declares-rift-valley-fever-outbreak-parts-eastern-lakes-state

211.Youssouf H, Subiros M, Dennetiere G, Collet L, Dommergues L, Pauvert A, et al. Rift Valley Fever Outbreak, Mayotte, France, 2018–2019. Emerging Infectious Diseases. 2020;26(4):769-72.

212.Vloet RPM, Vogels CBF, Koenraadt CJM, Pijlman GP, Eiden M, Gonzales JL, et al. Transmission of Rift Valley fever virus from European-breed lambs to Culex pipiens mosquitoes. PLOS Neglected Tropical Diseases. 2017;11(12):e0006145.

213.Mehand MS, Al-Shorbaji F, Millett P, Murgue B. The WHO R&D Blueprint: 2018 review of emerging infectious diseases requiring urgent research and development efforts. Antiviral Research. 2018;159:63-7.

214.RVFV infections 2000-2016. [cited; Available from: https://www.cdc.gov/vhf/rvf/outbreaks/distribution-map.html

215.Wu Y, Zhu Y, Gao F, Jiao Y, Oladejo BO, Chai Y, et al. Structures of phlebovirus glycoprotein Gn and identification of a neutralizing antibody epitope. Proc Natl Acad Sci U S A. 2017 Sep 5;114(36):E7564-e73.

216.Mancardi DA, Iannascoli B, Hoos S, England P, Daëron M, Bruhns P. FcγRIV is a mouse IgE receptor that resembles macrophage FcεRI in humans and promotes IgE-induced lung inflammation. Journal of Clinical Investigation. 2008;118(11):3738-50.

217.Bruhns P, Jönsson F. Mouse and human FcR effector functions. Immunol Rev. 2015 Nov;268(1):25-51.

218.Nimmerjahn F, Ravetch JV. Fcgamma receptors: old friends and new family members. Immunity. 2006 Jan;24(1):19-28.

219.Nimmerjahn F, Ravetch JV. Fcgamma receptors as regulators of immune responses. Nat Rev Immunol. 2008 Jan;8(1):34-47.

220.Taborda CP, Rivera J, Zaragoza O, Casadevall A. More Is Not Necessarily Better: Prozone-Like Effects in Passive Immunization with IgG. The Journal of Immunology. 2003;170(7):3621-30.

221.Lux A, Yu X, Scanlan CN, Nimmerjahn F. Impact of Immune Complex Size and Glycosylation on IgG Binding to Human FcγRs. The Journal of Immunology. 2013;190(8):4315-23.

222.Li D, He W, Liu X, Zheng S, Qi Y, Li H, et al. A potent human neutralizing antibody Fc-dependently reduces established HBV infections. eLife. 2017;6.

223.Wright D, Allen ER, Clark MHA, Gitonga JN, Karanja HK, Hulswit RJG, et al. Naturally Acquired Rift Valley Fever Virus Neutralizing Antibodies Predominantly Target the Gn Glycoprotein. iScience. 2020;23(11):101669.

224.Gerrard SR, Bird BH, Albariño CG, Nichol ST. The NSm proteins of Rift Valley fever virus are dispensable for maturation, replication and infection. Virology. 2007 Mar 15;359(2):459-65.

225.Bird BH, Albariño CG, Nichol ST. Rift Valley fever virus lacking NSm proteins retains high virulence in vivo and may provide a model of human delayed onset neurologic disease. Virology. 2007 May 25;362(1):10-5.

226.Reed LJ, Muench H. A SIMPLE METHOD OF ESTIMATING FIFTY PER CENT ENDPOINTS12. American Journal of Epidemiology. 1938;27(3):493-7.

227.Welsh CE, Miller DR, Manly KF, Wang J, McMillan L, Morahan G, et al. Status and access to the Collaborative Cross population. Mammalian Genome. 2012;23(9-10):706-12.

228.Iraqi FA, Churchill G, Mott R. The Collaborative Cross, developing a resource for mammalian systems genetics: A status report of the Wellcome Trust cohort. Mammalian Genome. 2008;19(6):379-81.

229.Morahan G, Balmer L, Monley D. Establishment of "The Gene Mine": a resource for rapid identification of complex trait genes. Mammalian Genome. 2008;19(6):390-3.

230.Chesler EJ, Miller DR, Branstetter LR, Galloway LD, Jackson BL, Philip VM, et al. The Collaborative Cross at Oak Ridge National Laboratory: developing a powerful resource for systems genetics. Mammalian Genome. 2008;19(6):382-9.

231.Bird BH, Bawiec DA, Ksiazek TG, Shoemaker TR, Nichol ST. Highly sensitive and broadly reactive quantitative reverse transcription-PCR assay for high-throughput detection of Rift Valley fever virus. J Clin Microbiol. 2007 Nov;45(11):3506-13.

232.McElroy AK, Albariño CG, Nichol ST. Development of a RVFV ELISA that can distinguish infected from vaccinated animals. Virology Journal. 2009;6(1):125.

233.Harmon JR, Barbeau DJ, Nichol ST, Spiropoulou CF, McElroy AK. Rift Valley fever virus vaccination induces long-lived, antigen-specific human T cell responses. NPJ Vaccines. 2020;5:17.

234.Gatti DM, Svenson KL, Shabalin A, Wu LY, Valdar W, Simecek P, et al. Quantitative Trait Locus Mapping Methods for Diversity Outbred Mice. G3: Genes|Genomes|Genetics. 2014;4(9):1623-33.

235.Hasebe R, Suzuki T, Makino Y, Igarashi M, Yamanouchi S, Maeda A, et al. Transcellular transport of West Nile virus-like particles across human endothelial cells depends on residues 156 and 159 of envelope protein. BMC Microbiol. 2010 Jun 8;10:165.

236.Liou ML, Hsu CY. Japanese encephalitis virus is transported across the cerebral blood vessels by endocytosis in mouse brain. Cell Tissue Res. 1998 Sep;293(3):389-94.

237.Salimi H, Cain MD, Jiang X, Roth RA, Beatty WL, Sun C, et al. Encephalitic Alphaviruses Exploit Caveola-Mediated Transcytosis at the Blood-Brain Barrier for Central Nervous System Entry. mBio. 2020 Feb 11;11(1).

238.Bai F, Kong KF, Dai J, Qian F, Zhang L, Brown CR, et al. A paradoxical role for neutrophils in the pathogenesis of West Nile virus. J Infect Dis. 2010 Dec 15;202(12):1804-12.

239.van Rooijen N, van Nieuwmegen R. Elimination of phagocytic cells in the spleen after intravenous injection of liposome-encapsulated dichloromethylene diphosphonate. An enzyme-histochemical study. Cell Tissue Res. 1984;238(2):355-8.

240.Daley JM, Thomay AA, Connolly MD, Reichner JS, Albina JE. Use of Ly6G-specific monoclonal antibody to deplete neutrophils in mice. J Leukoc Biol. 2008 Jan;83(1):64-70.

241.Earnest JT, Holmes AC, Basore K, Mack M, Fremont DH, Diamond MS. The mechanistic basis of protection by non-neutralizing anti-alphavirus antibodies. Cell Rep. 2021 Apr 6;35(1):108962.